Optimization of CFRP joints with fibre metal laminates

Daniel Gomes dos Santos

Supervisor: Prof. Lucas da Silva

Co-Supervisor: Dr. Ricardo Carbas

Dr. Eduardo Marques

U.PORTO

FEUP FACULDADE DE ENGENHARIA
UNIVERSIDADE DO PORTO

Integrated Master in Mechanical Engineering

June 2018

To my family

Abstract

The use of composite materials in the field of aerospace industry has been increasing, supported by the technological advances in the field of structural adhesives, needed to join these materials. Fibre metal laminates (FMLs) are a concept based on hybrid composite structures that consist in a combination of thin sheets of metal alloys and plies of fibre reinforced polymeric materials. This concept is able to combine the advantages of both types of material - in one side, the high bearing strength, impact resistance and reparability characteristics of metallic materials, and on the other, the high strength and stiffness, low density, fatigue and corrosion characteristics of the fibre reinforced polymers. Because of these combined properties FMLs have been the target of several studies made by major aerospace companies, such as Airbus and Boeing.

The aim of this project was to increase the peel strength of composite materials and increase the joint strength of composite adhesive joints by using different lay-ups of the adherends of an adhesively bonded joint based on reinforcements made using either additional adhesive layers or a concept similar to the FML concept. As the composite material, carbon fibre reinforced polymer (CFRP) was used and several alternative lay-up configurations were suggested using additional interlaminar adhesive layers, sheets of aluminium or sheets of titanium. An adhesive developed for the aeronautical industry, AF 163-2K, was chosen to manufacture several single lap joints (SLJs) for tensile testing. The main objective was to identify which configuration results in greater improvement of the SLJ mechanical properties, when compared to the reference (CFRP only configuration).

In order to determine the best lay-up, several configurations were manufactured and tested through tensile tests of SLJs with 50 mm of overlap length. In each manufacturing process, a combined cure of the adhesive and the CFRP plies of each joint was used, so that the overall curing time spent in the process could be minimized. To predict the failure load and the failure mode of each one of the joints, several numerical models, using finite element analysis (FEA), were created to simulate the experimental tensile tests of the adhesive joints manufactured, through the commercial software *Abaqus*®.

The best performing configuration tested was the configuration employing a combination of additional adhesive layers and titanium plies in the adherend of an SLJ, Ti-Adh-CFRP-Adh-Ti. For this optimal configuration the values of the failure loads obtained were improved significantly, when compared to the CFRP only reference configuration. Additionally, the delamination problem found in CFRP joints did not occur with the referred

configuration, being in this case, for every specimen tested, the failure mode present by the SLJ the cohesive failure in the adhesive.

Resumo

A utilização de materiais compósitos no contexto da indústria aeroespacial tem crescido ao longo dos últimos anos, sendo este aumento suportado por diversos avanços no campo da tecnologia dos adesivos estruturais, sendo estes necessários para a proceder à união deste tipo de materiais. Os *Fibre Metal Laminates* (FMLs) referem-se a um conceito baseado em estruturas híbridas que consistem numa utilização combinada de chapas finas de ligas metálicas e de camadas de materiais poliméricos reforçados com fibras. Este conceito permite combinar as vantagens de ambos os tipos de materiais - por um lado, assegura a resistência à propagação de fendas ao impacto, e reparabilidade dos materiais metálicos, e por outro, a elevada resistência mecânica e rigidez, densidade reduzida, e a boa resistência à fadiga e à corrosão características dos polímeros reforçados com fibras. Devido a esta combinação de propriedades, os FMLs têm sido alvo de projetos de estudo e desenvolvimento de importantes empresas aeroespaciais, como a *Airbus* e a *Boeing*.

Este projeto tem como objetivo melhorar a resistência ao arrancamento de materiais compósitos, bem como a resistência da própria junta adesiva que utiliza este tipo de materiais como substratos, utilizando diferentes empilhamentos para os substratos da junta adesiva, baseados em reforços que recorrem tanto à introdução de camadas adesivas adicionais como a um conceito semelhante ao empregue pelos dos FMLs. Utilizando como material compósito uma matriz epóxida reforçada com fibras de carbono (CFRP), várias alternativas para o substrato de referência, apenas CFRP, foram sugeridas usando camadas adesivas interlaminares adicionais, folhas de alumínio ou chapas de titânio para a produção das juntas de sobreposição simples (SLJs). O adesivo escolhido foi o AF 163-2K, bastante utilizado na indústria aeronáutica. O objetivo principal é identificar que configurações resultam numa maior melhoria em termos das propriedades mecânicas da junta, quando comparadas com a junta de referência (configuração utilizando apenas CFRP).

Com o propósito de descobrir a melhor configuração, vários *lay-ups* foram fabricados e testados, através de ensaios de tração de juntas de sobreposição simples com 50 mm de comprimento de sobreposição. Em todos os processos de fabrico das diversas juntas deste projeto, foi utilizada uma cura combinada do adesivo e das camadas CFRP, ou seja, ambos os materiais foram curados no mesmo ciclo de cura, de modo a que o tempo total despendido no processo pudesse ser otimizado. De forma a prever a força de rutura e o modo de falha de cada uma das juntas, vários modelos numéricos foram desenvolvidos, recorrendo a análises de elementos finitos, e utilizando o software comercial *Abaqus*®, para simular os resultados experimentais dos ensaios de tração das juntas adesivas fabricadas.

Foi possível verificar que a melhor configuração testada neste projeto foi a configuração referente ao uso combinado de camadas adicionais de adesivo e camadas de titânio no substrato de uma SLJ, configuração com o empilhamento Ti-Adh-CFRP-Adh-Ti. Para esta configuração "ótima", os valores obtidos para a força de rutura da junta foram melhorados significativamente, quando comparados com a configuração de referência (apenas CFRP). Adicionalmente, o problema de delaminação, recorrentemente verificado em juntas de CFRP, não foi observado nos substratos com a referida configuração, sendo que, com o empilhamento considerado “ótimo”, para todas as amostras testadas, o modo de falha obtido foi sempre falha coesiva no adesivo.

Acknowledgements

I would like to thank firstly, Ricardo Carbas, for his guidance, patience, and dedication during this months, for all the effort invested in this project and all the hours spent at the lab and in meetings.

Secondly, I would like to thank Professor Lucas da Silva, for sharing his knowledge and expertise during this dissertation, for all his straight and objective opinions and for his motivation in times when the project seemed to be going south.

To all the members of ADFEUP, particularly to the colleagues Marcos, Matheus and Xinlong with whom I spent so much time this semester, to them for all their help and advice.

I would like to thank my friends, with whom I started this journey 5 years ago, Luís Oliveira, Luís Alves, Moreira, Samuel, Rafa Vieira, João Costa, Chica, Bernardo, Ricardo, Rui, Pedro, Pires, Varela, Rosa, William, Pimenta, Kevin and Quinta, for their friendship and support, for making this journey easier since the beginning, and for the countless moments and memories that we shared along the way.

To my friends in my hometown, specially to all the guys from Moita Rugby Clube da Bairrada, for all the training sessions that I missed because I had to work.

To Francisca, Cortez, Patricia e Té, for all your love along the years, and for all the moments when I had you to hear me out.

A special thank you to my grandmother, I know that wherever she is, she is going to be proud of me for all the effort that I always put in everything I do. Finally, to my family still here, who supported me no matter what, for being there whenever I needed, and without whom I would have never become the engineer that I am becoming and, more importantly, without whom I would have never learned how to be the person that they know that I am today.

Contents

Nomenclature

Acronyms

ARALL – Aramid reinforced aluminium laminate
BARALL – Basalt reinforced aluminium laminate
CARALL – Carbon reinforced aluminium laminate
CFRP – Carbon fibre reinforced polymer
CTE – Coefficient of thermal expansion
CZE – Cohesive zone elements
CZM – Cohesive zone model
DCB – Double cantilever beam
DLJ – Double lap joint
ENF – End notched flexure
FEA – Finite element analysis
FEM – Finite elements method
FML – Fibre metal laminate
FRP – Fibre reinforced polymer
GLARE – Glass reinforced aluminium
HTCL - Hybrid titanium composite laminate
SLJ – Single lap joint
TAST – Thick adherend shear test

Symbols

Adh - Adhesive
Al – Aluminium
b – Width of the joint
E – Young's Modulus
G – Shear modulus
G_{IC} – Fracture energy in mode I
G_{IIC} – Fracture energy in mode II
l – Overlap length
P – Load
t – Thickness of the adherend
Tg – Glass transition temperature

Ti – Titanium

δ - Displacement

τ – Shear stress

υ – Poisson’s ratio

Figures

Tables

1 Introduction

1.1 Background and motivation

Composite materials have been increasingly replacing the more traditional metallic alloys mainly due to their combination of excellent mechanical properties and their low weight. For some applications, specifically in the transport industry, these are major factors to consider, based on the objectives of designing low weight structures that can operate with low energy consumption, important to ensure reduced overall costs and minimize environmental impact, but are still able to respect quality and safety standards. Nowadays the percentage of composite materials used in, for example, a modern airplane can reach over 50% in structural weight, as is the case of the Boeing 787 Dreamliner [1].

Adhesion bonding technology has been developed side by side with composite materials allowing its usage in large scale. Composite materials, however, show a major decrease in their mechanical properties when holes are needed for joining either by using rivets or bolts. This low performance is mainly due to the low bearing and shear strengths and to the higher notch sensitivity they exhibit when compared to metals [2]. To avoid these joining methods, adhesive bonding appears as an ideal technology to be applied allowing higher stiffness, more uniform stress distributions and extremely low weight.

Most of the composite materials used are fibre reinforced plastics, materials which exhibit an anisotropic behaviour and so, with out of plane loading, can experience peel stresses and fail in the transverse direction – a phenomenon known as delamination.

Many research studies have proposed methods to mitigate the disadvantages of composite materials being one of those solutions the concept of fibre metal laminates. FMLs are hybrid composite materials in which plies of fibre reinforced plastics are reinforced with alternatively stacked sheets of metallic alloys. This allows to combine the properties of the metallic material, such as the high bearing strength, impact resistance and an easier

reparability, with the properties of the plastic reinforced composites, namely the excellent fatigue and corrosion resistance in addition to the high strength and stiffness [3].

In this project two concepts were used to improve the peel strength of a basic composite material substrate in an adhesively bonded joint and to increase the overall performance of the joint itself, one based on the introduction of additional layers of adhesive material in the substrate and other based on a concept similar to the concept of FML.

1.2 Objectives

The main aim of this thesis is to study the influence of different lay-up configurations, starting from a basic CFRP substrate, in the performance of an adhesively bonded SLJ.

The several lay-ups that were suggested in this project use additional adhesive layers in between the plies of the CFRP as well as metallic plies using a concept similar to the one used in FMLs.

Therefore, the main objective is to find the configuration that offers the best improvement in the peel strength of the composite, maximizes joint strength of composite adhesive joints, and avoids the occurrence of delamination.

To test and find that optimal configuration, several numerical and experimental studies were made. The CFRP composite suffered a hybridization through its thickness, by including combinations of sheets of film adhesive, titanium plies and aluminium plies, depending on the configuration.

1.3 Research methodology

To achieve the objectives purposed the following work plan was followed:

a) Literature review on composite materials, mostly carbon fibre and FMLs, adhesive bonding, FML's and SLJ's failure mechanisms;

b) State of the art, focusing on the FML concept and its applications;

c) Review of previous data obtained by studies performed in the context of the Adhesives Group of the Faculty of Engineering of the University of Porto;

d) Manufacture SLJs using substrates with different lay-up configurations using additional adhesive layers, titanium and aluminium;

d) Performance of experimental tests of SLJs for different combinations and analysis of the respective results;

e) Numerical simulation of the tensile tests made with SLJs using *Abaqus*® software to correlate with the experimental results;

f) Numerical study of the behaviour of the suggested configurations under impact conditions.

1.4 Outline of the thesis

This thesis comprehends eight major chapters, that will be presented, in terms of content, as follows.

In the first one, an overview of the project its background, motivation and purpose are presented, as well as the main objectives and this outline that was followed.

The second chapter consists on a literature review focused on adhesive bonding, composite materials, the FML concept, and several methods regarding the strength prediction of adhesively bonded joints.

In the third chapter, the technical details, the several conceptual approaches taken during this project and the experimental procedures are described.

The fourth chapter regards the presentation of the experimental results obtained for the tensile tests performed on the several lay-up configurations suggested for the SLJs.

In the fifth chapter, the finite element analysis is discussed, with the description of the models developed for this project and the presentation of the numerical results obtained.

In the sixth chapter, the results from both FEA and the tensile tests are compared and discussed, in terms of failure load and failure mode obtained by the several lay-up configurations suggested.

The seventh chapter presents the conclusions drawn from the results of this project.

Finally, in the eight chapter, suggestions for future investigations and ideas to follow the work developed in this thesis are given.

2 Literature review

2.1 Adhesive bonding

2.1.1 Introduction

An adhesive can be defined as “a material which when applied to surfaces of materials can join them together and resist separation”. Many kinds of adhesives have been used by humankind throughout history as a mean of joining materials, but the modern technical progress of this technology only started by mid 1940s [4].

In the context of engineering applications, structural adhesives are often referred, and can be defined, by adhesives that can withstand substantial loads (shear strength superior to 5-10 MPa) and that are used to ensure the strength and stiffness of a structure [5].

Adhesive bonded joints are gaining ground as an alternative to mechanical joints due to their many advantages, as for example:

- The uniformization of the stress distribution along the bonded area, originating improvements in stiffness and load transmission, and reducing the overall weight and costs;
- The ability to join dissimilar materials, using the adhesive flexibility to compensate the thermal expansions due to different coefficients of thermal expansion (CTEs). An example of an automotive vehicle, where several dissimilar materials are used and bonded using adhesive joints is shown in Figure 1;
- The ability to join thin sheet materials. Despite of strength values that are lower than those presented by metallic materials, when used to join thin sheets the strength is considered adequate;
- Cost effective technique, being the application of adhesive an operation that can often be easily automated;
- Improvements in corrosion resistance, in overall appearance of the joints and in the design flexibility.

However, it is also important to identify the disadvantages of this technology, being these disadvantages the drive for the development of more studies. As main disadvantages, it can be pointed that, for example [6]:

- In environments where the temperature and humidity conditions are severe, problems of limited resistance can be detected, based on the polymeric nature of adhesives;
- There is still a lack of effective non-destructive techniques to assess adhesion problems in adhesive joints, making the quality control process more difficult;
- The manufacturing process can have a great weight on economic costs because many types of adhesives need certain temperature levels to ensure the hardening process and the bond, which is not usually instantaneous, requires the use of tools to maintain the substrates in the correct position of assembly.

There are nowadays many examples of structural applications where the main components transfer their load through an adhesive layer being the main areas of such applications the aerospace, automotive, marine (and offshore) and construction industries. In all these technological areas, the use of adhesive bonding technology is becoming more and more important as the need for weight savings and for joining dissimilar materials increases [7].

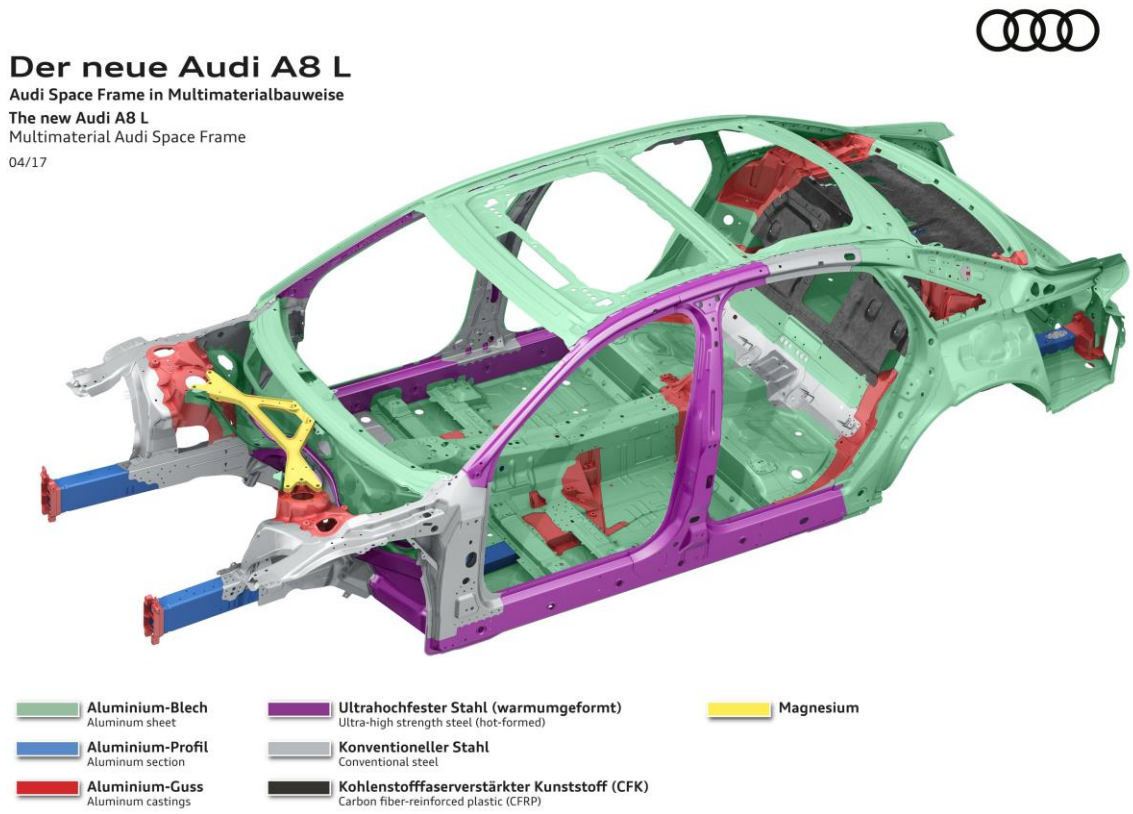

Figure 1: Adhesively bonded parts for Audi A8 L [8].

2.1.2 Types of adhesives

Adhesives can be divided according to many different classification methods, being one of the most general classification the division related to the source of the adhesive, that can be synthetic or natural. Synthetic, if the adhesive is manufactured using man-made products, as is the case for polymeric adhesives, natural, if the adhesives are manufactured with products that are sub products of natural origin. However, this division is too wide for many applications and it is necessary to classify adhesives according to their objectives and that classification can be organized by function, chemical composition, physical form, reaction mode among other forms of classification.

Within the functional classification adhesives can be divided in structural and non-structural being, as already referred in this work, the structural adhesives, those with high strength and performance, and having the function of keeping a structure bonded while resisting high loads without excessive deformation. The common types of structural adhesives and their main advantages and disadvantages are presented in the Table 1.

Table 1: Most relevant adhesive families and their properties [4]

Adhesive	Advantages	Disadvantages
Epoxies	High strength, good toughness, temperature resistance and relatively low cost	Short pot life, exothermic reaction, requires precise chemical formulation
Polyurethanes	Good strength and toughness at low temperatures, resistance to fatigue, impact resistance, good durability	Moisture sensitive, poor heat resistance, short pot life
Phenolics	High hardness, excellent thermal stability, low cost	Brittle with low peel strength, requires very high cure pressures
Silicones	Environmental stability, high degree of flexibility, capability of bond materials of dissimilar natures, excellent resistance to temperature and moisture	High cost, lower mechanical properties at room temperature
Cyanoacrylates	Rapid room temperature cure, good mechanical strength, long pot life, good adhesion to metal	Expensive, poor durability, poor heat resistance
Modified acrylates	Good peel and shear strengths, does not requires extensive surface treatments, room temperature cure	Limited resistance to thermal variation, difficult to process, toxic and flammable
Aromatics	Very good heat resistance	Expensive, hard to process, very brittle at room temperature

Regarding the chemical composition adhesives can be divided into thermosets, thermoplastics and as a mixture of both. This classification is further subdivided into several types. Thermoplastic adhesives are cured by cooling from a melted state or by loss of solvent. They can be melted after curing if subjected to temperatures above *Tg* (glass transition

temperature). Thermosetting adhesives, after the cure cycle, cannot be heated and melted again.

In terms of physical form, adhesives are available in many forms such as liquids, pastes, films and powder. This classification is very important due to its implications in the joint manufacturing process. For example, while liquid adhesives have good gap filling capabilities because they can easily flow into the bondline during manufacture, paste adhesives must be spread with the use of spatulas or pressure guns. Additionally, these adhesives can be supplied with or without solvent and, when without solvent, in one or two parts. Solid adhesives, as are the film adhesives, struggle to wet the surfaces but have advantages, as being adhesives with only one component, dismissing the steps of dosage and mixing and can be applied with very low waste.

The reaction method is also an important classification parameter with practical importance in the final application of a specific adhesive, as it divides adhesives according to the way they react or solidify (cure). Adhesives can cure by chemical reaction, by loss of solvent, by loss of water or by cooling from melted state [9].

2.1.3 Solicitation modes

To understand the mechanical behaviour of an adhesive joint it is first important to understand the type of stresses that can be applied, Figure 2. There are four types of stresses involved in the mechanics of an adhesive joint such as normal (or direct) stresses, shear stresses, cleavage stresses and peel stresses.

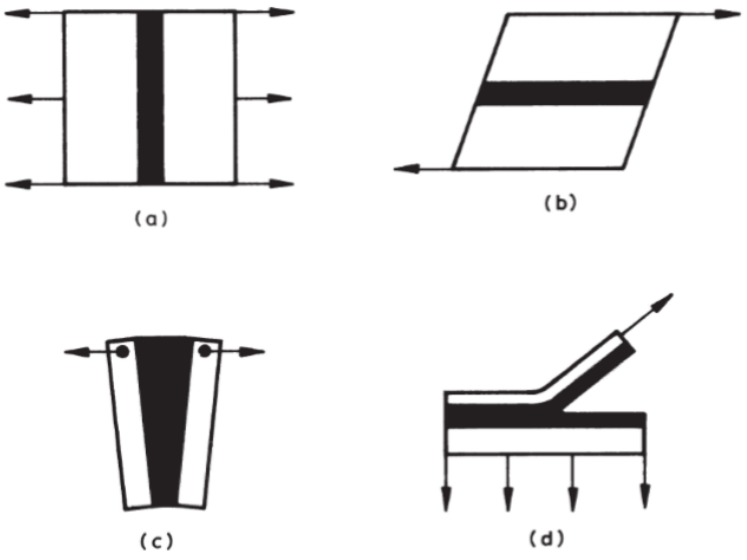

Figure 2: Failure loads in adhesive joints. a) Normal stress b) Shear stress c) Cleavage stress d) Peel stress [4].

Normal stresses are, as the designation indicates, normal on the plane in which they act, can be tensile or compressive and are uniformly distributed across the adhesive. Shear stresses are parallel to the plane on which they act and represent the preferred mode in which an adhesive should be loaded. These two types represent the components in which the resultant stress can be divided on any plane.

Additionally, it is important to identify other two types of stresses – cleavage and peel. In cleavage stresses, one of the adherends is subjected to stress while the other is theoretically under no stress, which arises as the result of an offset tensile force or bending moment or in the case of the usage of two stiff adherends. Peel stresses occur in cases where one, or both, adherends are flexible.

Knowing that, in real-world applications, it is very hard to design a joint in which only one type of stress is present and thus the main goal of a design study of an adhesive joint is to keep stresses to a minimum and to distribute the loads in the adhesive as a combination of compressive and shear stresses avoiding, as possible, tensile, cleavage and peel stresses [4].

2.1.4 Joint configuration

A wide variety of joints are available and the most analysed in the literature are single-lap joints, double-lap joints, scarf joints, and stepped-lap joints being the main objective of its design to minimize stress concentrations, being the peel stresses the main load to avoid [5]. In Figure 3 a schematic view of several types of joints is shown.

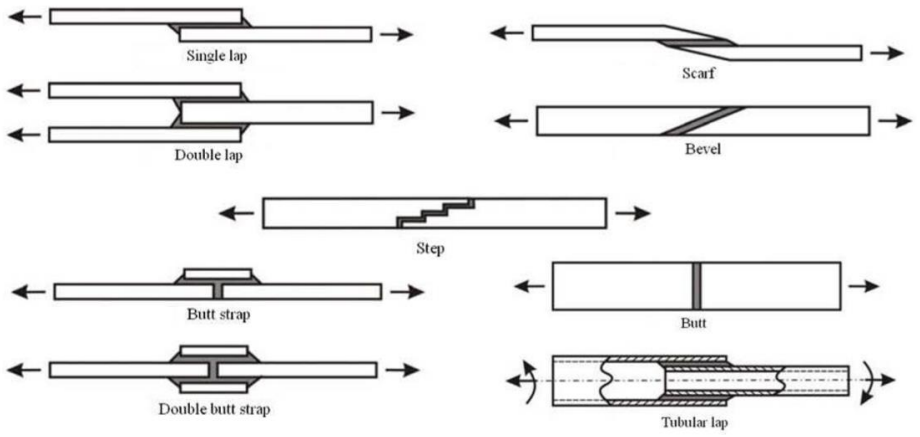

Figure 3: Examples of joint configurations [5].

The single-lap joint is the most common joint and it is widely used mainly due to its simplicity and efficiency. However, this type of design is associated with stress distributions

(shear and peel) that are concentrated at the ends of the overlap. Researchers have adopted various techniques to improve the efficiency of the single-lap joints such as altering the adherend geometry [10].

2.1.5 Failure modes

The failure modes of adhesive bonding are related with the description of the way in which bonded joints fail. These modes are related with the quality of the bond on the surfaces off the adherends, with the joint geometry and the types of loading that are applied and can be categorized in three main types, that can be observed in Figure 4.

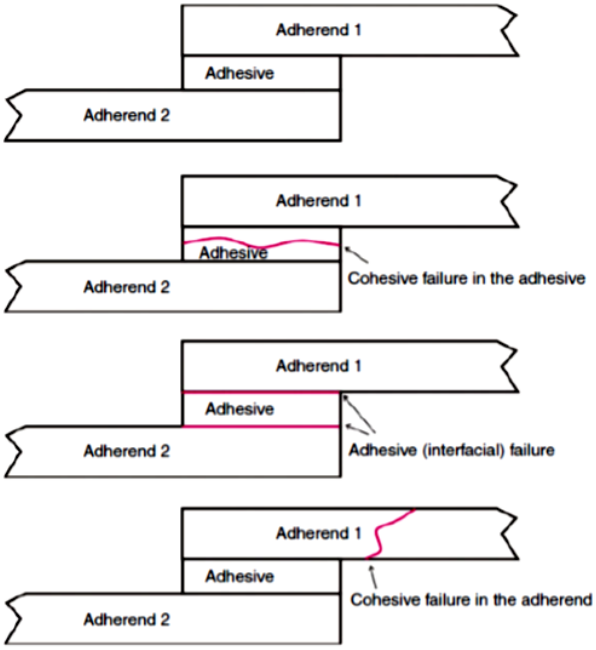

Figure 4: Failure modes in adhesive joints [6].

Cohesive failure designates the case when the failure occurs in the adhesive layer and is characterized by the presence of adhesive material on both surfaces of the adherends. This kind of failure is normally associated with poor design of the bonded joint or even with high porosity of the adhesive layer. The main type of loading related to this mode of joint failure is shear loading, even though a combination of shear and peel loads can also be the cause for cohesive failures [11].

Adhesive failure is used to describe cases where the failure occurs in the interface between the adhesive layer and one of the adherends. This kind of failure is associated with the manufacturing process of the joint and can be originated by surface contamination of the

surface of the adherend, insufficient or inappropriate surface treatment or by insufficient cure of the adhesive, not allowing the bond to fully form [12].

The ideal failure mode presented by an adhesive joint is to observe an adherend failure. This situation is achievable, in joints that are well designed and fabricated, and allows the facilitation of certification processes since that, in this kind of situation, the adhesive will present a higher strength than the adherend itself, allowing that, for testing, only the demonstration of the capacity of the adherend is needed to ensure the structural integrity of the bonded joint.

In many occasions the failure mode observed is a combination of more than one of the failure modes described above, being this case designated as a mixed failure and described as a percentage to cohesive or adhesive failure based on the fraction of the contact surface area that has failed cohesively or adhesively [13].

2.1.6 Surface treatments

Surface preparation is one of the most important steps to ensure the quality of an adhesive bond, because its final strength depends on this operation. The bonding of joints is achieved either by mechanical interlocking of the polymer with the adherend surface, or by chemical bonding of the polymer molecules with the metal oxide [14]. To improve bond strength and achieve a durable adhesive joint between different substrates, surface preparation is a necessary pre-treatment prior to adhesive bonding.

The goal of this step is to ensure that the weakest link in an adhesive joint is within the adhesive or adherend, not at the interfaces between them. With a good surface preparation, the failure should not occur in the interface due to a weak boundary layer (contaminant layers which do not promote bonding between the adhesive and the adherend) or insufficient wetting of the surface, in other words, the ideal, and most common, mode of failure of a bonded joint should be the cohesive failure [13].

This surface preparation can be a single or a combination of the following actions: removal of material, chemical modification of the surface, or changing of the surface topography, and these effects can be achieved through several treatments that can be grouped as mechanical, chemical, electrochemical, coupling agents or dry surface treatments that are preformed to increase surface tension, increase surface roughness and change the surface [3, 15].

Substrate	Treatment Method	Effect of Treatment
Metals	Degreasing	Cleaning of the surface
Metals	Grit blast	Loose material (weak boundary) removal from the surface and increase in contact surface area
Metals	Acid etch/liquid pickling	Surface oxidation
Metals	Anodizing	Surface oxidation
Plastics	Corona treatment	Weak boundary layer removal and surface oxidation
Plastics	Flame treatment	Weak boundary layer removal and surface oxidation
Plastics	Chemical etching	Weak boundary layer removal and surface oxidation
Fluoroplastics	Chemical etching	Surface defluorination and oxidation

Figure 5: Common surface treatments to enhance adhesion [13].

Choosing the surface treatment method depends on the type of materials of both adhesive and adherend, as shown in Figure 5. Additionally, cost and availability must also be considered and balanced against the requirement for reliability, maintainability and performance needed for a specific joint.

2.2 Fibre reinforced plastics

2.2.1 Introduction

Since the first flight of history, in December 17, 1903, by the Wright Brothers, the plane as a mean of transportation has been developed tremendously in terms of capacity and performance. Therefore, the development of new technologies and materials is of major importance to the aviation industry. The first break through was the introduction of the all metal aircraft that allowed air traffic to become intercontinental and available to the public, but the growth in the demand for air traffic required materials that could lower production and operating costs while maintaining the safety level of the aircrafts [16].

Composite materials and, specifically, the fibre reinforced plastics (FRP) have gained considerable importance during last decades. They were firstly applied in military applications in the aircraft industry after World War II and, nowadays, their uses and studies have spread to commercial aircraft and aerospace industries.

The drive for innovation in these industries is to achieve a lighter aircraft, reducing costs of fuel consumption and the reduction of the environmental impact of this sector [17].

Composite materials are replacing the more traditional materials, such as steel or aluminium, because of their strength/stiffness weight ratio and the flexibility to manufacture more aerodynamic structures. Additionally, they provide excellent fatigue properties and corrosion resistance [3]. The major trade-off of the aircraft industry is still the balance of the weight reduction with the structural integrity, price, and durability and, despite the increase in composite materials usage, as showed in Figure 6, metallic materials continue to be fundamental.

As examples of the growing importance of composite materials in commercial aircraft it can be pointed out the 22% composite material ratio of the total weight in the Airbus A380 and the example of Boeing, that already has models, such as the Boeing 787 Dreamliner (Figure 7), that uses composite materials for around 50% of the aircraft structure weight, enhancing the saving in fuel consumption, maintenance, and operating costs [1, 18].

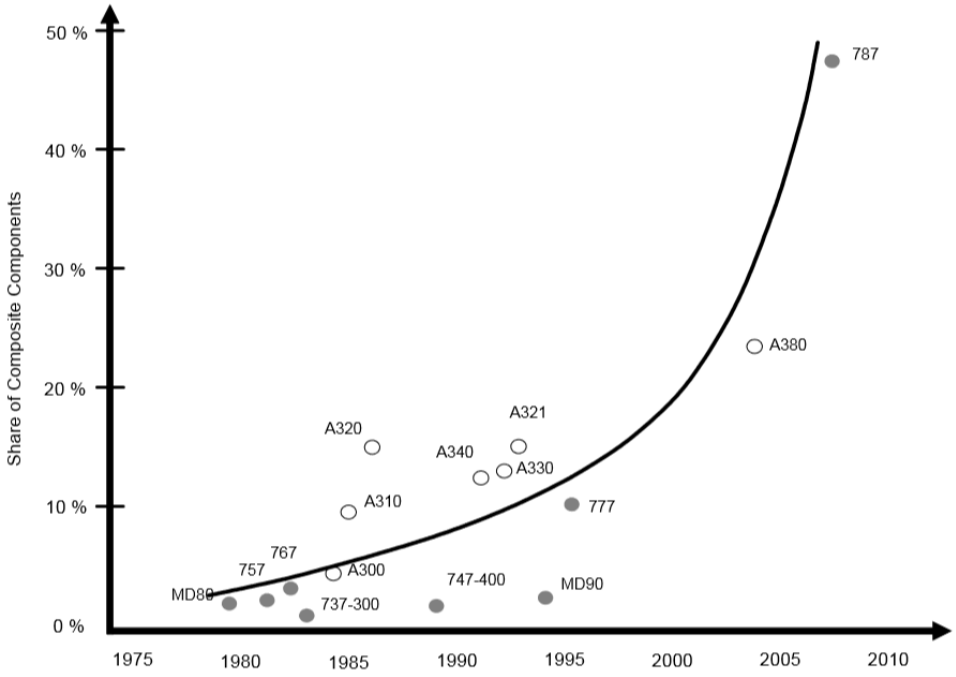

Figure 6: Evolution of the share of composite components in commercial aircraft [19].

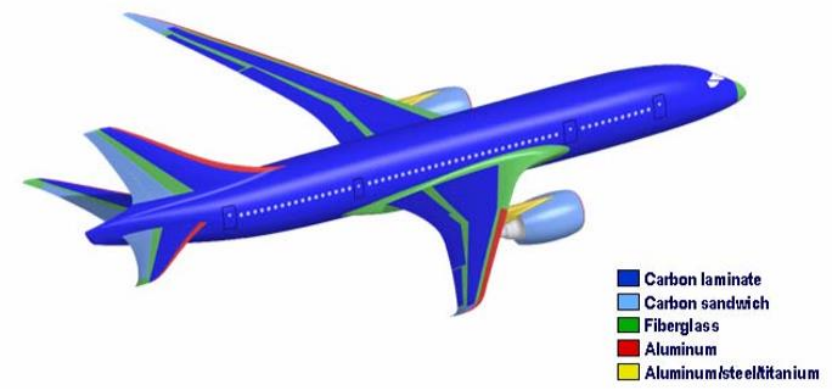

Figure 7: Composite materials in the Boeing 787 [19].

2.2.2 Failure modes in FRP adherends

It can be referred that a failure occurs when a structural element does not perform in a satisfactory way anymore, so the practical definition of failure can vary from application to application.

In the case of composite materials, such as FRP, generally the internal material failure starts much before any macroscopic change can be observed. These internal failures can occur in different forms, separately or combined, such as breaking of the fibbers, separation of fibres from the matrix (debonding or matrix failure) and separation of the laminas in a laminated composite (delamination), as shown in Figure 8 [20].

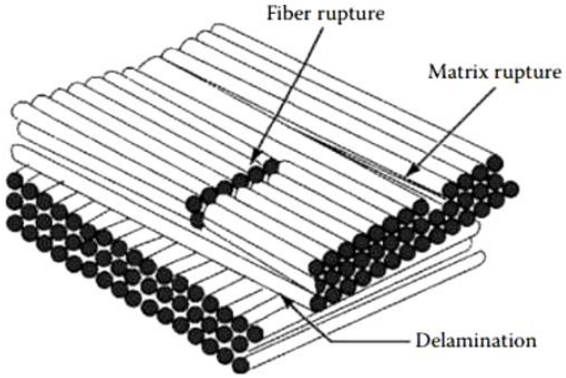

Figure 8: Failure modes in FRP adherends [21].

2.2.3 Failure modes in adhesively bonded FRP adherends

Regarding adhesively bonded FRP adherends, there are seven typical modes of failure that, similarly to the failures related with adhesive bonding, are influenced by parameters such as the specimen geometry, the quality of the bond at each interface and the loading. The observed modes are adhesive failure, cohesive failure, thin-layer cohesive failure, fibre-tear failure, light-fibre-tear failure, stock-break failure, or mixed failure, shown schematically in the Figure 9.

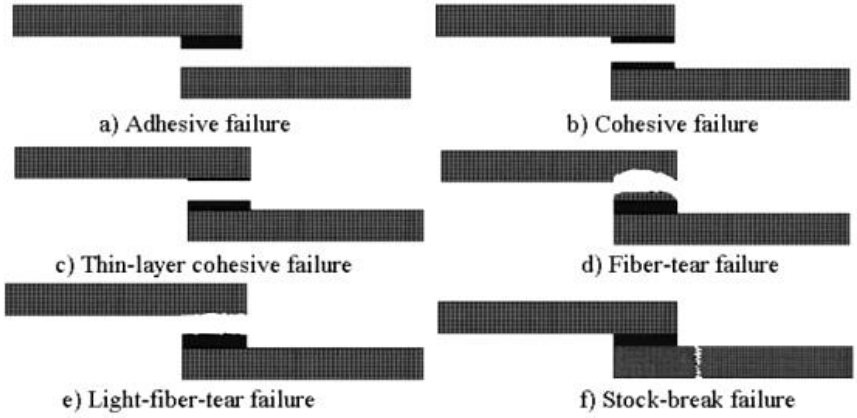

Figure 9: Failure modes in adhesively bonded FRP adherends [22].

In the case of FRP composite substrates, there is an additional concern. The peel stresses, that have peak values at the ends of the overlap, can cause an interlaminar failure by delamination near the points of the singularities due to the low transverse tensile strength in the through-thickness direction (Figure 10) [9].

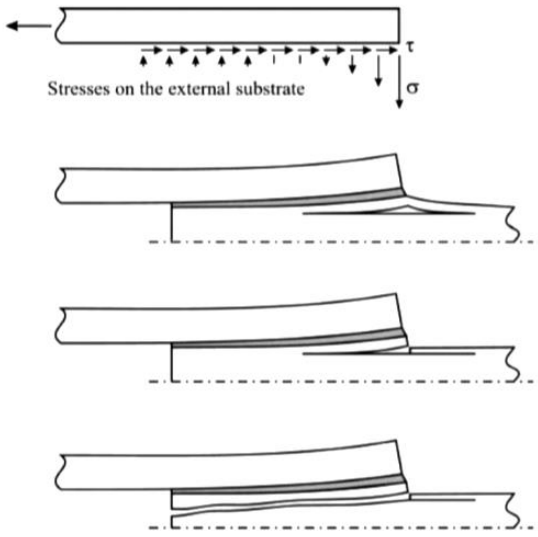

Figure 10: Peel stress failure in adhesively bonded FRP adherends. Adapted from [23].

To address the problem of the low transverse tensile strength of an FRP adherend, several techniques have been suggested, such as adherend and adhesive shaping (Figure 11) and the utilization of z-pins (Figure 12).

Because the maximum values of stresses in adhesive bonds are at the edges of the adhesive layers, one way of increasing the joint strength is by modifying the geometry of the joint in these regions. These modifications significantly increase the strength of the joint particularly when using a combination of adherend tapering and a fillet of adhesive at the

edge of the overlap. As the concentration in transverse tensile stress in the FRP is reduced, premature interlaminar failure can be avoided and the failure occurs in the adhesive [24].

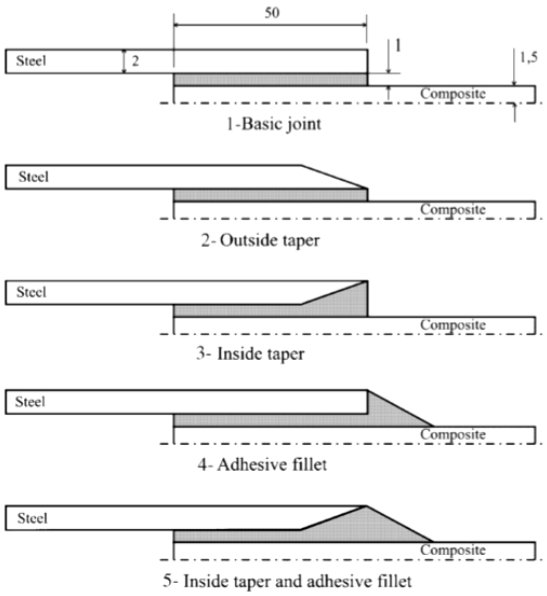

Figure 11: Designs of DLJs (double lap joints) - shaping of the adherends and the adhesive [10].

The z-pin technique consists of using thin metal rods that lock the laminate plies together using friction and adhesion. This technique was first used in laminates in 1970, starting with manual application of the pins and later being developed into an automated process. The most common materials for these pins are titanium alloys, steel or fibrous carbon composite – all high strength and stiffness materials – with pin diameters ranging from 0.2 to 1.0 mm. The overall pin content usually ranges from 0.5 to 4.0 vol% and its usage increases the delamination resistance, impact damage tolerance and joint strength of prepreg laminates [25].

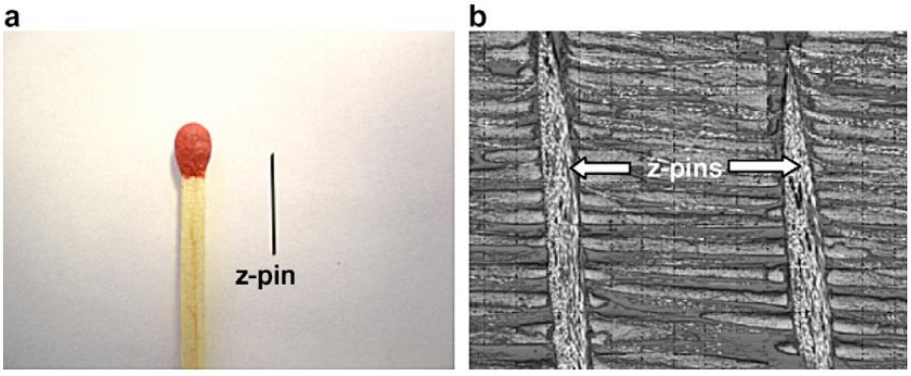

Figure 12: Introduction of z-pins to reinforce composite materials. a) typical size of a z-pin b) z-pins in a prepreg composite [25].

There are still other techniques that have been used to reinforce the through-thickness direction of composites, and thus improving their resistance to delamination, such as 3D weaving or stitching [26]. The stitching process, a technique that is unique for composite materials, involves basically sewing high tensile strength yarn (glass fibre, carbon fibre or Kevlar), through an uncured prepreg laminate or dry fabric plies using industrial sewing machines. The use of polyester thread is also possible, but Kevlar is the most popular yarn material due to its high strength and flexibility.

In 3D weaving, warp yarns are fed into the weaving loom through a lifting mechanism, which selects and lifts the required yarns and creates a space (the shed) into which the weft yarns are inserted at right angles to the warp. The sequence in which the warp yarns are lifted controls the interlinking of the warp and weft yarns, and thus the pattern is created in the fabric. This technique can produce complex near-net-shape structures, with relative low cost, and 3D woven composites have higher delamination resistance, ballistic damage resistance, impact damage tolerance, higher tensile strain-to-failure values and higher interlaminar fracture toughness properties [27]. An example of a 3D woven structure is shown in Figure 13.

Figure 13: Example of a 3D woven structure [27].

2.3 Fibre metal laminates

2.3.1 Introduction

One of the most important factors to consider in designing an aircraft transport is the weight of the overall structure. In order to achieve low weight structures the adoption of high specific strength materials is fundamental [28]. However, in the design of a modern aircraft fuselage structure there are additional problems that require the use of more advanced techniques and improved materials, being one of the most relevant considerations the possibility of observation of skin cracks resulting from fatigue.

To face this, it is necessary to select materials and stress levels, so that these cracks can be identified in an inspection interval prior to their reaching a critical crack length, meaning that a crack which may initiate after an inspection should not propagate to a critical length, before the next inspection, during which the crack should be detectable.

Damage and failure of aircraft structures have been documented and investigated over the years, as is example the failure reports of 71 Boeing 747. By analysing these reports, it was found that out of the total 688 repairs, 90 (13%) were caused by impact of foreign bodies, 202 (29.4%) were cause by corrosion problems and 396 (57.6%) were cause by fatigue cracks, pointing out the importance that fatigue cracks have on aircraft service life [29].

To summarize, crack growth behaviour is a decisive factor and the approach should be to develop new aircraft materials with better fatigue resistance and, preferably, with higher specific strength and lower density.

2.3.2 Development and concept

As seen, in the search for an optimal design, studies have been made during the last decades in order to replace the widely used in the past aluminium alloys, for a material that combines high strength, low density, high elasticity modulus, improved toughness, corrosion resistance and fatigue properties. Fibre reinforced plastics mostly appear as an ideal material for this purpose, although their low fracture toughness is cause for concern [3]. The low fracture toughness is the factor behind the idea of using two materials to create a hybrid composite material able to avoid most of the disadvantages faced when using aluminium alloys or fibre reinforced plastics alone [29].

In 1978, at the Faculty of Aerospace Engineering at Delft University of Technology, while studying methods to increase fatigue performance in aluminium alloys, it was observed

an improvement in fatigue properties by introducing a high strength aramid fibre into the adhesive layers of a laminate sheet.

These studies introduced ARALL (Aramid Reinforced Aluminium Laminates), the first fibre metal laminate (FML), that consists in alternating thin aluminium alloy layers with uniaxial or biaxial aramid fibre prepreg. It was patented in 1984 and industrially manufactured by the Alcoa Company [28]. Nowadays, there are several standards for ARALL materials, each one related with the different aluminium alloys that can be used for the laminate.

The resistance to crack growth in FMLs is achieved due to bridging of fatigue cracks, in other words, when a crack occurs in the aluminium layers, some limited delamination is observed at the interface metal-fibres and, the stresses are redistributed from the metal to the unbroken fibres. This phenomenon of crack bridging, provided by the strength of the fibres that are located between the aluminium layers, limits crack opening and reduces crack growth in the metal layers (Figure 14) [30].

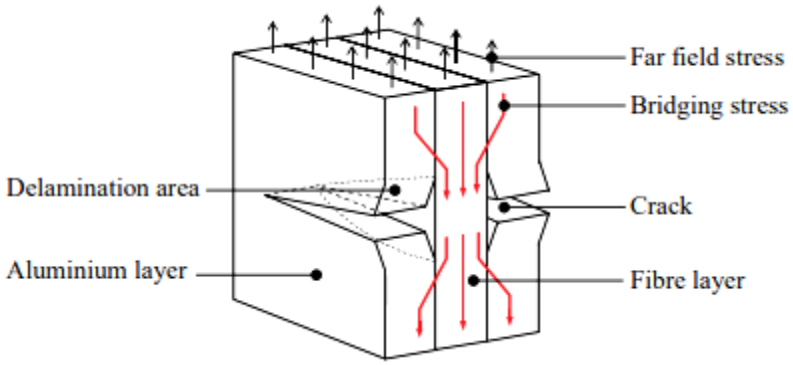

Figure 14: Crack bridging of the fibres in a FML [31].

The successor of ARALL laminates was GLARE, developed in 1990, that uses high strength glass fibre instead of aramid fibres. GLARE is still widely used in the aerospace industry, being applied, as an example, in the main fuselage skin and leading edges of the Airbus A380 [32].

With later developments of this technology, other types of laminate materials were developed, CARALL, that differ from ARALL in the utilization of carbon fibres instead of aramid fibres, resulting in a much stiffer material with low crack growth rates, and BARALL, that uses basalt fibres as the reinforcement.

Regarding CARALL, its performance is still limited by some unsolved problems associated with this material. Firstly, the utilization of carbon fibres, in combination with aluminium, often results in a problem of galvanic corrosion due to different electrochemical potential of these two materials. A related, but distinct issue is caused by the thermal

expansion coefficients of aluminium and carbon, as these differences induce high thermal residual stresses to the final component [33]. Due to these problems, and to the limitations regarding operation temperature and damage tolerance of aluminium based FML, researchers have been developing titanium based FML, also known as Hybrid Titanium Composite Laminates (HTCL) and studies indicate that these kind of laminates can provide a stronger, stiffer and more damage-tolerant alternative for high temperature use [34, 35].

In summary, the FMLs combine the good properties of either metal and fibre-reinforced composites, presenting better mechanical properties, when compared to the conventional lamina, using only of fibre-reinforced lamina, or to the monolithic aluminium alloys, as can be seen by analysing the study shown in Figure 15. The main disadvantage of this material is, however its long processing cycle, necessary to cure the matrix of the composite plies, increasing manufacturing time and overall costs of FMLs [36].

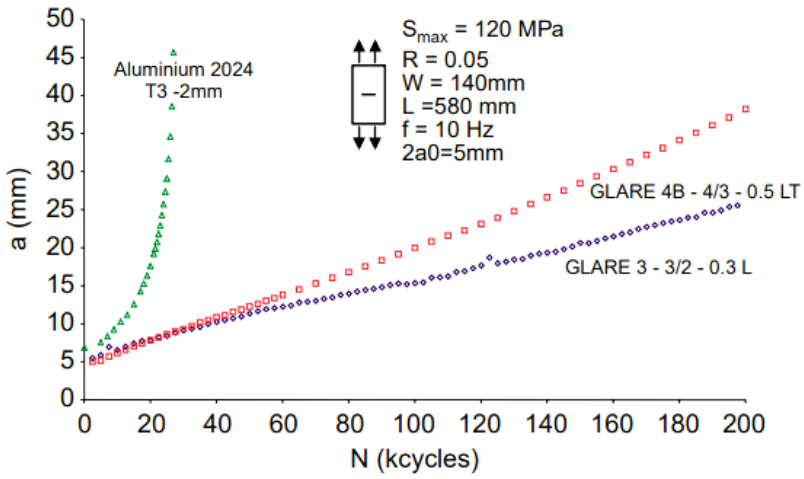

Figure 15: Crack growth curves of aluminium 2024-T3, Glare 3-3/2-0.3 L and Glare 4B-4/3-0.5 LT for constant amplitude fatigue loading [31].

2.3.3 Previous work performed in ADFEUP group

ADFEUP is an investigation group based in the Faculty of Engineering of the University of Porto that works in the field of adhesive technology. Regarding FMLs there are some previous studies done in the group that are important to mention due to their importance as sequence for this master's dissertation.

In 2016, Palmares [37], performed a research work in a master's dissertation regarding FMLs, using aluminium as the metal. In this work, different lay-up configurations were studied for CFRP-Aluminium FMLs to assess which one could be more interesting in terms of

failure load and failure mode. The optimal configuration was found to be the one presented in Figure 16 and the failure mode observed was a mixed failure (adhesive and cohesive failure in the adhesive).

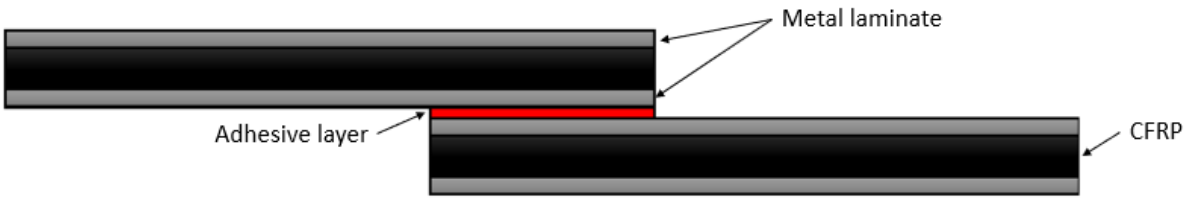

Figure 16: Optimal lay-up configuration found in Palmares and Martins works. Adapted. [38].

In 2018, Martins [38], also studied several FMLs configurations during a master's dissertation using titanium as the base metallic material, because of its previously referred, advantages in terms of proximity of values of coefficient of thermal expansion with the values presented by the CFRP, when compared with aluminium. The most efficient and available (in terms of lab conditions) surface treatment for CFRP-Titanium FMLs was studied, leading to the conclusion that, for this type of laminates, the surface treatment of the metal should be grit-blasting. Several lay-up configurations of the FML were also studied, reaching a conclusion similar to that of Palmares [37], in terms of optimal layup configuration that should be used.

In Martins' [38] case, it is important to refer that, in the optimal lay-up configuration, the failure mode observed was, as stated by the author, a "progressive failure", where an adhesion failure between the metal and the CFRP can be observed, with some delamination, followed by a plastic deformation of the titanium, as illustrated in Figures 17 and 18.

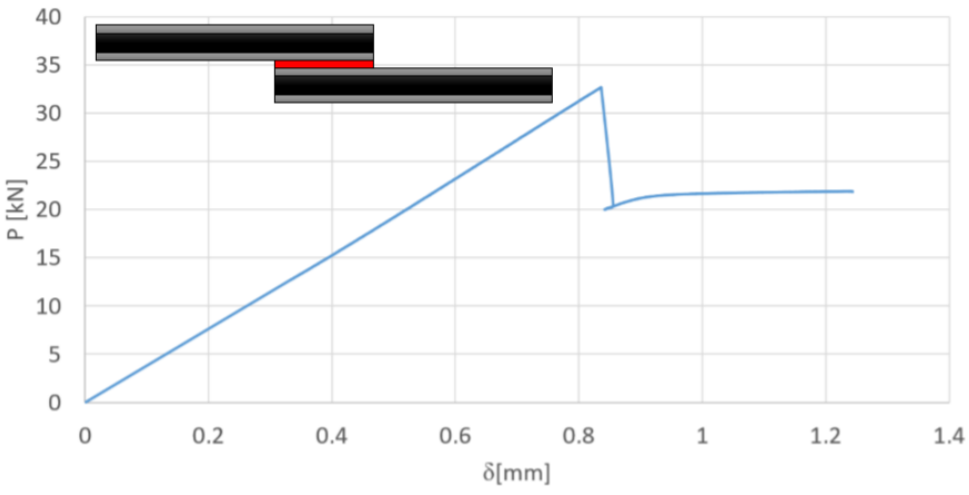

Figure 17: Load vs displacement of a Ti-CFRP-Ti SLJ with a 50 mm overlap [38].

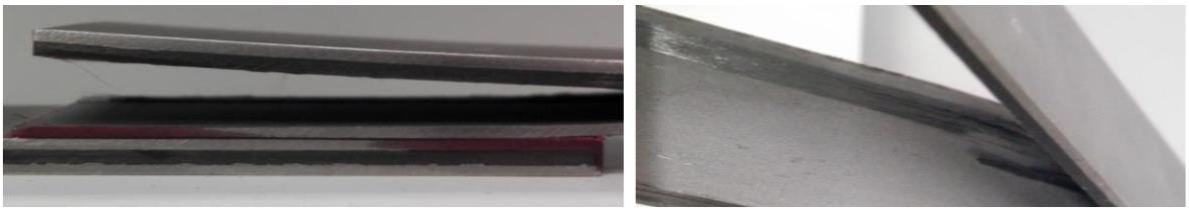

Figure 18: Failure surface of a 50 mm overlap Ti-CFRP-Ti SLJ [38].

Both Palmares [37] and Martins [38] used the same adhesive used in this thesis and manufactured all their FMLs following the same base manufacture process, which consisted in manually stacking all the CFRP layers, heat curing the CFRP laminates, followed by the application of metal laminates, adhesive layers and, finally, performing an additional heat cycle to cure the adhesive.

2.4 Impact loads

Ensuring adequate behaviour under impact loading conditions of vehicle strictures is crucial to ensure passenger safety and meet standing legal requirements, which as led to extensive research on how to improve impact performance.

Specifically, impact damage of aircraft structures can be originated by several sources, as collisions between service vehicles or cargo with the structure, maintenance damage (dropped tools), runway debris, bird strikes, ice from propellers striking the fuselage and engine debris. Additionally, in military applications, it is even important to consider the damage caused by ballistic impacts. For commercial aircraft, it is of the utmost importance to ensure a certain degree of damage resistance and inspectability, of the results of this kind of impacts [39].

In terms of testing, static tests are often done to simulate collisions of high masses at very low velocities (example of collisions at low velocities of service trucks and cargo containers); low velocity tests (up to 10 $m.s^{-1}$), that simulate damages from maintenance mishaps (dropped tools); and tests with high impact velocities (up to 100 $m.s^{-1}$), at velocities that closely match those found during collisions with runway debris and hail strikes [40].

Regarding the adhesives, it is known that due to their polymeric nature, their properties are in general strain rate dependent. Harris and Adams [41], tested several substrates and adhesives and concluded that energy absorption is not directly dependent on the adhesive but is derived instead from the plastic deformation of the adherend.

As a ductile and strong adhesive was being used, the plastic deformation of the substrate is what determined the failure load and the energy absorbed. High strength substrates produced high failure loads but very low absorbed energy, while the opposite occurred for more ductile substrates [42].

Figure 19 shows that, for SLJs with the same adherend (soft aluminium was the material used in the study), ductile adhesives perform better, due to the better stress distribution along the overlap leading to failure in the substrate.

Figure 20 allows the conclusion that brittle adhesives break very easily and are unable to allow the metal substrates to deform plastically, leading to very small absorbed energy. In contrast, ductile adhesives can hold the joint together during the impact and enable large energy absorption, especially when used in conjunction with, low strength, ductile substrates.

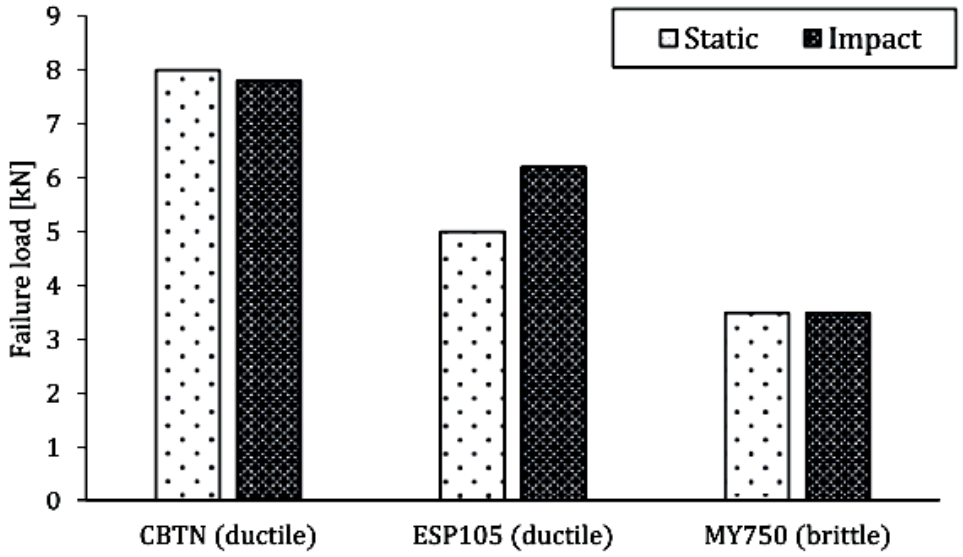

Figure 19: Effect of the strain rate in failure load of joints with soft aluminium substrates and three different adhesives. Adapted from Harris and Adams [41].

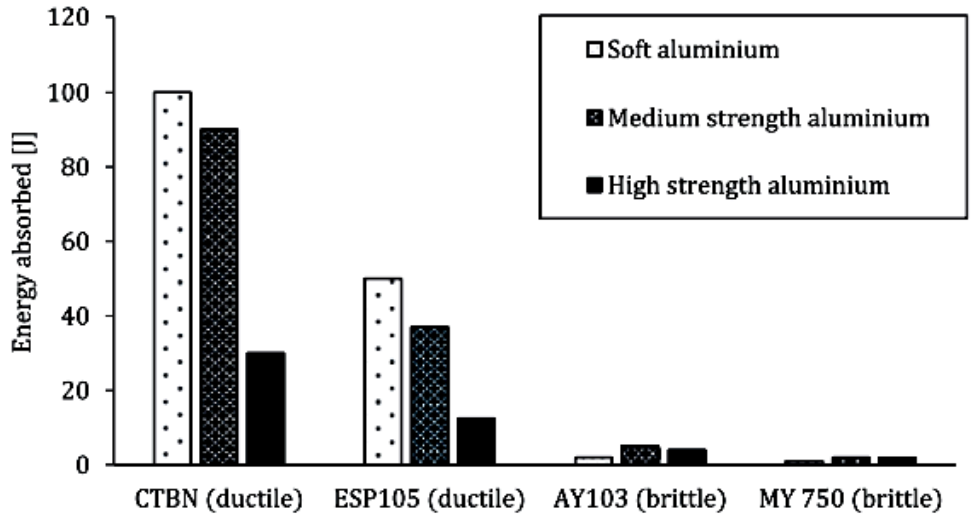

Figure 20: Effect of the strain rate in absorbed energy for three types of substrates and two types of adhesives. Adapted from Harris and Adams [41].

FMLs perform well under impact loads as they effectively combine the advantages of metal and composites to amplify their impact damage resistance. In metallic structures, impact is not a severe threat, due to their ductility, metals can absorb a large amount of impact energy in the elastic region up to yield, and the material may develop large strains before failure. In contrast, most composite materials are brittle in nature and the absorption of impact energy occurs only in elastic region before failure occurs.

There are some studies on the impact damage resistance of FMLs and other aircraft structural materials, as exemplified in a study by Vlot [40], where a low velocity drop weight impact tester was used to calculate the impact energy at which the first fibre failure occurs called minimum cracking energy.

In this study, the static, low velocity and high velocity tests were performed with a hemispherical steel tip indentor, with 7.5 mm of radius. The static tests were performed with a loading rate of 1 $mm.min^{-1}$. The low velocity impact tests were performed with a drop weight impact tester, with an impactor mass of 575 g. The maximum drop height was 12 m, with a corresponding maximum velocity in the order of 10 $m.s^{-1}$. The high velocity impact tests were performed with a gas gun - after burning through the membrane of the gas gun, the expanding air accelerated a projectile with a mass of 23.3 g up to a maximum velocity of 100 $m.s^{-1}$.

By analysing the results of the referred study, presented in the Figure 21, it can be concluded that, for all loading conditions, GLARE 3, – a FML that consists of 0.3 mm Al 2024-T3 layers and intermediate layers of glass/epoxy prepreg oriented in two directions - appears to show superior performance when compared to other materials and, still for

GLARE 3, the minimum cracking energy increases with the rate of loading due to the strain rate dependent behaviour of the glass fibre. It was also found that a clear residual dent was present on the surface of the impacted FML, whereas impact was often difficult to detect in the composite materials [43].

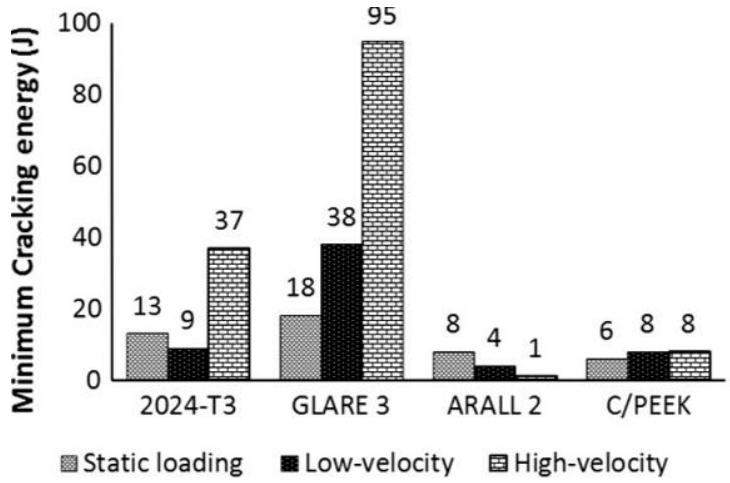

Figure 21: A comparison of minimum cracking energy of aircraft structure materials [40].

However, there are several parameters that are still being, or yet to be, studied related with the response of FMLs to impact, such as the type of metal, the fibre, matrix, stacking sequence, metal volume fraction, impactor geometry, target shape, post-stretch percentage, and this interdependency of parameters turns the optimization of FMLs a difficult job.

Other particular aspect of the aircraft industry is the extreme service temperatures that are required. Many applications range approximately from -20ºC to 80ºC. Regarding temperature and other environmental effects (like moisture) there are few published studies on the structural response of FMLs subjected to conditions of impact [44].

2.5 Strength prediction

As seen in the previous subsections, adhesive bonding technology is gaining more usability due to their improved mechanical performance and the prediction of joint strength is a crucial part of the approach of adhesive bonding utilization. To allow this prediction is necessary to have the stress distribution and a proper failure criterion [45].

Throughout the years of investigating adhesive joints many models have been suggested, all of them with some pros and limitations in terms of condition of applicability.

2.5.1 Analytical solutions

2.5.1.1 Simple linear elastic analysis

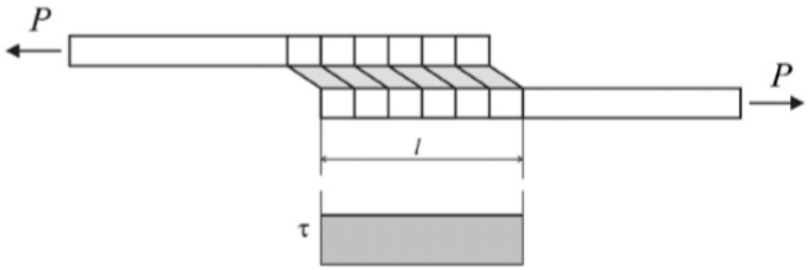

Figure 22: Deformations and stresses in SLJ according to the simple linear elastic analysis [45].

The simple linear elastic analysis is the most basic analysis for a SLJ, in which the adhesive is considered to deform only in shear, the adherends are considered rigid and the shear stress (constant over the overlap) is given by

$$\tau = \frac{P}{bl}$$

Where P is the applied load, b is the joint width and l is the overlap length. This analysis does not represent realistically the distribution of the shear stress along the adhesive layer but, is widely used as the basis for quoting the shear strength in many test situations. The schematic view of this analysis is shown in Figure 22.

2.5.1.2 Volkersen's analysis

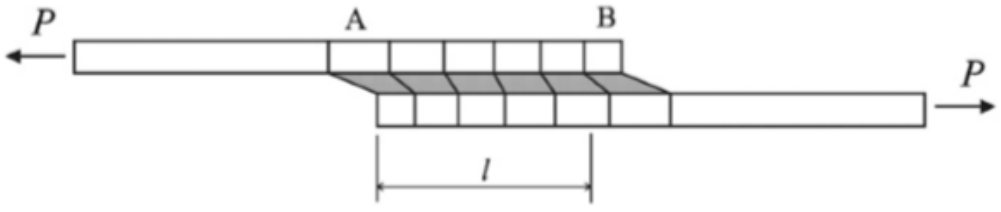

Figure 23: Deformations of SLJ according to Volkersen [45].

The Volkersen's analysis [46], considers the adhesive as a linear elastic solid, that only deforms in shear, and the adherends not rigid, but deformable in tension (Figure 23). Both adherends bear the full load, P, just before the joint overlap, being A, the point of maximum value of tensile stress, and transmitting the load gradually to the other adherend

through the adhesive layer, making the point B a point of zero tensile stress, so the strain will also progressively reduce from point A to point B. This phenomenon is valid for both adherends and combined with the continuity of the adhesive/adherend interface cause a non-uniform shear strain (and stress) distribution in the adhesive.

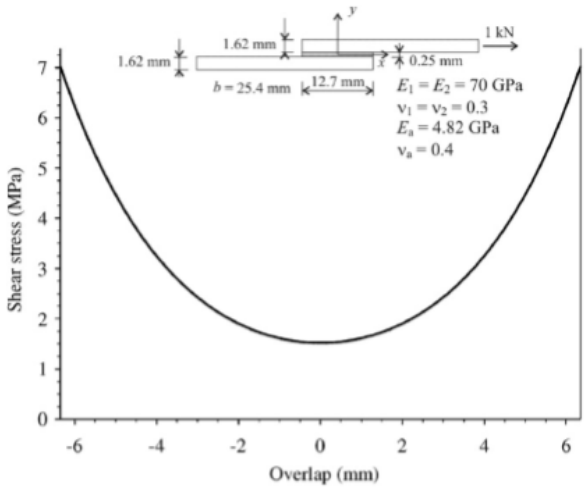

Figure 24: Adhesive shear stress distribution according to Volkersen's [46].

As seen in the shear stress distribution plot, Figure 24, the shear stress presents its maximum values at the ends of the overlap decreasing towards the centre.

2.5.1.3 Goland and Reissners's analysis

The Volkersen's analysis presented previously, is incomplete because it does not consider the bending effect due to eccentric loading of the SLJ, being its application more suitable for designs where this is not an issue, as in the case of the double lap joint.

This effect of an eccentric path applied to the single lap jap, was first considered in 1944, by Goland and Reissner [47], and it causes a bending moment and a transverse force applied to the joint ends, as shown in Figure 25. The joint will now rotate to align the direction of the tensile forces, reducing the bending moment and creating a nonlinear geometric problem where the effects of large deflections of the adherends must be considered.

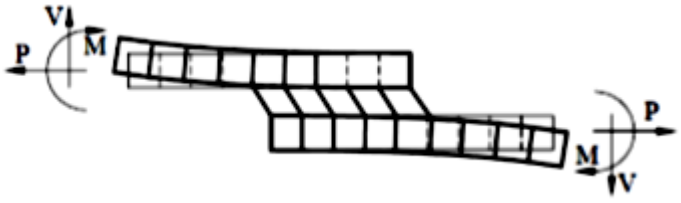

Figure 25: Goland and Reissner's model [47].

The shear stress distribution is similar to the one found using Volkersen's analysis, considering the same joint design – SLJ – however, the Goland and Reissner's analysis predicts higher values of shear stress values at the ends of the overlap, Figure 26, explained by the existence of peel stresses that cause additional shear stresses.

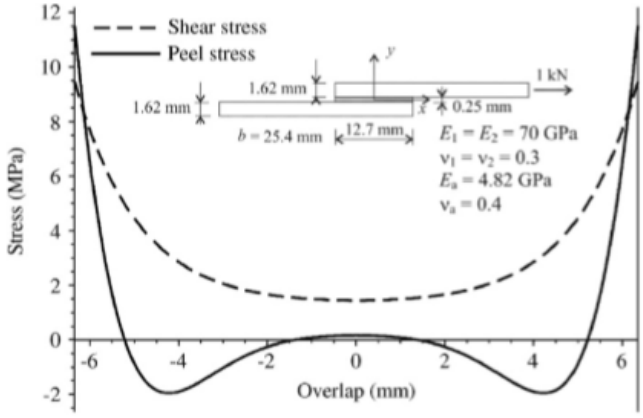

Figure 26: Shear and peel stresses distribution along the overlap according to Goland and Reissner's [45].

Both Volkersen's and Goland and Reissner's analysis establish the basis for the stress analysis in adhesive bonded joints, however, they do have some features that are considered incorrect or overlooked, such as the violation of the stress-free condition at the ends of the overlap, and they both don't take into account the plastic deformation of the adherends and the yielding of the adhesive, being better suited for brittle adhesives.

2.5.1.4 Hart-Smith's solution

The previous analyses, Volkersen's and Goland and Reissner's, don't consider the plastic behaviour of the adhesive. Hart-Smith's work considered this factor for both SLJ [48] and DLJ [49].

Hart-Smith's solutions modelled the adhesive using an elastic–plastic shear stress model, in which ultimate shear stress and strain are equal to the ultimate shear stress and strain of the adhesive, the two curves having the same strain energy, and it used maximum shear strain as the failure criterion.

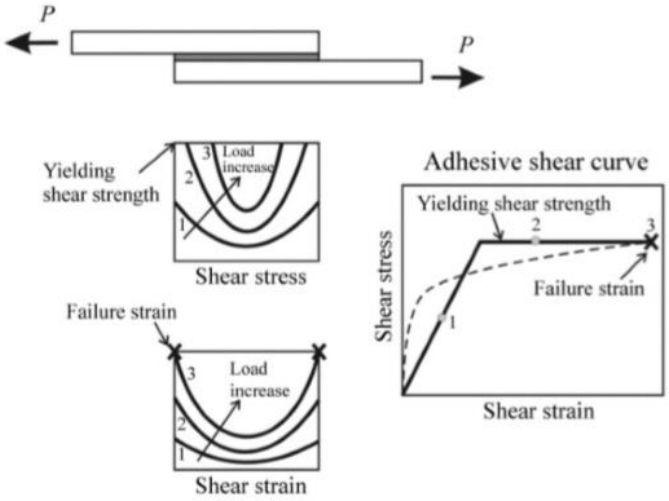

Figure 27: Hart-Smith's solution [49].

With his work, Hart-Smith showed that if the adhesive plasticity is considered, the joint strength prediction is higher than for an elastic analysis – a ductile adhesive will work in plasticity and can stand additional loading until the ultimate strain is reached [9]. Schematically, Hart Smith's solution is presented in Figure 27.

2.5.1.5 Global yielding

Other methodology was purposed by Adams [5], and considers the effect of overlap length on the strength of the adhesive bond for ductile adherends and adhesives.

For ductile adhesive, with more than 20% shear strain to failure, the joint strength is considered approximately proportional to the overlap, an increase in the overlap will increase the joint strength, and in this case the failure criterion is the global yielding of the adhesive, which is ruled by the equation

$$P_{GY} = \tau_y . b . l$$

Where P_{GY} is the failure load of the adhesive due to global yielding, τ_y is the yield strength of the adhesive, b is the joint width and l is the overlap length.

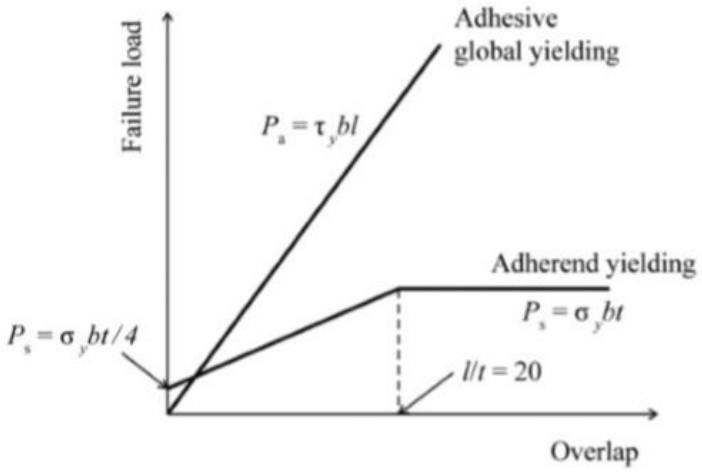

Figure 28: Global yielding criterion for SLJs based on adherend yielding [6].

For adherends that deform plastically, the failure criteria considered is the adherend yielding, the following equations are applied, depending on the ratio overlap length over adherend thickness

$$\begin{cases} P_y = \sigma_y . b . \frac{t}{4} \quad for \ \frac{l}{t} < 20 \\ P_y = \sigma_y . b . t \quad for \ \frac{l}{t} \geq 20 \end{cases}$$

Where P_y is the maximum load which creates adherend yielding, σ_y is the yield strength of the adherend, b is the joint width, l is the overlap length and t is the adherend thickness.

This criterion, Figure 28, has been applied with successful results but, in cases where the adhesive and the adherends are brittle, the model is not applicable and the finite element method can be used [6].

2.5.2 Numerical approach

2.5.2.1 Finite element method

While analytical models are able to describe the behaviour of a few well defined joint geometries and loading, more powerful models are sometimes necessary to describe the mechanical behaviour of complex adhesive joint geometries and loadings. The finite element model (FEM), is a very useful tool for this purpose, being able of solving differential equations to deal, in an easier way, with aspects such as the plasticity of the adhesives and adherends or the rotation of the joint. It is important to refer that a numerical model that is suited for every problem does not exist and so it is important to evaluate the limitations of each approach to each particular case [50]. This method is based on the concept of dividing a complicated object into smaller pieces to simplify the problem.

To predict the joint strength using the finite element method it is necessary to determine the stress distribution and select a suitable failure criterion. Several approaches can be applied for this purpose, taking into account continuum mechanics, fracture mechanics or damage mechanics (a combination of continuum and fracture mechanics). These will be introduced and discussed next.

2.5.2.2 Continuum mechanics

The continuum mechanics approach uses as the failure criterion the maximum values of stress, strain or strain energy predicted by the finite element analysis and then, compares them with the allowable values of the specific material in study, assuming the bond between adhesive and adherends is perfect, or that the structure and its materials are a continuum [51].

Due to the existence of singularity points, when using the finite element analysis, the maximum strain and stress values will inevitably be found in those points and the value will be highly dependent on the mesh size used.

In fact, due to the manufacturing process of joints, these corners are rounded and not sharp, and as showed by Adam and Harris [52], this rounding, Figure 29, removes the singularities and turns the value of the stress dependent on the value of the radius of the corner, facilitating the application of the, at first not applicable, maximum strain or stress criterion.

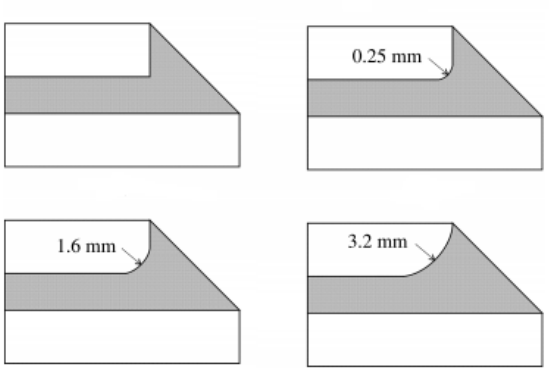

Figure 29: Different degrees of rounding of the corners [51].

2.5.2.3 Fracture mechanics

The main assumption of continuum mechanics is that the structure and its material are continuous and does not consider defects or materials with re-entrant corners. The most relevant defects in structures are cracks and fracture mechanics approach has been developed to deal with this particular case of singularities where stresses and local strains are greatly increased, serving often as initiation points for structural failures [53].

The failure is based on relation between the material resistance to crack propagation and the energy required to separate adjoining elements, assuming the material to be linear elastic and the pre-existence of a crack.

2.5.2.4 Cohesive zone model

Cohesive zone models (CZMs) were developed by combining the continuum approach to model damage initiation and the fracture mechanics approach to deal with crack propagation. In CZMs, fracture is viewed as a gradual phenomenon where separation takes place across an extended crack “tip”, or so called cohesive zone, and is resisted by cohesive traction [54, 55].

CZMs have been studied and tested to simulate crack behaviour in cohesive, interfacial problems (zero thickness interface), and composite delamination situations and can be incorporated in finite element models to study the fracture behaviour of some materials, such as adhesively bonded joints.

A CZM simulates the macroscopic damage along its path by the specification of a traction-separation response between initially coincident nodes on either side of the pre-existing crack. Upon unloading, the nodes start to separate and then finally completely de-

bond [56]. The simulation consists on the establishment of traction–separation laws, designated CZM laws, to model interfaces or finite regions and observe the damage growth. No initial crack is needed, and damage propagation takes place without user intervention. However, it is still necessary to know the critical regions where damage is more likely to occur so that the cohesive elements can be placed in those regions [57].

In the majority of CZM laws, the traction–separation relations represent the same behaviour, Figure 30, – when load is applied and when the interfacial separation increases, the traction forces across the interface reach a maximum, then decrease and eventually disappear allowing the complete decohesion [58]. Its application requires the values of energy release rate in tension, and in shear, and respective critical values or toughness. Additionally, the cohesive strengths in tension are other required parameters and pertain to damage initiation in the CZM laws [59].

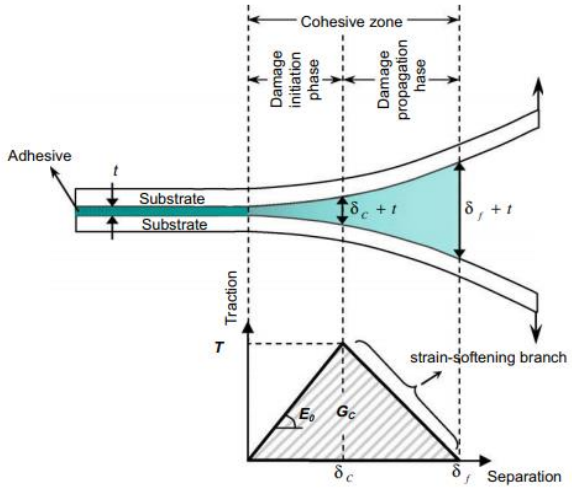

Figure 30: Schematic representation of the damage process zone and corresponding bi-linear traction–separation law in an adhesively bonded joint [60].

Two of the most common cohesive laws used in bonded joints simulation are the triangular and the trapezoidal law, shown in Figure 31. The triangular cohesive law is the most used due to its simplicity, being well suited for brittle or moderately ductile adhesives, and the trapezoidal law, is more suited for ductile adhesives. There are many other CZM laws such as linear-parabolic, polynomial, or exponential cohesive laws.

The predictions obtained by a CZM are generally accurate, when the CZM law is chosen accordingly to match the behaviour of the material being studied and, by using them in combination with FEM, extensive experimentation for design validation can be reduced, lowering the design cost and overall time consumption.

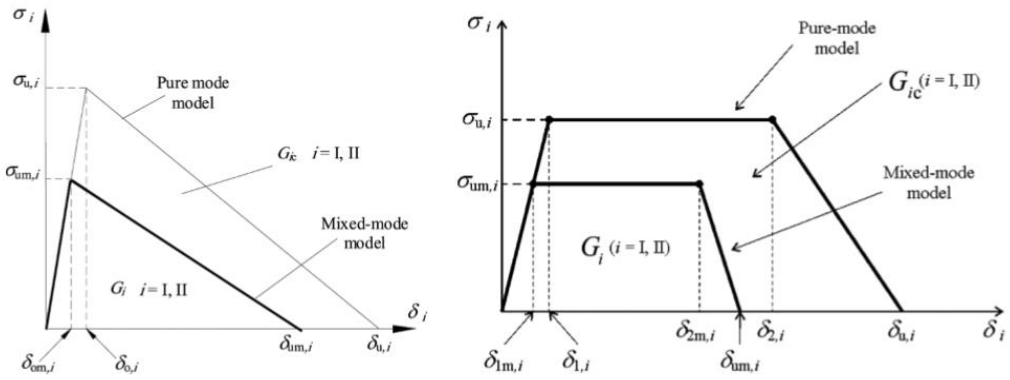

Figure 31: The triangular and trapezoidal cohesive laws for pure and mixed-mode [54].

3 Experimental details

3.1 Adhesive

The adhesive used in this study was a modified epoxy structural adhesive in film form. The commercial reference of the adhesive used is AF 163-2K and was supplied by 3M Scotch-Weld (Maplewood, Minnesota, USA) [61]. Several manufactures in the aeronautical and aerospace sectors use this structural ductile adhesive.

The technical datasheet provided by 3M contains several parameters that were ensured during the experimental procedures. One of these parameters is the proper cure cycle of AF 163-2K, that can be changed according to the temperature ranges desired, a highly relevant aspect to be considered when the cure cycles of adhesive and CFRP are combined.

In order to enable the application of a numerical simulation approach to predict the behaviour of the adhesive being studied it is necessary to determine its mechanical properties. These properties for AF 1632-2K were determined in a previous master's thesis realized by Palmares [37] in his work within the ADFEUP group. Palmares [37] determined the fracture energy of the adhesive in pure mode I and mode II, performing double cantilever beam (DCB) and end notched flexure (ENF) tests respectively, and performed the bulk tensile test to determine the adhesive's stiffness and tensile strength, and the thick adherend shear test (TAST) to identify its shear strength. The results for the values of the adhesive properties obtained are shown in Table 2. These values allow the definition of the adhesive's cohesive law necessary to implement the numerical models in *Abaqus*®.

Table 2: AF 163-2K mechanical properties [37]

Tensile strength (MPa)	46.93 ± 0.63
Young's Modulus (MPa)	1521.87 ± 118.29
Shear strength (MPa)	46.86 ± 2.57
Shear Modulus (MPa)	563.67
G_{Ic} (N/mm)	4.05 ± 0.07
G_{IIc} (N/mm)	9.77 ± 0.21

3.2 Adherends

3.2.1 CFRP

The CFRP used was a unidirectional 0° carbon-epoxy composite, HS 160 T700, supplied in a prepreg roll by the company Composite Materials (Legnano, Italy). For the adherend's preparation, prepreg sheets of 300 by 300 mm were cut and manually stacked. Each CFRP layer had 0.15 mm of thickness, so the final thickness of CFRP depends on the number of layers that are stacked and on the configuration that is being studied. After the introduction of metal laminates, the specimens were cured in a hot plates press machine, to obtain the final hybrid laminate.

The work of Campilho [62] was used as a source for the mechanical properties of the CFRP, presented in Table 3.

Table 3: Orthotropic elastic properties for an unidirectional CFRP ply, x-axis [62]

E_x (MPa)	E_y (MPa)	E_z (MPa)	ν_{zy}	ν_{yz}	ν_{xz}	G_{xy} (MPa)	G_{yz} (MPa)	G_{xz} (MPa)
109000	8819	8819	0.342	0.342	0.380	4315	4315	3200

3.2.2 Titanium alloy

The titanium alloy used for the fibre metal laminates configurations where this material was used as the reinforcement, was the titanium Ti-6Al-4V alpha-beta (Grade 5), annealed, and was provided by Smiths Metal Centres Ltd (Biggleswade, UK) [63, 64]. This specific titanium alloy has been widely used in aerospace applications such as bolts, seat rails (in airframes) and fan blades (in engines) [65].

The alloy was supplied in sheets of 300 mm by 300 mm with 0.8 mm thickness. Only adherends with titanium laminates with the provided 0.8 mm thickness were manufactured, as thin was the thinner thickness supplied by the manufacturer. The mechanical properties of this titanium alloy are presented in Table 4.

Table 4: Mechanical properties of Ti-6Al-4V alpha-beta, annealed [64]

Young's Modulus (GPa)	**Yield Strength (MPa)**	**Poisson's ratio**	**Elongation (%)**	**Coefficient of thermal expansion ($\mu m/m.K^{-1}$)**
113.8	900	0.342	14	8.6

3.2.3 Aluminium alloy

The aluminium alloy that was used during this work was the 2024-T3 Alclad, with copper being the main alloying metal. This specific alloy has been extensively applied in aerospace applications, including in the manufacture of fibre metal laminates [3]. This material was supplied in sheets with the dimensions of 300 mm by 300 mm, 0.4 mm thick, and was provided by AMI Metals, Belgium. The mechanical properties of this alloy are presented in Table 5.

Table 5: Mechanical properties of Al-2024-T3 Alclad [66]

Young's Modulus (GPa)	**Yield Strength (MPa)**	**Poisson's ratio**	**Elongation (%)**	**Coefficient of thermal expansion ($\mu m/m.K^{-1}$)**
66	350	0.33	12	23.22

3.3 Specimens

3.3.1 Concept

As referred in the literature review section, in previous researches related to this work, the initial step in the specimen manufacturing process was always the manufacturing of the CFRP plates, followed by the addition of the laminates and manufacturing of the SLJ, with the utilization of two cure cycles, one to cure the CFRP and another to cure the adhesive layer.

However, it was also mentioned that one of the disadvantages of using fibre metal laminates is the long processing cycle needed in the manufacturing process to cure the CFRP and, after that, the adhesive layer.

A new approach suggested in this work is to combine the two cure cycles, for the CFRP and for the adhesive AF 163-2K, to reduce the necessary production cycle time.

To reinforce the basic CFRP substrate, in addition to the FML concept, the introduction of additional layers of film adhesive in the interfaces between the CFRP and the metal laminates of the FML was considered, to improve adhesion between CFRP and metal, preventing the occurrence of any adhesion failure.

Other approach suggested to reinforce the CFRP adherend, was by the introduction of additional film adhesive layers between laminas of the prepreg CFRP used in lay-up configurations studied without the usage of metal.

All the SLJ manufactured are approximately 3.2 mm thick, are 25 mm wide and have an overlap length of 50 mm. The dimensions of the SLJs are shown in Figure 32.

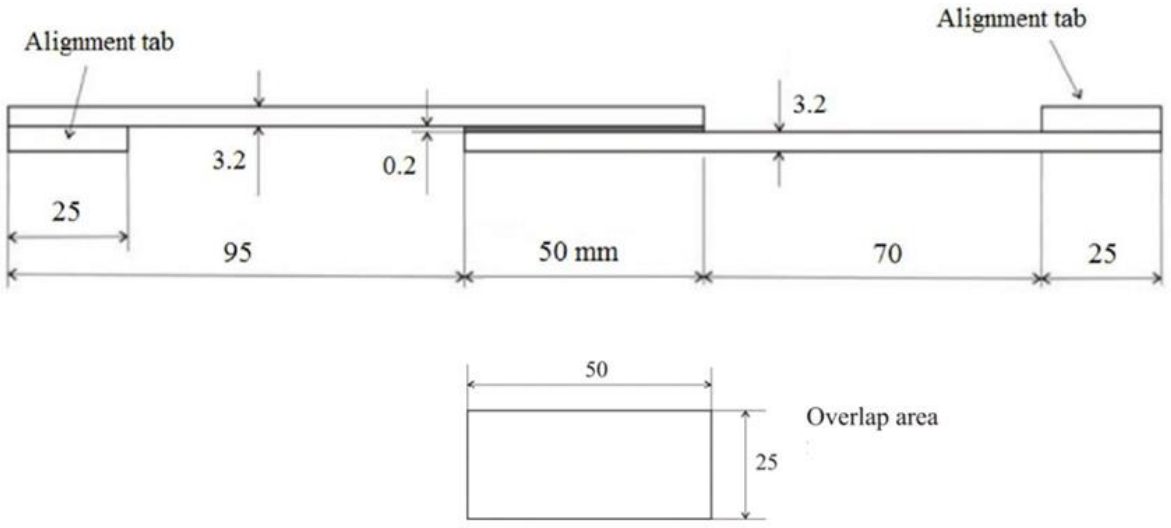

Figure 32: SLJs geometry schematization. Adapted from [37].

3.3.2 CFRP

The CFRP used was manufactured from several 300 mm by 300 mm sheets, cut from a unidirectional the prepreg roll. Each sheet had a 0.15 mm thickness thus it was needed to stack those sheets so that compact laminates with the intended thickness could be created.

The manufacturing process, related with the CFRP, is described below:

I. The prepreg roll is removed from the freezer and left to warm until it reaches room temperature (about 26°C);

II. While the prepreg is defrosting, the mould components, which were used to manufacture the laminates, are cleaned and degreased. This cleaning and degreasing is done using a sandpaper, in a first approach to remove the solid impurities, and then with an organic solvent, in this experimental work the solvent used was acetone. After this, it is crucial to apply a release agent to the mould components so that the plate's removal may be easier at the end of the cure cycle. Two coats of release agent are applied in each side of the components. The product used for this purpose was Loctite® Frekote 770-NC, provided by Henkel (Dusseldorf, Germany);

It is important to notice that, in this particular work, as the CFRP sheets are not going to be cured in their original 300 mm by 300 mm geometry it was necessary to manufacture a new mould to guarantee a good positioning and the dimensions of all the SLJs tested. The manufactured mould and its application scheme can be seen in the Figure 33.

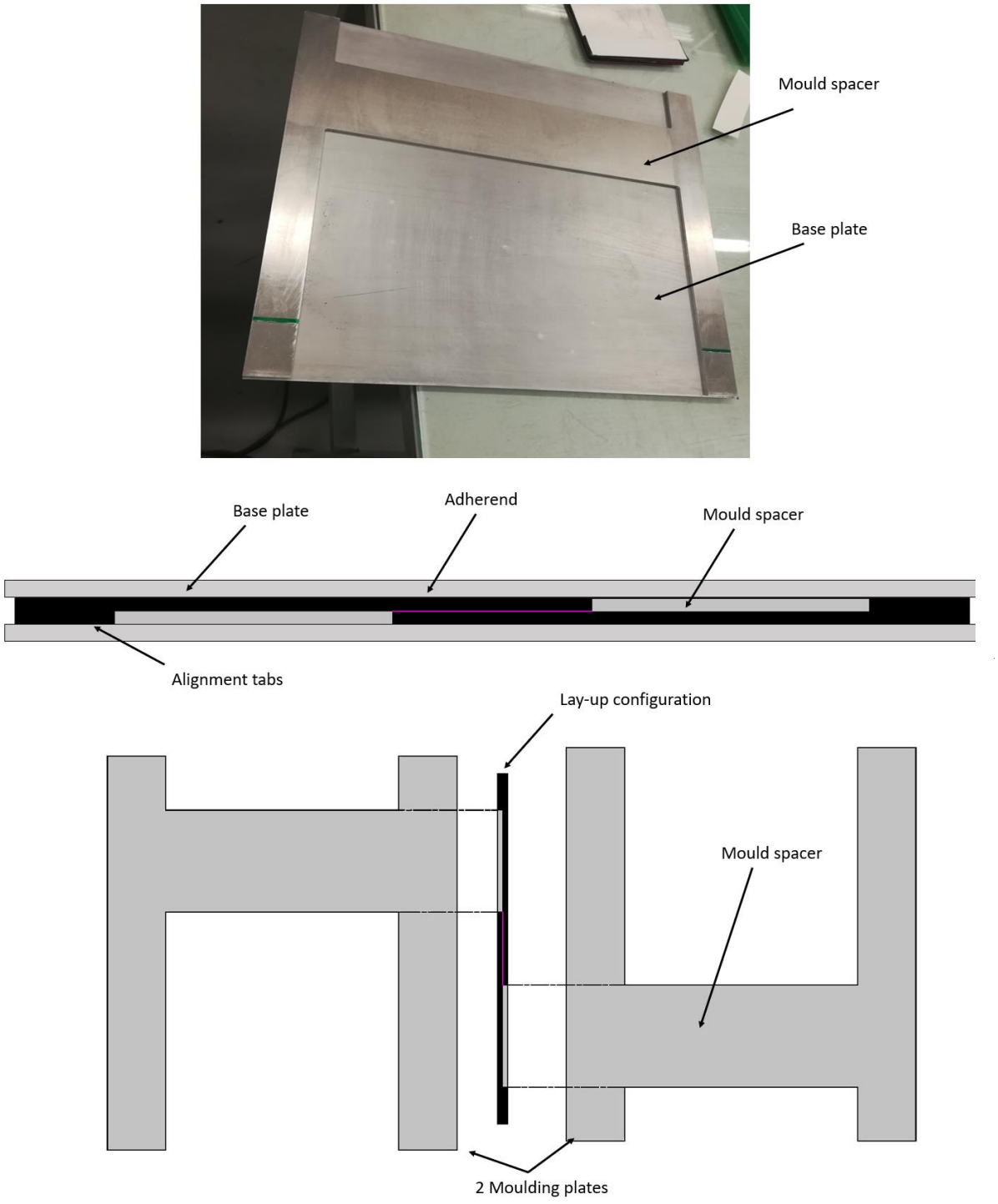

Figure 33: Manufactured curing mould.

III. When the prepreg reaches the room temperature, several 300 mm by 300 mm sheets are cut to use in different configurations and the roll is re-stored in the freezer.

3.3.2.1 Stacking process of CFRP

For this step a hand lay-up method was used, by stacking the metal laminates, the CFRP and the adhesive in such a way, that the proposed configurations were obtained. To obtain a unidirectional final plate, every single layer must have the fibres oriented in the same direction as the previous one.

To improve the bond quality between the CFRP layers, a hot air gun was used applying heat to make the material more malleable and tacky. Layer by layer, the stacking is made applying pressure with a scraper to release any air bubbles existing between the bonding interface. The protective wax paper coating of every layer is removed, and the next layer is applied to continue the process. The 300 mm by 300 mm sheets stacked are cut into smaller 100 mm by 300 mm sheets, making possible to re-stack into the intended configuration and discarding as little material as possible.

The number of layers stacked in each configuration varied according with the lay-up, in such a way that the final FML could be approximately 3.2 mm thick for all the specimens manufactured.

3.3.3 CFRP lay-up configurations

To initiate the study of the effect of different lay-up configurations on the failure mode and failure load of a fibre metal laminate SLJ, it was decided to, at first, study configurations that could, without using metal, reinforce a SLJ made with CFRP substrates, using in alternative, only additional interlaminar adhesive layers.

In this study three different lay-up configurations were suggested for CFRP joints. One, serving as the most basic case, where the goal was to have a CFRP only SLJ, this being the case with which all the results obtained after (new configurations) could be compared. This configuration was also important to access the feasibility of performing the CFRP and adhesive cures simultaneously.

For the application of the concept regarding the reinforcement of the CFRP only adherend using additional adhesive layers of film adhesive, two different configurations were suggested. One configuration in which an additional adhesive layer, located between the first layer of CFRP prepreg and the second on both extremities, was used. Other, based on the previous one, but instead of employing only one additional layer of adhesive film in between the first laminas of prepreg on the extremities of the CFRP adherend, three interlaminar

additional adhesive layers were applied, altering between a CFRP layer and an adhesive layer, as can be seen in the Figure 34.

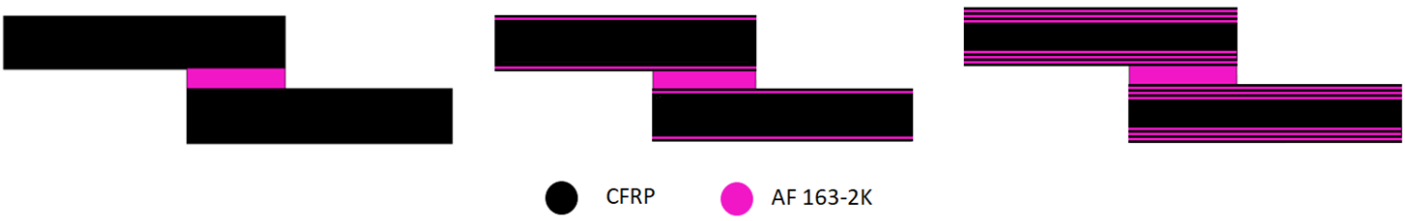

Figure 34: CFRP SLJs lay-up configurations studied.

3.3.4 Aluminium lay-up configurations

For the study with the 2024-T3 Alclad aluminium as the metal laminate for the CFRP FML, only one lay-up configuration was considered. Having the optimal configuration obtained by Palmares [37] as the basis, two additional layers of adhesive, AF 163-2K, were introduced, between the interfaces of CFRP and aluminium. The configuration suggested is presented in Figure 35.

In the study performed by Palmares [37], major differences between the numerical and experimental results were observed, and in terms of surface preparation, the phosphoric acid anodizing was not sufficient to avoid the occurrence of adhesion problems in the specimens and the consequent observation of a mixed failure. In this thesis, the additional adhesive layers in the interfaces Al-CFRP were suggested so that these already identified adhesion problems wouldn't occur. This configuration has 3.2 mm of thickness, with the aluminium laminates having 0.4 mm of thickness, being this the lowest available thickness of material at the time of the experimental work done for this dissertation.

The aluminium laminates used in this section of the experimental work were treated using sandpaper in the surfaces in direct contact with the adhesive. A phosphoric acid anodizing was not used due to problems with the anodizing setup and was considered that, due to the utilization of the interfacial adhesive layers between CFRP and metal, the adhesion between materials could be guaranteed. Conclusions about the need for anodizing the aluminium plies will be taken when the experimental results are analysed.

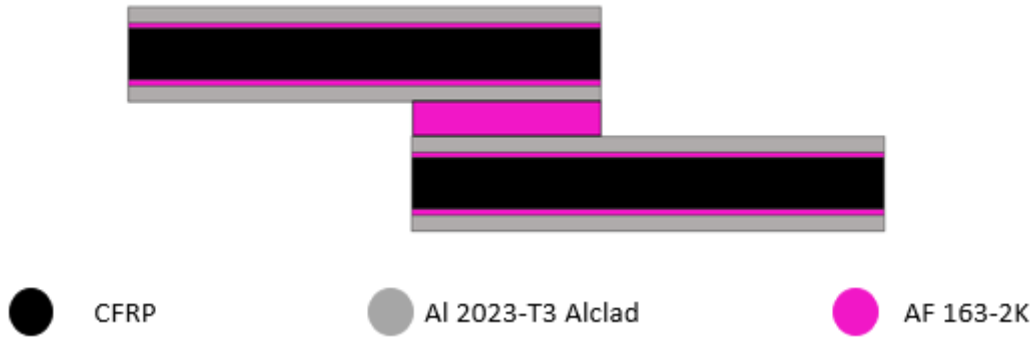

Figure 35: Aluminium lay-up SLJ configuration studied.

3.3.5 Titanium lay-up configurations

In the case where the Ti-6Al-4V alpha-beta (Grade 5), was used as the metal of the laminate three different lay-ups were suggested. Again, all the FMLs manufactured are approximately 3.2 mm thick, but the thickness of the titanium laminate is 0.8 mm (instead of the 0.4 mm used in the case of study with aluminium), due to the restrictions imposed by the availability of material by the supplier.

Based on the work done by Martins [38], the first lay-up suggested was the same as the optimal one suggested in his work, but again, with the manufacturing process involving only one cure cycle, for adhesive and CFRP.

Secondly, a configuration was suggested where two additional layers of AF 163-2K adhesive, with an approximate thickness of 0.2 mm, were used between the interfaces of CFRP and titanium, so that no adhesion problems occur, an issue that was observed by Martins [38].

At last, a third configuration was suggested with additional layers of adhesive between the CFRP and the metal, only applied in half of the laminate length. This technique ensures that, should an adhesive failure occur (“progressive failure” in Martins’ [38] work), the failure would propagate until the point where the additional adhesive layers start to be loaded and then try to force the plastic deformation of the titanium. In this configuration, the adhesive layers between CFRP and the titanium were pressed, with the combined action of the hot plates press machine and of the manufactured mould, so that its thickness can be considered as negligible.

In Figure 36, a schematic representation of the 3 suggested lay-up configurations of this study can be seen.

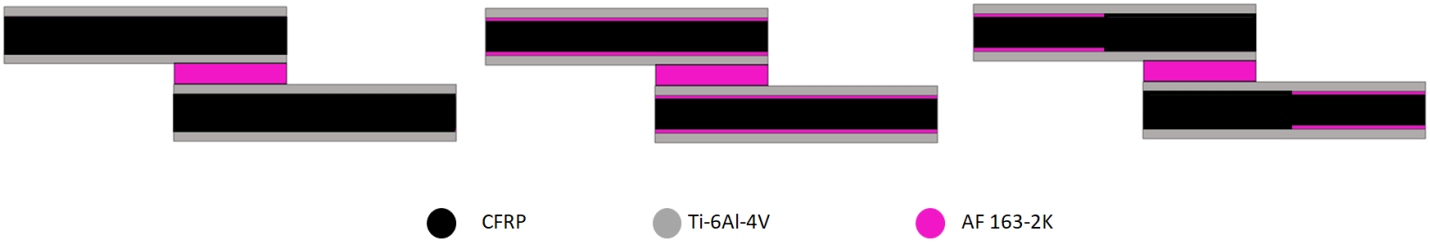

Figure 36: Titanium SLJs lay-up configurations studied.

3.3.5.1 Titanium grit-blasting

Grit-blasting is a mechanical surface treatment that is used to produce a clean macroscopically rough surface without surface contaminants. This mechanical process uses a machine that projects an abrasive material against the surface, such as alumina (particle size of 45 μm), with several passes at a distance of about 15-20 cm from the surface being treated, under high pressure [67].

The surface of the titanium laminate was placed on the surface of the interior of the machine and blasted alternately on both sides several times, to prevent the titanium's bending due to the differential release of internal stresses.

The surface was at first cleaned with acetone, to remove some ink marks presented on the sheet surface (codes written by the supplier) and then the grit-blasting process was performed. Afterwards, the laminates were degreased and cleaned again with acetone to remove the last impurities. The machine used in this work was a grit blaster model 705 GM, produced by de Laurentiis.

The manufacture of the final FMLs was done immediately after the grit-balsting process was completed, to avoid any kind of contamination.

3.4 Cure cycle

After the stacking process was completed, the stacked specimens were assembled in the manufacturing mould and placed on the hot plates press, in order to initiate the cure cycle.

Although the curing cycles used for the adhesive in previous works refer a plateau of cure temperature of 120ºC, it is possible, based on the information on the datasheet provided

by the manufacturer of this specific adhesive, AF 163-2K, to combine the cure of both adhesive and CFRP, in a single step. The cure cycle used is presented in Figure 37.

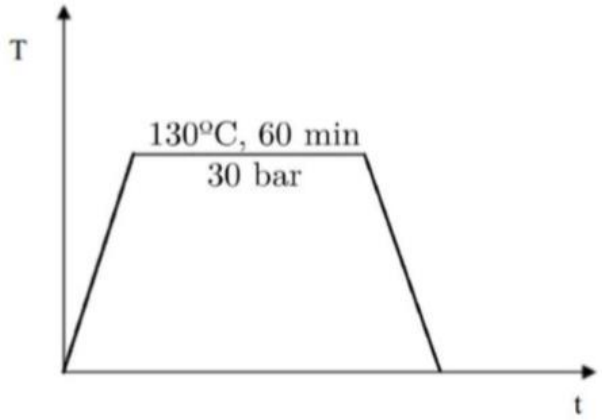

Figure 37: Cure cycle used for CFRP and for AF 1632-2K [61].

All the supplier recommendations were followed, including a heating rate of 4°C/min until the temperature of 130°C is achieved. Once the cure cycle was completed and the plate cooled to room temperature, it was removed from the press.

Due to the way the mould is setup, the final product of the curing process is a 100 mm wide and 250 mm long adhesively bonded joint, so in order to obtain SLJ specimens with the intended configuration, 25 mm by 240 mm, it is necessary to cut the plates. For each configuration suggested, 3 specimens where cut from the cured adhesively bonded plates.

The machine used was the model DV 25 Batisti Meccanica, made in Italy, equipped with a diamond disc as the cutting tool.

3.5 Testing conditions

All the 3 SLJs specimens manufactured for each configuration suggested, were tensile tested in a servo-hydraulic machine, MTS® model 810, with a load cell of 100 kN. The several tests were performed at a constant crosshead speed of 1mm/min, at laboratory ambient conditions (room temperature of 23ºC, relative humidity of 55%).

The SLJs were fixed using clamps that hold the free extremities of each specimen. Dowel pins were also used to align the sample and the clamps. The 4 bolts that hold the two parts of each clamp were tightened using a torque wrench. The torque was applied progressively, up to 40 N.m, ensuring an even clamping force.

4 Experimental results

All the specimens manufactured were tested in tension, allowing the plotting of *P-δ* curves (load-displacement). For each case, only one representative curve will be presented, with the reference of the standard deviation of the results obtained. The failure mode observed in each configuration will also be stated and analysed.

The main objective of the dissertation was to find the best lay-up configuration that offers good results in terms of failure load and failure mode observed, having as basis the results obtained for the basic configuration of a CFRP only SLJ.

It is relevant to refer that the slope obtained experimentally for the *P-δ* curves was corrected considering the influence of the stiffness of the gripping system, since the displacement measured by the machine is affected by the stiffness of the tool steel setup used to fix the specimens. In a previous work, Palmares [37] verified significant differences in the slope of numerical and experimental curves, which is thought to have been caused by excessive compliance of the testing system. To correct this error, the authors tested a steel specimen with the same thickness of the SLJs and subtracted the elastic deformation of the steel, calculated using Hooke's Law, from the total measured displacement. The resultant displacement is then the contribution from the gripping system. If this displacement is subtracted to the total displacement in a SLJ test, it is possible to obtain the *P-δ* curve for the specimen only. The data obtained by this methodology was applied for all the specimens.

It is also important to remind that all the SLJs manufactured had 50 mm of overlap length and the cure cycle of the CFRP and the adhesive AF 163-2K was performed in one single step.

4.1 CFRP SLJs

4.1.1 CFRP only

The typical *P-δ* curve obtained for the CFRP only configurations manufactured can be observed in the Figure 38.

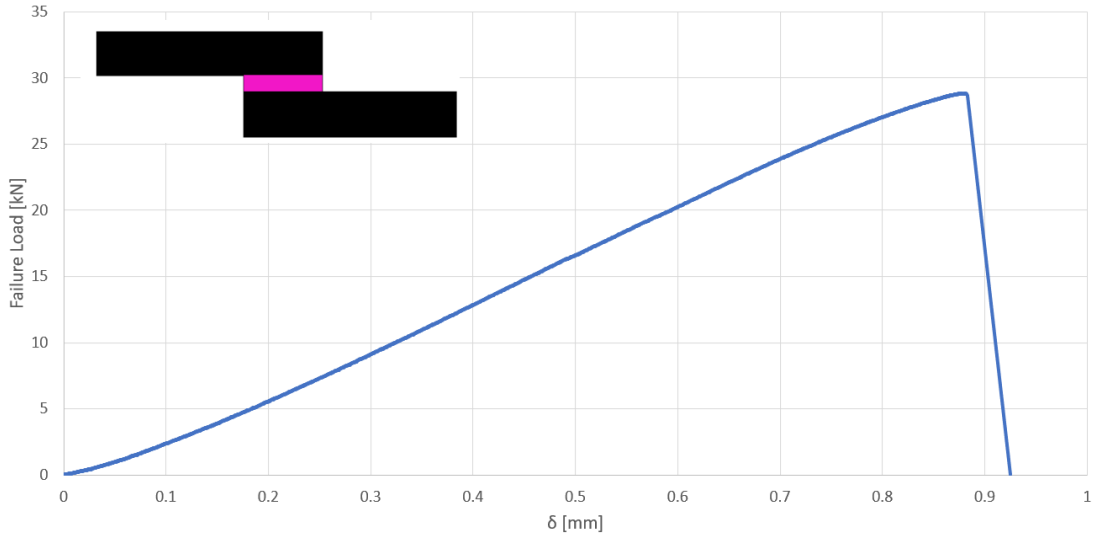

Figure 38: Typical load vs displacement curve of a SLJ using the configuration CFRP only (50 mm overlap).

The type of failure of the tested specimens was delamination of the CFRP fibres, as shown in Figure 39. The average failure load for CFRP only SLJs was 29.44 ± 0.82 kN.

Figure 39: Typical failure surface of a SLJ using the configuration CFRP only (50 mm overlap).

As referred previously, this result will be the basis of comparison for the results obtained with all the other configurations tested. In a first analysis, to assess the single step cure concept feasibility, the results obtained with this configuration can be compared with the results obtained by Martins [38] because in his work two cure cycles were used, while in the

current study, the manufactured process of the SLJs was done differently, with the referred cure in one single step, for CFRP and for the adhesive.

Analysing the comparison between the results of this project and the results obtained by Martins [38], Figure 40, it can be concluded that, although the results obtained for the average failure load of the specimens using the one step cure process are lower (reduction of 13.5 %), the saved curing time is 60%. These results for the CFRP only configuration also validate the curing process chosen for this project.

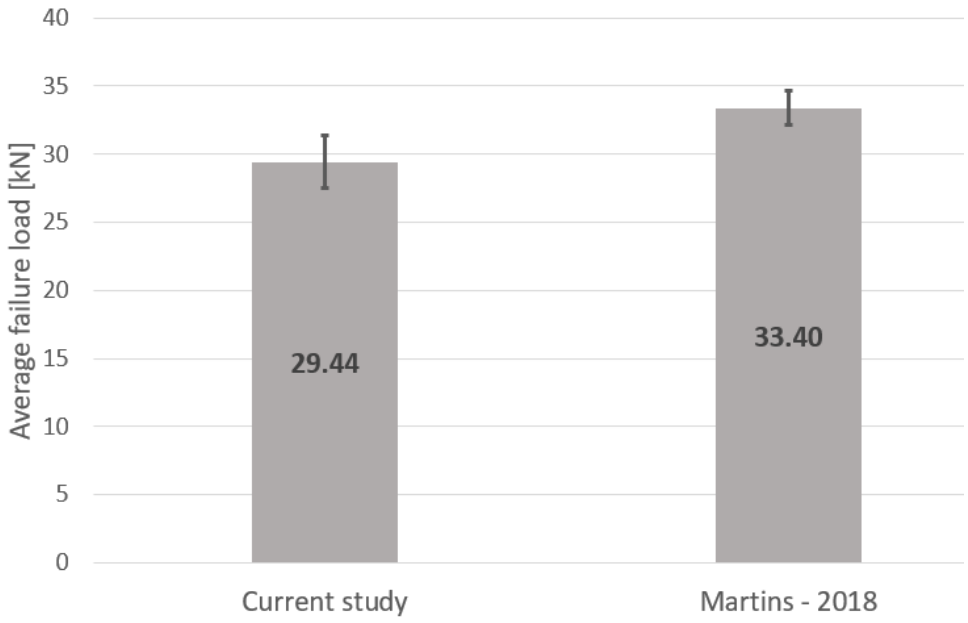

Figure 40: Comparison between the failure load values obtained for a SLJ using the configuration CFRP only (50 mm overlap), in this project and in Martins' [38] project, using different cure processes.

In a practical application this result must be taken into account, and for the studied adhesive, a balance between average failure load needed for each specific application and the curing time spent should also be made according to economic aspects.

4.1.2 CFRP with 1 interlaminar adhesive layer

The typical *P-δ* curve obtained for the CFRP specimens with 1 interlaminar adhesive layer manufactured can be observed in the Figure 41. In these specimens, the failure load was expected to be higher than the value obtained in the CFRP only configuration.

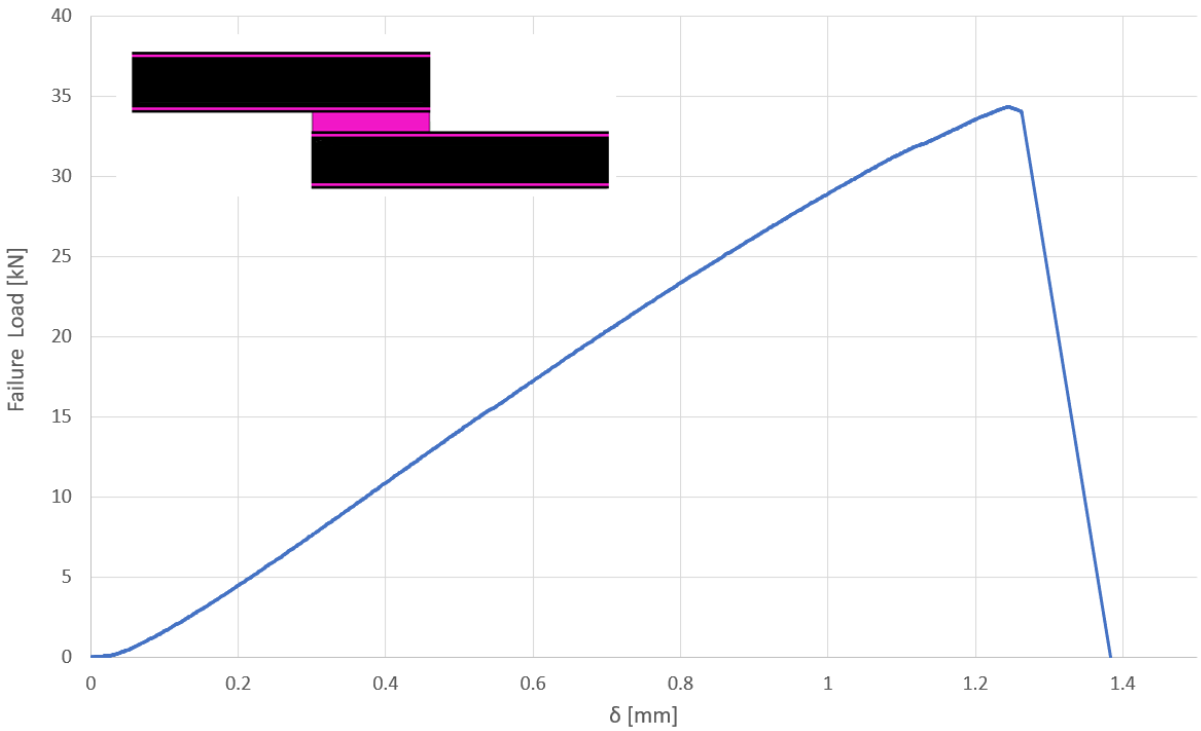

Figure 41: Typical load vs displacement curve of a SLJ using the configuration CFRP with 1 interlaminar adhesive layer (50 mm overlap).

Figure 42: Typical failure surface of a SLJ using the configuration CFRP with 1 interlaminar adhesive layer (50 mm overlap).

The type of failure of the tested specimens was delamination of the CFRP fibres, as shown in Figure 42 and the failure load obtained by testing the specimens was 34.49 ± 1.49 kN.

4.1.3 CFRP with 3 interlaminar adhesive layers

The typical *P-δ* curve obtained for the CFRP specimens with 3 interlaminar adhesive layers manufactured can be observed in the Figure 43. The failure load obtained was higher

than the two previously analysed configurations but, the increase, in comparison with the utilization of only 1 interlaminar additional adhesive layer, was not very relevant.

The typical failure mode obtained with this configuration is again delamination, Figure 44. This delamination occurred through all the CFRP layers that were in contact with the additional films of adhesive. For this configuration the values for the failure load obtained was 35.31 ± 0.82 kN.

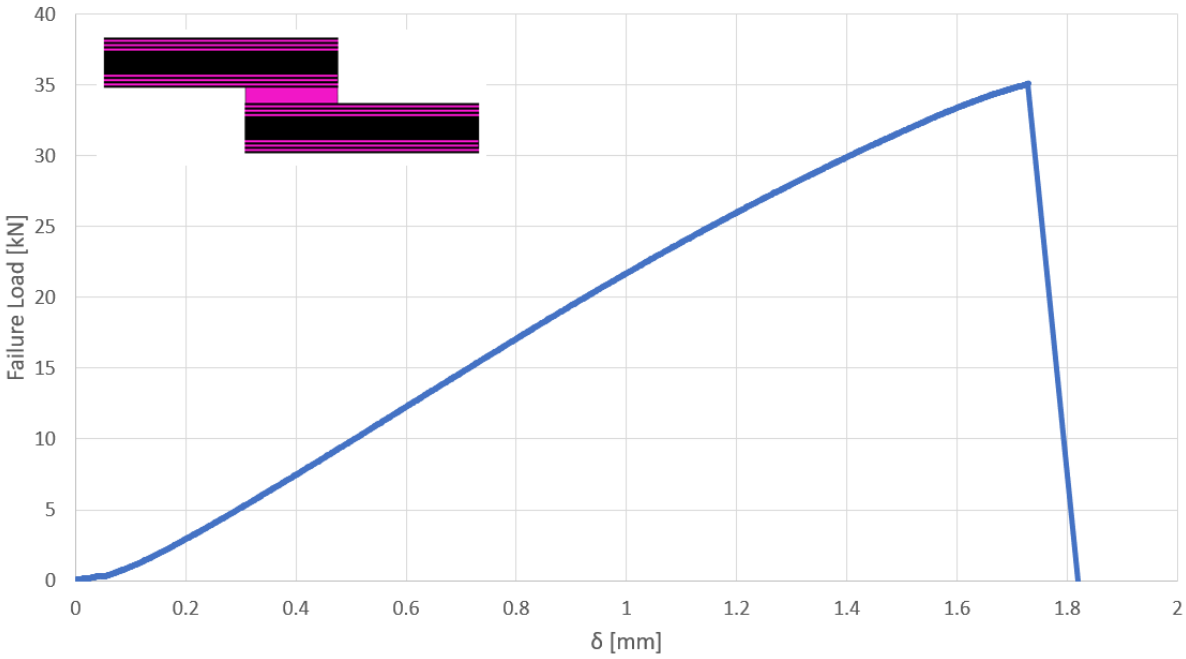

Figure 43: Typical load vs displacement curve of a SLJ using the configuration CFRP with 3 interlaminar adhesive layers (50 mm overlap).

Figure 44: Typical failure surface of a SLJ using the configuration CFRP with 3 interlaminar adhesive layers (50 mm overlap).

4.2 Aluminium SLJs

4.2.1 Al-Adh-CFRP-Adh-Al

The typical *P-δ* curve obtained for the Al-Adh-CFRP-Adh-Al specimens can be observed in the Figure 45.

The failure mode obtained with this configuration is cohesive in the adhesive, Figure 46, being this change of failure mode from delamination (in the CFRP lay-up configurations) to cohesive failure, the main improvement offered by this configuration.

The results obtained allow to state that the surface preparation step using phosphoric acid anodizing might be discarded, if the good adhesion between the CFRP and the aluminium is guaranteed by the application of an additional adhesive layer. Again, the economic impact of using additional adhesive compared to the materials and time needed to perform the anodizing process should be taken in to account.

In terms of values obtained, the failure load obtained with this lay-up configuration was 31.3 ± 1.09 kN

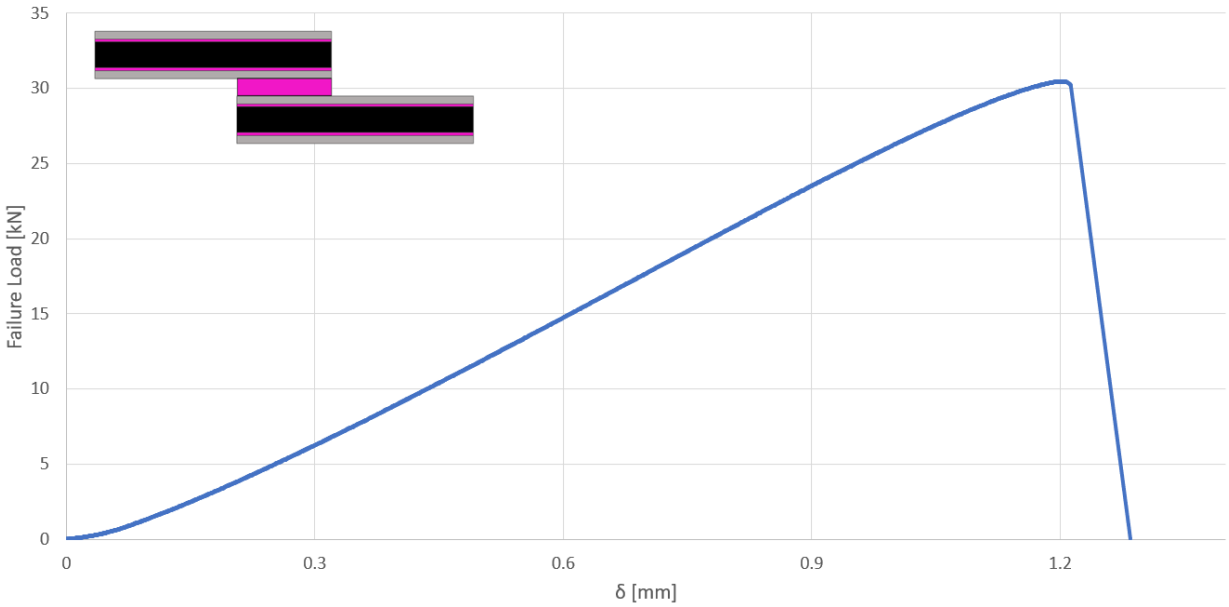

Figure 45: Typical load vs displacement curve of a SLJ using the configuration Al-Adh-CFRP-Adh-Al (50 mm overlap).

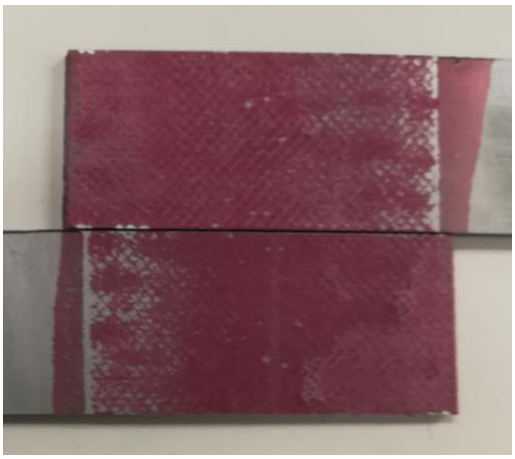

Figure 46: Typical failure surface of a SLJ using the configuration Al-Adh-CFRP-Adh-Al (50 mm overlap).

4.3 Titanium SLJs

4.3.1 Ti-CFRP-Ti

Regarding the study with titanium FML SLJs, for the Ti-CFRP-Ti lay-up configuration, the typical *P-δ* curve obtained was the one presented in the Figure 47.

The failure mode obtained was, as in the aluminium FMLs case, cohesive in the adhesive and can be seen in the Figure 48. The observation of this failure mode allows to draw the conclusion that the surface preparation of the titanium was done correctly.

The values for the failure load obtained with this lay-up configuration were 34.27 ± 1.67 kN

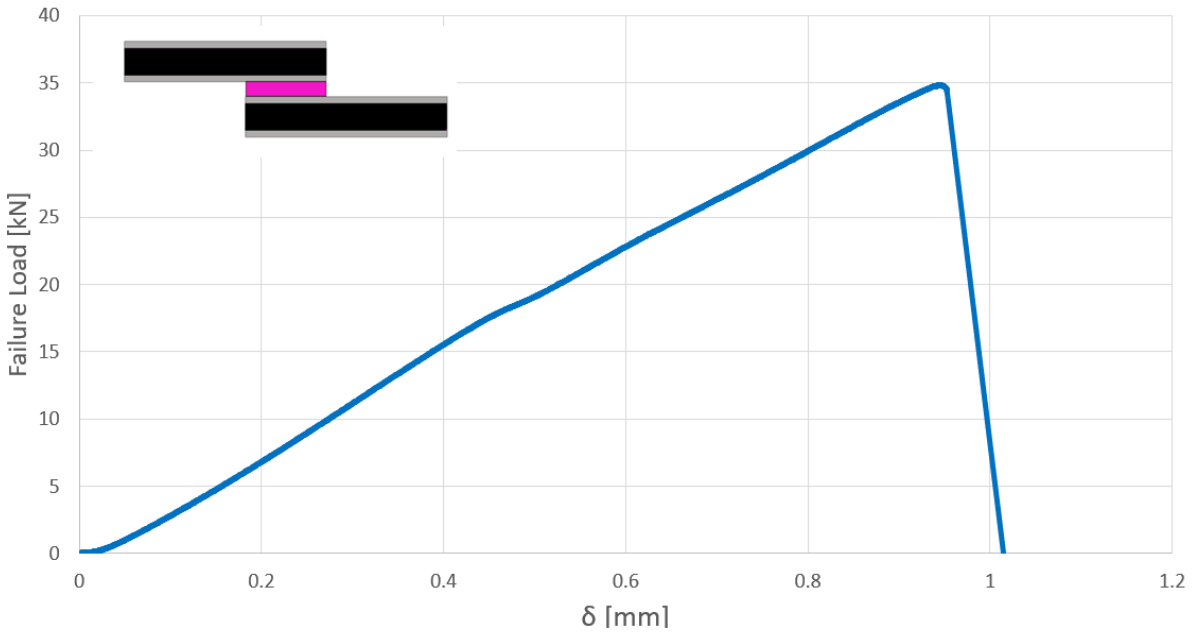

Figure 47: Typical load vs displacement curve of a SLJ using the configuration Ti-CFRP-Ti (50 mm overlap).

Figure 48: Typical failure surface of a SLJ using the configuration Ti-CFRP-Ti (50 mm overlap).

As referred previously, one of the observations in Martins' work [38], was the observation, with this configuration, Ti-CFRP-Ti, of a designated "progressive failure", that defined an observed failure mode in which the SLJ test failed in the interface between the titanium and the CFRP, with some degree of delamination. The occurrence of this type of failure was analysed as being a desirable phenomenon, when applied to an aerospace industry application, because if this failure mode could be reproduced consistently, it would be a major improvement for aerospace structures, in terms of reparability and inspectability of damaged components before total failure occurs.

Event though, through the utilization of the same configuration in this dissertation, the "progressive failure" could not be observed, it was considered that trying to achieve this failure mode was worth a deeper investigation. Thus, to furthermore study this configuration and the possibility of replicating the "progressive failure", interesting from the point of view of controlling the safety of a structure, an additional set of specimens was manufactured, using the same lay-up configuration, but with a surface treatment less severe, with the objective of forcing an interfacial adhesion failure to occur. For this new batch of specimens, the surface of the titanium laminates was only cleaned with acetone, with the single purpose of removing the ink marks, printed on the metal by the supplier – no grit-blasting was used.

The comparison of the obtained results can be analysed in Figure 49, where a reduction in the average failure load of the specimens that have not been subjected to the grit-blasting process can be detected. The values for the failure load obtained in this additional study were 32.88 ± 1.26 kN.

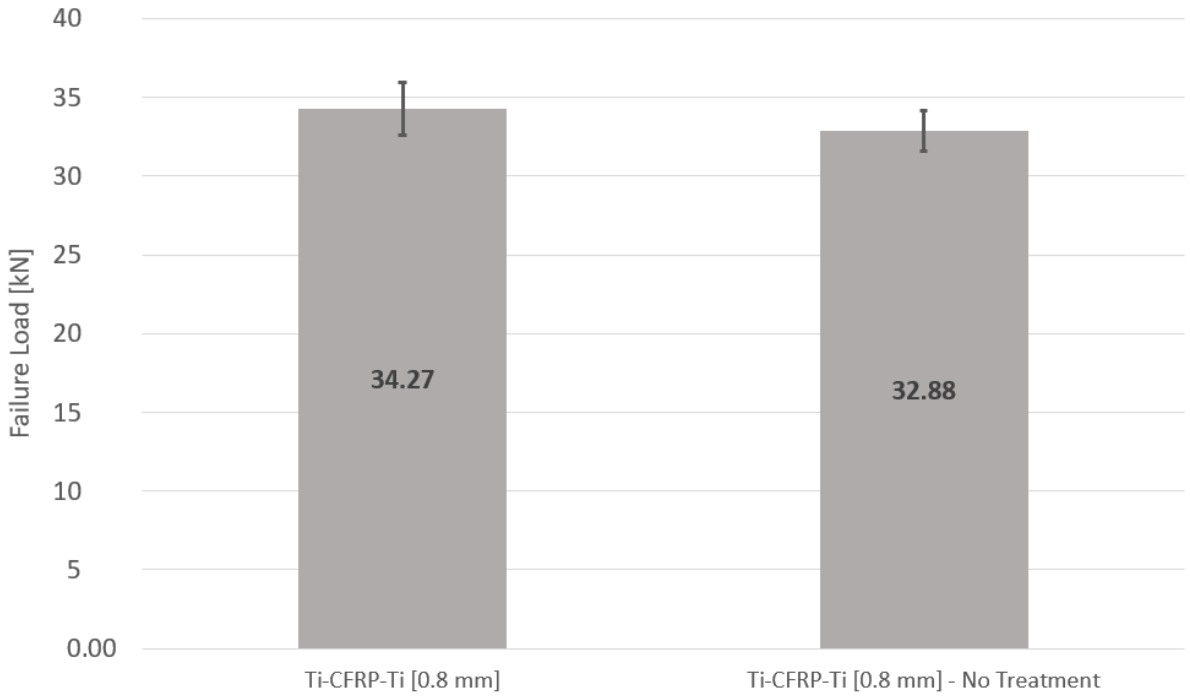

Figure 49: Comparison between the failure load values obtained for a SLJ using the Ti-CFRP-Ti (50 mm overlap), with grit-blasting and without grit-blasting ("No treatment") of the titanium plies.

The failure mode observed in the specimens where grit-blasting was not performed was again cohesive failure in the adhesive layer, Figure 50. With these results, it can be concluded that the reproducibility of the "progressive failure", obtained in other projects, is not good enough to ensure that this referred failure mode occurs in each case employing the Ti-CFRP-Ti configuration, with 0.8 mm thick titanium sheets. In this study, the titanium sheets were supplied with a protective coating that ensures good surface finishing and provides, in the supplied state, an already adequate level of surface energy for bonding, not allowing the occurrence of adhesion problems in the interfaces CFRP-Ti.

Figure 50: Typical failure surface of a SLJ using the configuration Ti-CFRP-Adh-Ti, without using grit-blasting on the titanium laminates surface (50 mm overlap).

4.3.2 Ti-Adh-CFRP-Adh-Ti

In the case where an additional adhesive layer is introduced in the interface between the CFRP and the titanium the typical *P-δ* curve is shown in the Figure 51.

This configuration was the one which presented the best results in terms of failure load, with correspondent values of 38.50 ± 0.35 kN. It is important to note that additionally to the higher average failure load obtained the standard deviation of the results is relatively low. In the load-displacement curve there is a slight change in the slope of the curve, that does not represent an experimental failure of the joint but is due to the gap between the holes of the specimens and the fixing clamps, and the pins that are used to fixate the testing setup, leading to a small occurrence of sliding (visible in the curve).

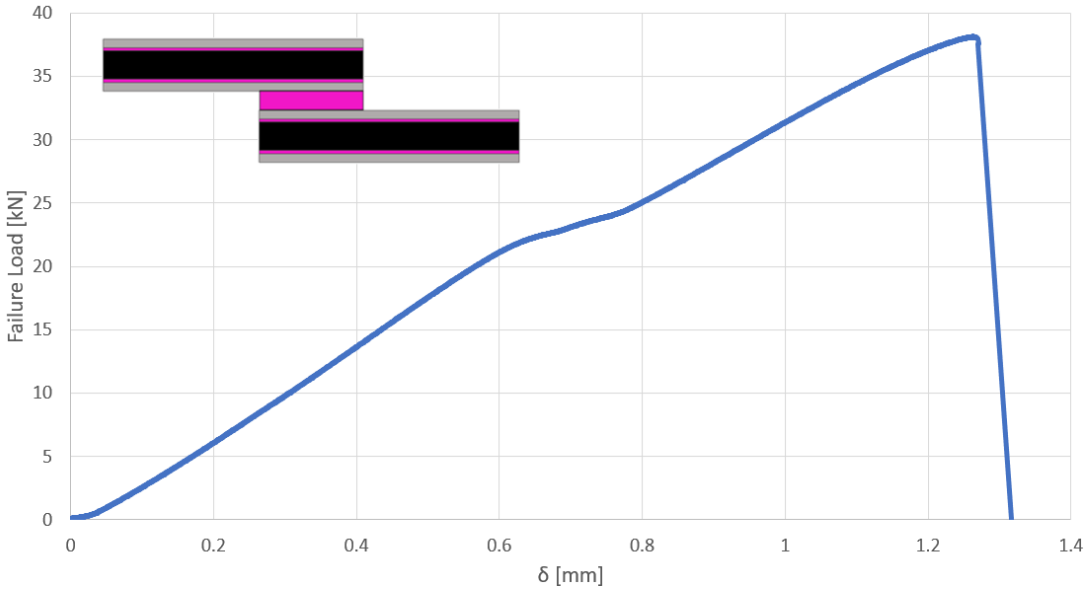

Figure 51: Typical load vs displacement curve of a SLJ using the configuration Ti-Adh-CFRP-Adh-Ti (50 mm overlap).

The failure mode can be observed in Figure 52, showing that with this configuration a cohesive failure in the adhesive is obtained. This result, regarding the failure mode, is in accordance with the expectations because, as the additional interfacial layers of adhesive are used in combination with the grit-blasting of the titanium plies, the adhesion between metal and CFRP was guaranteed. Once again, the issue of the occurrence of delamination in the CFRP appears to be solved with this suggested lay-up configuration.

Figure 52: Typical failure surface of a SLJ using the configuration Ti-Adh-CFRP-Adh-Ti (50 mm overlap).

4.3.3 Ti-1/2 Adh-CFRP-1/2 Adh-Ti

With the third titanium-based configuration suggested, with only half of the joint length with an additional film of adhesive, the typical *P-δ* curve obtained was the one presented in Figure 53.

Regarding the failure load, these specimens reached an average value of 37.56 ± 1.93 kN, which represents a noticeable improvement when compared with the basis configuration of CFRP only.

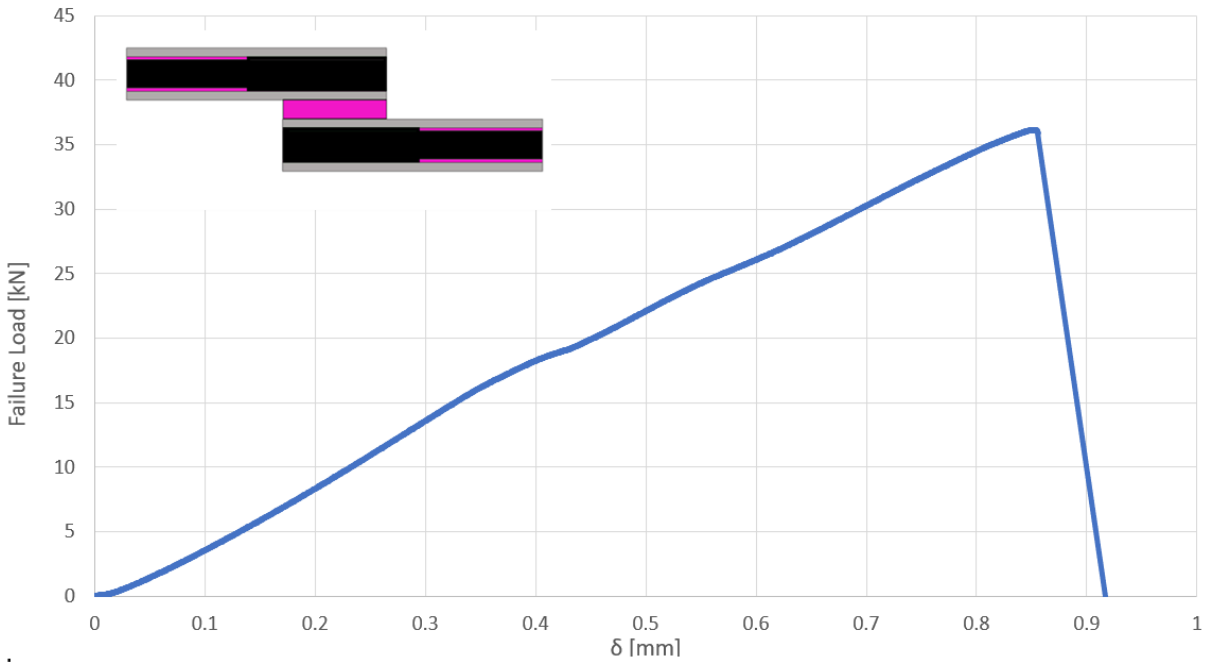

.

Figure 53: Typical load vs displacement curve of a SLJ using the configuration Ti-1/2Adh-CFRP-1/2Adh-Ti (50 mm overlap).

The typical failure mode was again the cohesive failure in the adhesive layer of the SLJ, Figure 54. This configuration was suggested in an attempt to have, in an initial phase, of an adhesion failure between the CFRP and the titanium. This failure would then be retarded (in terms of progression) by the additional adhesive used. This scenario did not occur because the titanium used already had adequate surface preparation in the supplied state and also because the plies were grit-blasted, making its surface well prepared for bonding without adhesion problems.

Figure 54: Typical failure surface of a SLJ using the configuration Ti-1/2Adh-CFRP-1/2Adh-Ti (50 mm overlap).

4.4 Summary

In order to better understand the influence of the effect of all the lay-ups configurations suggested for SLJs with 50 mm of overlap length a table was built, Table 6, with the summary of the results obtained for the average failure load obtained and for the typical failure mode for each configuration studied.

Table 6: Failure load and failure mode for the lay-up configurations studied (50 mm overlap)

Lay-up Configuration	Schematization	Average Failure Load ± Standard Deviation (kN)	Failure Mode
CFRP only		29.44 ± 0.82	Delamination
CFRP with 1 interlaminar adhesive layer		34.49 ± 1.49	Delamination
CFRP with 3 interlaminar adhesive layers		35.31 ± 0.82	Delamination
Al-Adh-CFRP-Adh-Al	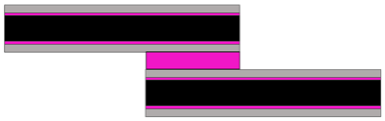	31.3 ± 1.09	Cohesive failure in the adhesive
Ti-CFRP-Ti		34.27 ± 1.67	Cohesive failure in the adhesive
Ti-Adh-CFRP-Adh-Ti		38.50 ± 0.35	Cohesive failure in the adhesive
Ti-1/2Adh-CFRP-1/2Adh-Ti		37.56 ± 1.93	Cohesive failure in the adhesive

Analysing the previous table, it is possible to conclude that by including interlaminar additional layers of adhesive AF 163-2K, in between the top layers of CFRP, it is possible to increase the overall failure load presented by the SLJs. Despite the occurrence of

delamination, as the main failure mode, the improvement in the failure load should be seen as a supporting argument, for using adhesive as the reinforcement for the through-thickness of CFRP joints in cases where the usage of metal layers is not favourable. There is an improvement of approximately 17.2%, when comparing the results of the CFRP only configuration with the ones obtained with the CFRP with 1 interlaminar adhesive layer lay-up. It could also be identified that the usage of 3 interlaminar layers of adhesive, instead of only 1 additional layer, does not have a significant impact on the final average failure load of the joint – leading to an improvement of only approximately 2.4 %, from the reinforcement with 1 additional adhesive layer.

Regarding the usage of metal layers for manufacturing an FML, in all the suggested configurations, a cohesive failure in the adhesive was the typical failure mode obtained, which makes the control of the failure process much easier from a mechanical design approach. This result also fulfils the goal of avoiding delamination that was initially purposed with this concept.

The Al-Adh-CFRP-Adh-Al lay-up presented an improvement, when compared to the basic configuration of CFRP, of only 6.3 %. The main advantage of this lay-up is the already referred cohesive failure and the good level of adhesion between the aluminium plies and CFRP, provided by the adhesive layer in this interface, that allow the possibility of manufacturing of the SLJs without the need for phosphoric acid anodizing the aluminium.

All the titanium configurations tested presented improvements in terms of both failure load and failure mode to the original lay-up, having been the Ti-Adh-CFRP-Adh-Ti configuration the one with which the best results were obtained. With this configuration, it was possible to obtain an improvement in terms of average failure load of 30.8 % and no adhesion problems were detected. This improvement, in terms of failure load, obtained by performing the tensile tests on the manufactured joints with this configuration, is thought to have implications with the fact that, with the introduction of additional adhesive in the adherend, layers with lower rigidity are created, allowing the stresses to be redistributed and absorbed, explaining the higher values of failure load registered in this study, when the Ti-Adh-CFRP-Adh-Ti configuration is used.

The configuration using the Ti-1/2Adh-CFRP-1/2Adh-Ti lay-up, did not exhibit the expected behaviour because the CFRP-Ti interface never had suffered adhesion failure, a case where the additional portion of film adhesive would try to stop the interfacial failure. This can be explained by a good surface preparation of the titanium layers during the manufacturing process of the specimens.

5 Numerical analysis

5.1 Model description

The numerical model used to simulate a tensile test of a SLJ was developed using the *Abaqus*® software, with the main goal of numerically reproducing the results obtained with the experimental tests, in terms of both failure load and failure mode. The model is based on a 2D planar deformable shell part with the specific properties of the materials in each case being the properties referred above in the section 3.

A traction-separation law was applied to the adhesive layers of the model in order to introduce damage evolution in the cohesive elements during the analysis. For this dissertation, the same trapezoidal cohesive law used by Martins [38] was employed, mainly due to the semi-ductile nature of the adhesive used.

In the section of the model using CFRP, it was also necessary to include a cohesive zone with cohesive zone elements (CZE) following a traction separation law with the parameters present in the Table 7, with the aim of modelling composite delamination. This cohesive layer was modelled using a thickness of 0.02 mm and was placed 0.15 mm away from, depending on the configuration, the adhesive layer or the metal layer. This value of 0.15 mm was used because it is the value of the thickness of a single CFRP prepreg layer.

Table 7: Cohesive parameters for CFRP interlaminar failure [62]

	Mode I	**Mode II**
σ_R (MPa)	32	30
G_c (N/mm)	0.66	1.13

An example of the placement of the several cohesive layers used in the developed model is shown and described in Figure 55.

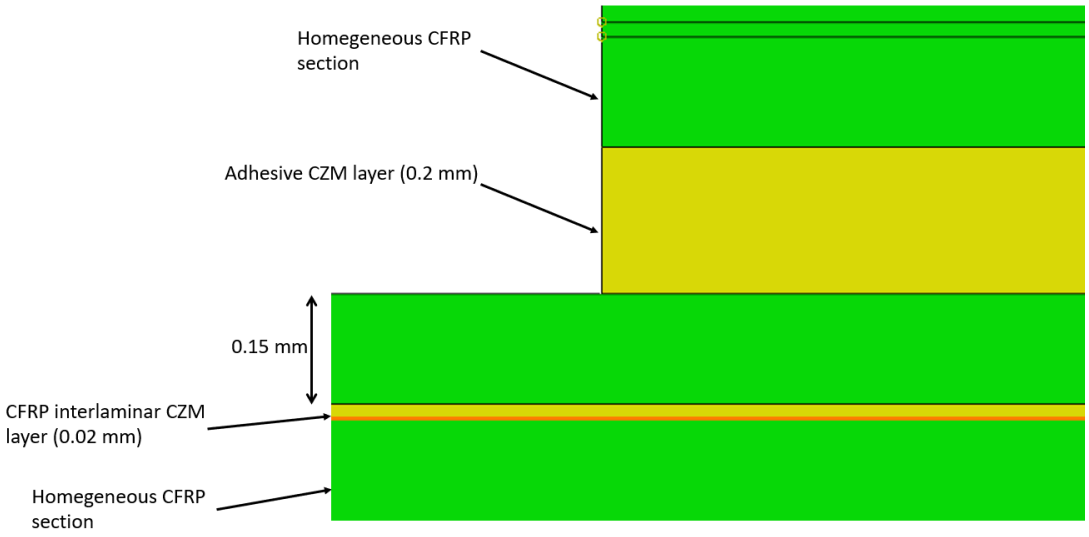

Figure 55: Schematization of the placing of the several CZE layers throughout the SLJ in the numerical model.

Two calculation steps were applied to the model, one to represent the curing process during the manufacture of the SLJ, and another related to the boundary conditions needed to simulate the tensile test.

The thermal residual stresses due to the difference in the thermal expansion coefficient are a very important concern especially in the study regarding CFRP and aluminium. To take this factor into account, and to make the model as realistic as possible, a primary step was introduced before applying the displacement, in which a thermal field was imposed to the model, imposing at first, the cure temperature applied experimentally, followed by the imposition of room temperature conditions, therefore simulating the temperature changes that occur during the cure cycle process.

The several coefficient of thermal expansions used were 0 $\mu m/m.K^{-1}$, for CFRP, 8.6 $\mu m/m.K^{-1}$, for the titanium and 23.22 $\mu m/m.K^{-1}$ for aluminium.

The boundary conditions of the model were selected to closely match those that occur in a tensile test. A constant displacement was applied at the right end of the joint, while the left end was fixed in every direction. Also, for both edges, the movement was limited in the vertical direction, representing the forces imposed by the griping system of the test machine. A schematic representation is presented in Figure 56.

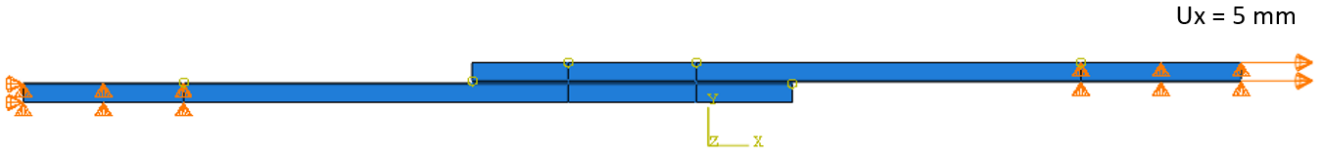

Figure 56: Schematic view of the physical boundary conditions in *Abaqus*®, quasi-static conditions.

The mesh used was refined until the element spacing was set at 0.2 mm, Figure 57, a value corresponding to the modelling of the adhesive layer thickness. The elastic sections of the model were modelled using 8-node bilinear plane strain elements, CPE8R and the cohesive sections employed a 4-node two-dimensional cohesive element, COH2D4.

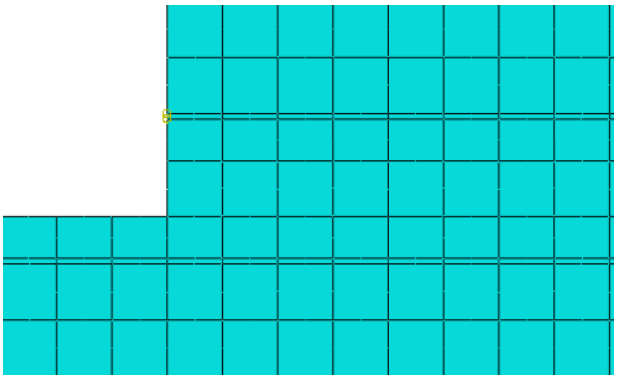

Figure 57: Square mesh used, with 0.2 mm refinement.

5.2 Numerical results

In this section the numerical results obtained by running numerical analysis for each of the specimen lay-up configurations under study will be presented. For every case, a tensile test was simulated based on the model described earlier, and the *P-δ* curves and failure surfaces obtained numerically will be presented and compared with the experimental results, which were previously shown and discussed on the chapter regarding the experimental results.

5.3 CFRP SLJs

5.3.1 CFRP only

The numerical *P-δ* curve for the base configuration, CFRP only, obtained from *Abaqus*®, using a trapezoidal traction-separation law for the adhesive CZEs, is presented in Figure 58.

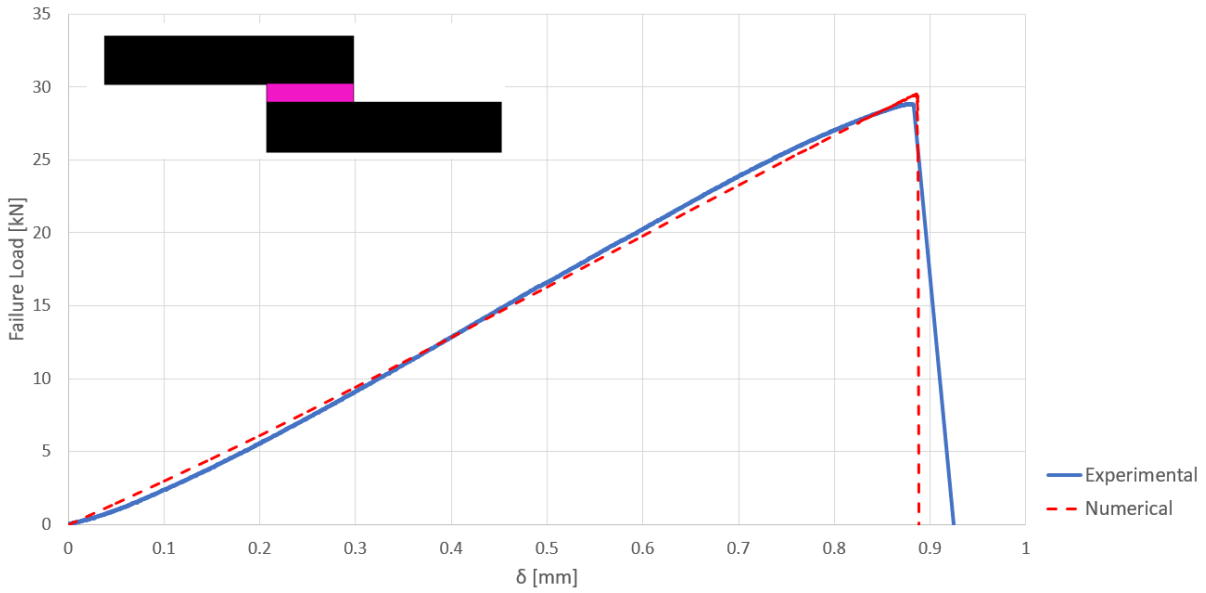

Figure 58: Numerical P-δ curve vs experimental P-δ curve, for a 50 mm overlap SLJ, with the configuration CFRP only.

The failure mode obtained numerically was delamination, Figure 59, being the failure mode consistent with the one observed experimentally.

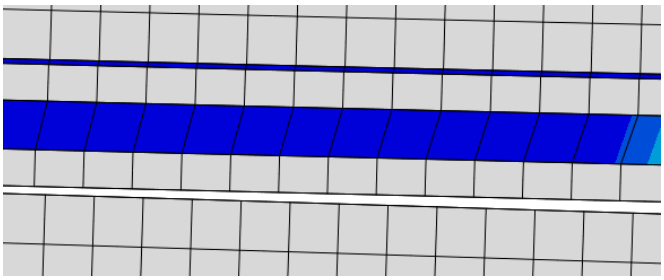

Figure 59: Numerical failure surface, for a 50 mm overlap SLJ, with the configuration CFRP only.

5.3.2 CFRP with 1 interlaminar adhesive layer

Regarding the configuration using CFRP with 1 interlaminar adhesive layer the *P-δ* curve is presented in the Figure 60.

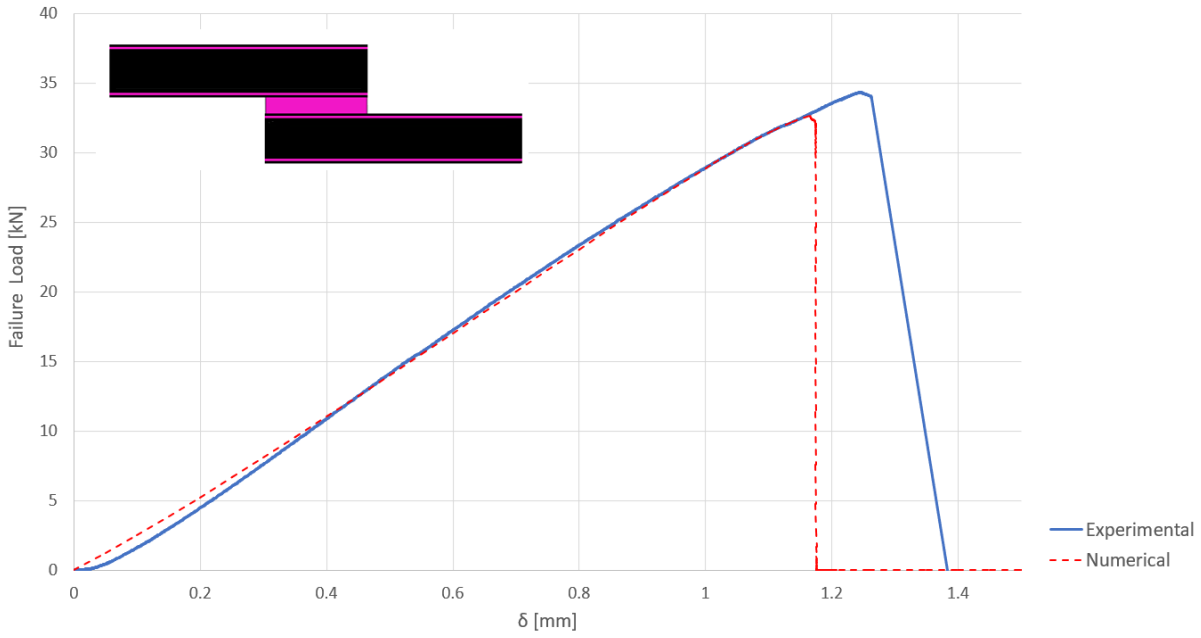

Figure 60: Numerical P-δ curve vs experimental P-δ curve, for a 50 mm overlap SLJ, with the configuration CFRP with 1 interlaminar adhesive layer.

The failure mode obtained numerically was a cohesive failure in the adhesive layer, Figure 61. This failure mode does not correspond to the experimentally observed failure, where the specimens presented delamination of the CFRP fibres.

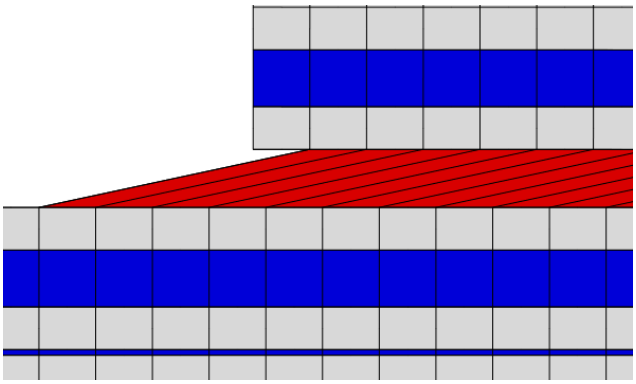

Figure 61: Numerical failure surface, for a 50 mm overlap SLJ, with the configuration CFRP with 1 interlaminar adhesive layer.

5.3.3 CFRP with 3 interlaminar adhesive layers

For the configuration using CFRP with 3 interlaminar adhesive layers the numerically obtained *P-δ* curve is presented in the Figure 62. By examining the curve, it is possible to understand that the failure load obtained by the FEM software is lower than the value obtained with the experimental testing of the specimens.

Also, in terms of failure mode, the model applied could not replicate the experimental results, and in the Figure 63, it can be seen that a cohesive failure in the adhesive was numerically predicted for this lay-up configuration.

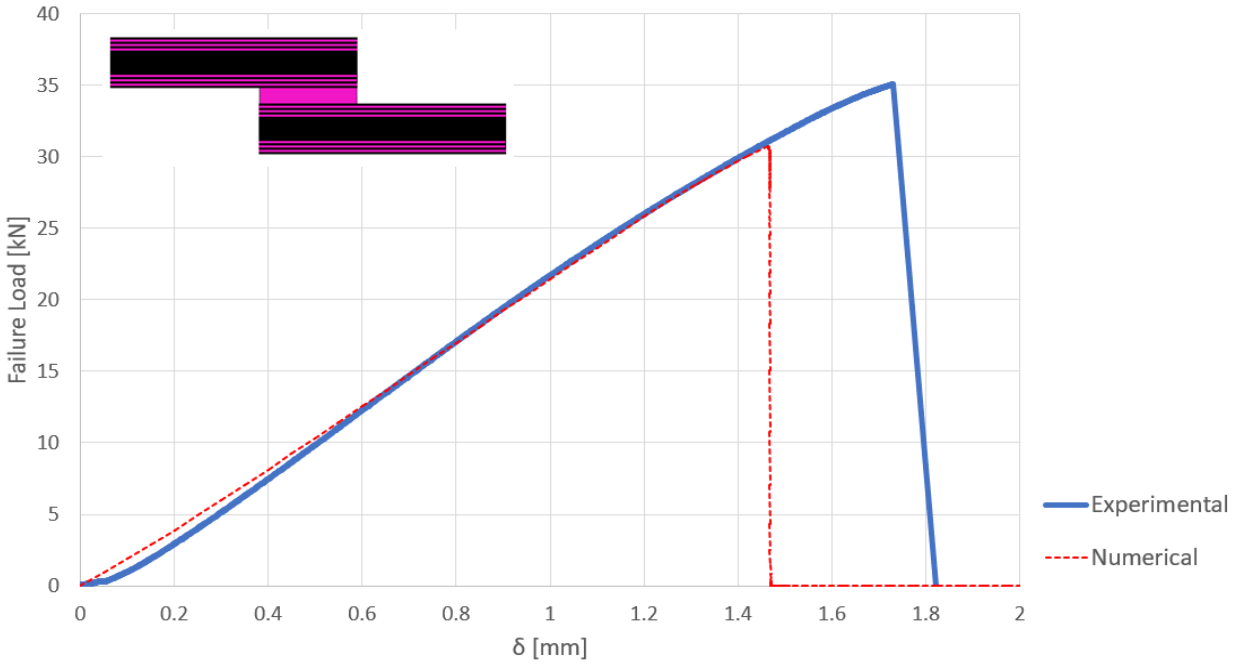

Figure 62: Numerical P-δ curve vs experimental P-δ curve, for a 50 mm overlap SLJ, with the configuration CFRP with 3 interlaminar adhesive layers.

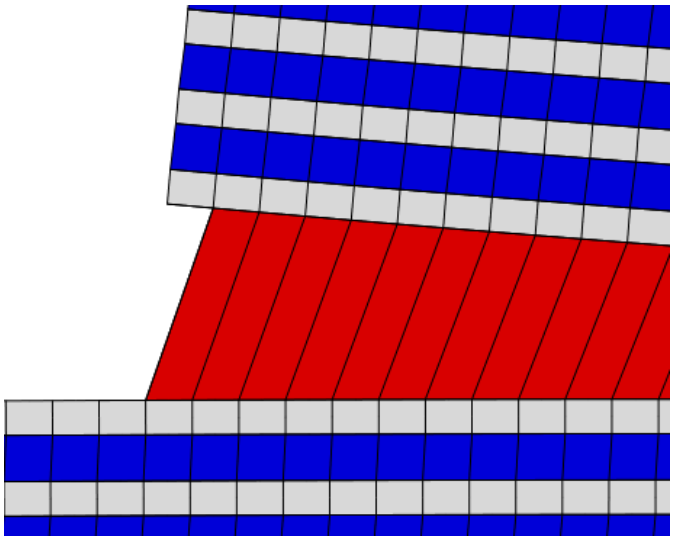

Figure 63: Numerical failure surface curve, for a 50 mm overlap SLJ, with the configuration CFRP with 3 interlaminar adhesive layers.

5.4 Study of the adherend's stiffness under peel stresses

To start the numerical analysis regarding the utilization of the FML concept combined with the utilization of additional adhesive layers as the reinforcement for the basic CFRP adherend, it was considered relevant to evaluate the distribution of the peel stresses in the optimal lay-up configuration found in previous works performed by the adhesive's research group of the Faculty of Engineering of University of Porto.

In terms of the developed model to perform this study, the software used was also the *Abaqus*® software, and the analysis performed differed of the previous explained model by being an elastic analysis. In terms of boundary conditions, everything was equal to the described in the previous section, except for the right end of the SLJ in which, in this case, a constant load of 30 kN was applied for every stiffness level studied, instead of a displacement, Figure 64.

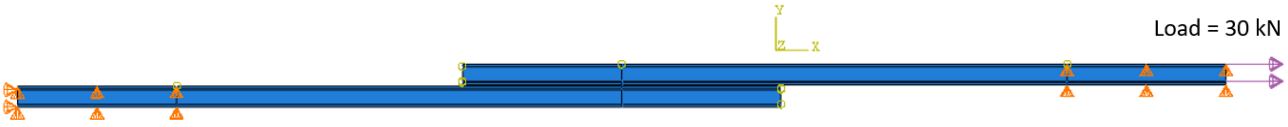

Figure 64: Schematic view of the physical boundary conditions in *Abaqus*®, quasi-static conditions, for the study of the effect of the adherend's rigidity on the peel stresses.

Starting from the referred lay-up configuration, Figure 65, the stiffness of the material used in the extremities was modified and the peel stresses were evaluated using a "path", both

along the overlap of the joint and in at the end of the first layer of CFRP pre-prepreg, Figure 66. This procedure allows to understand the effect of the material used in an FML and to check if using aluminium and titanium was a correct approach.

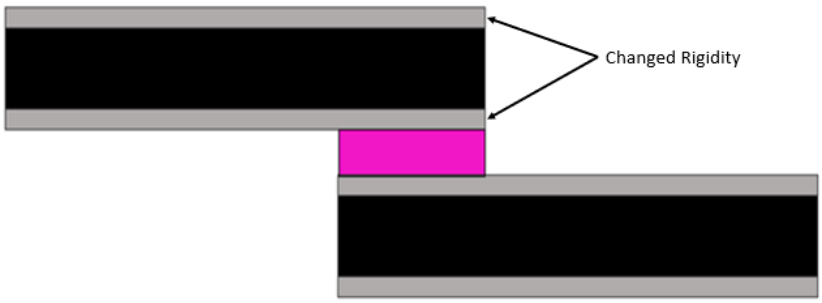

Figure 65: Configuration used to vary the rigidity of the material used to reinforce an FML SLJ.

Figure 66: Location of the paths where the peel stresses were analysed.

The results obtained for the case in which the peel stresses were taken along the adhesive overlap can be seen in the Figure 67. It can be noted that with the increase of the stiffness of the material used in the FML, the maximum peel stresses along the overlap tend to reduce.

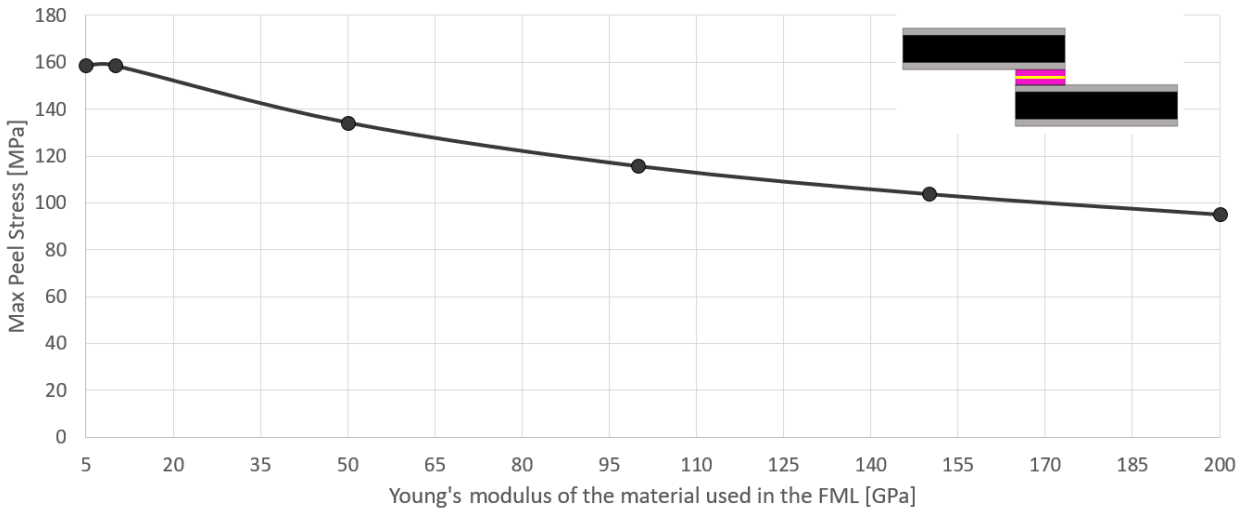

Figure 67: Evolution of the maximum peel stresses along the overlap with the variation of the Young's modulus of the material used in the FML.

The results obtained for the case in which the peel stresses were measured on the location after the first layer of the CFRP prepreg can be analysed in the Figure 68, allowing to conclude that, with the increase of the stiffness of the material used in the FML, the maximum peel stresses tend to reduce.

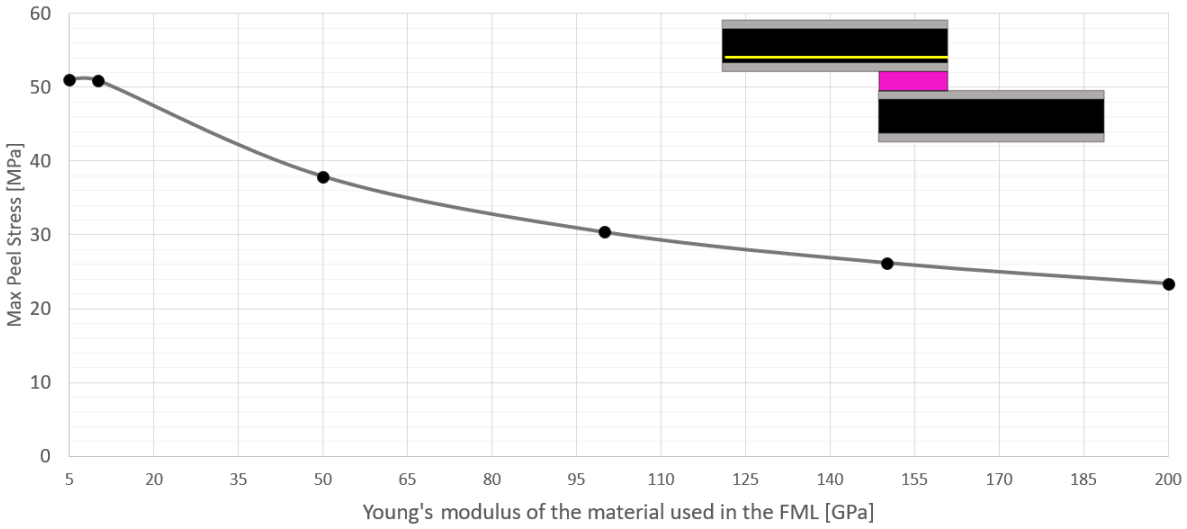

Figure 68: Evolution of the maximum peel stresses along the first layer of the CFRP prepreg with the variation of the Young's modulus of the material used in the FML.

In aeronautical applications, as referred in the literature review section, one of the major aspects to consider is the weight of the structures. Thus, it is important to reach a point of balance between the density of the materials and, in this case, the peel stresses obtained by the utilization of a certain material. A study comparing the peel stresses taken in one of the cases above and the general material's densities for the studied stiffnesses is shown in Figure 69, where it can be seen that there is a "go to" area where it is possible to have a good balance of the mentioned factors.

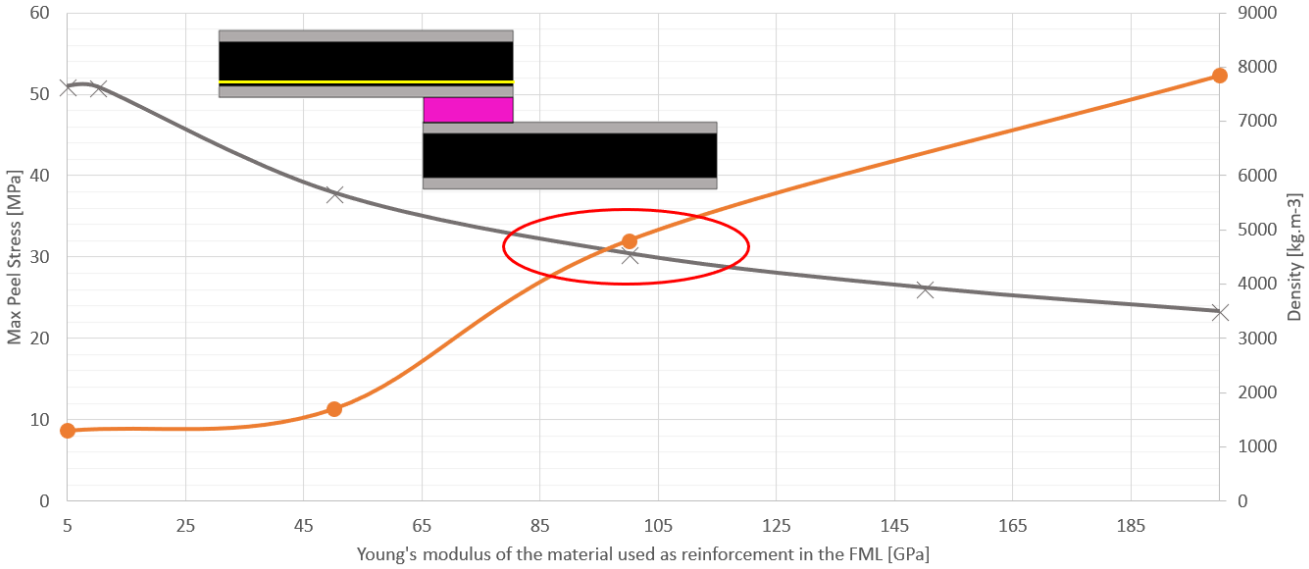

Figure 69: Evolution of the maximum peel stresses in an FML with the variation of the Young's modulus of the material used compared with the variation of material's densities.

Considering the materials under study in this dissertation, Al 2023-T3 (66 GPa) and Ti-6Al-4V (113.8 GPa), titanium seems to be the one that is more suited for the intended application. The plots also help to understand why this dissertation did not focus on more rigid materials, such as steel – although the utilization of steel would result in lower peel stresses on the adherend, its higher density makes it less compatible with the light weight condition needed for aviation applications.

5.5 Aluminium SLJs

5.5.1 Al-Adh-CFRP-Adh-Al

In the case were the configuration regarding the Al-Adh-CFRP-Adh-Al lay-up was modelled, the numerical results obtained using *Abaqus*® software were very close to those obtained experimentally, both in terms of failure load, Figure 70, and in terms of failure mode (cohesive failure in the adhesive), Figure 71.

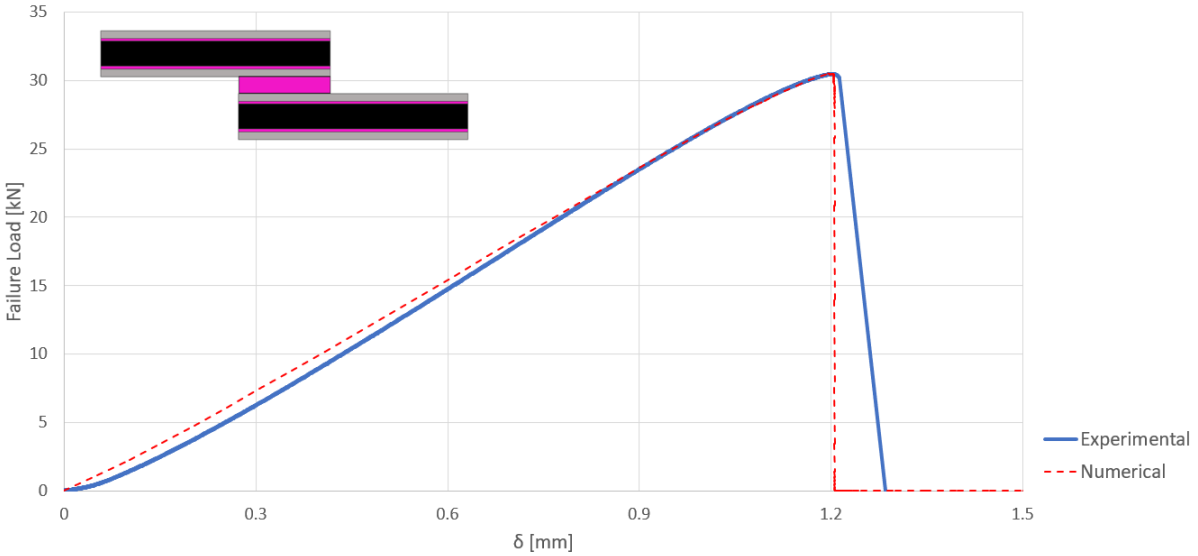

Figure 70: Numerical P-δ curve vs experimental P-δ curve, for a 50 mm overlap SLJ, with the configuration Al-Adh-CFRP-Adh-Al.

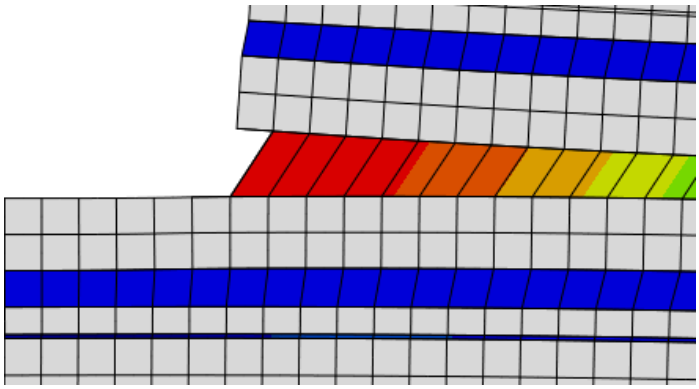

Figure 71: Numerical failure surface, for a 50 mm overlap SLJ, with the configuration Al-Adh-CFRP-Adh-Al.

5.6 Titanium SLJs

5.6.1 Ti-CFRP-Ti

The model described earlier was also used for the suggested titanium-based lay-up configurations. For the configuration with the Ti-CFRP-Ti lay-up, the *P-δ* curve obtained is presented in Figure 72. The failure load obtained numerically is coherent with the one obtained experimentally.

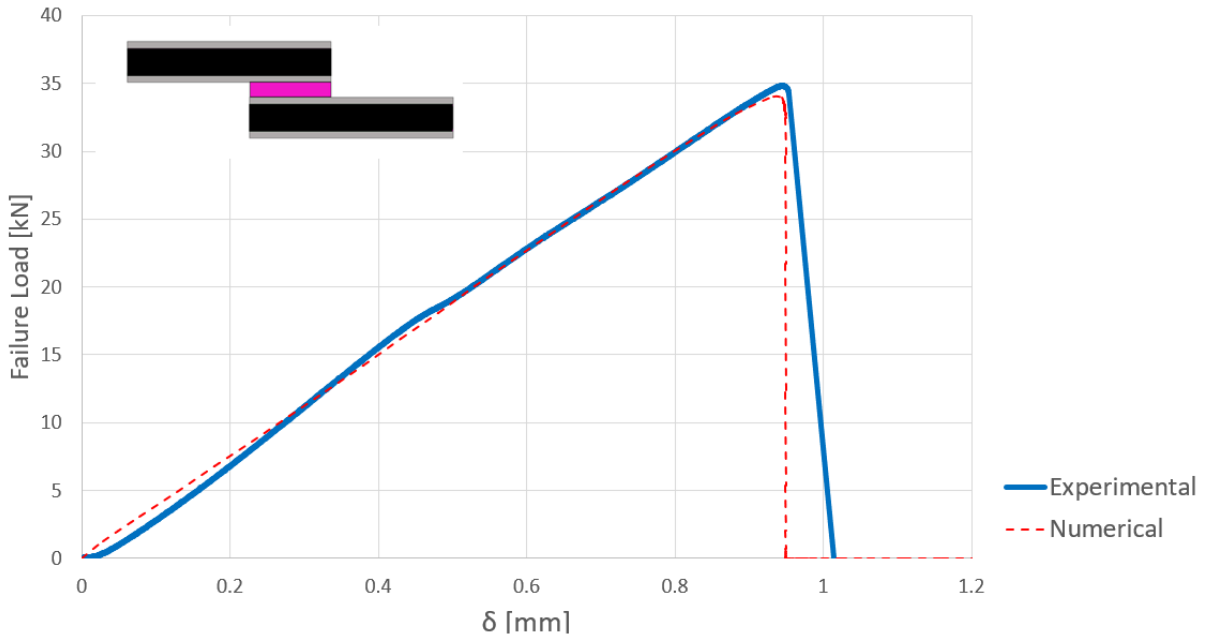

Figure 72: Numerical P-δ curve vs experimental P-δ curve, for a 50 mm overlap SLJ, with the configuration Ti-CFRP-Ti.

Regarding the failure mode, it was possible to observe a cohesive failure in the adhesive layer of the modelled SLJ, Figure 73, this result also being coherent with the experimental results obtained.

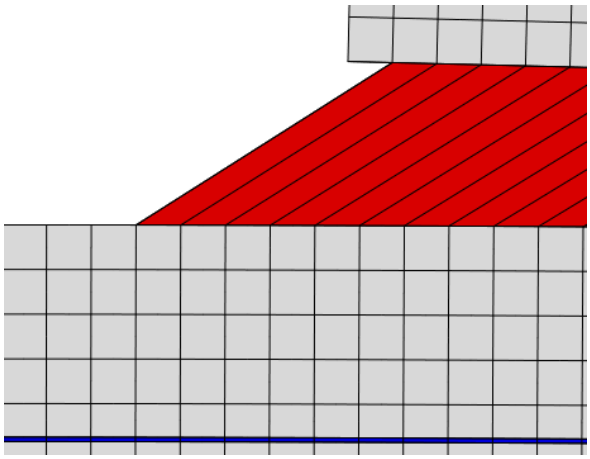

Figure 73: Numerical failure surface, for a 50 mm overlap SLJ, with the configuration Ti-CFRP-Ti.

5.6.2 Ti-Adh-CFRP-Adh-Ti

For the configuration using the Ti-Adh-CFRP-Adh-Ti lay-up the *P-δ* curve obtained numerically is presented in Figure 74. The numerical failure load of this joint configuration is lower than the values obtained for the experimental tensile test performed. In terms of failure mode, the numerical prediction is coherent with the results obtained by experimentally testing the specimens, being observed, in both cases, a cohesive failure in the adhesive, Figure 75.

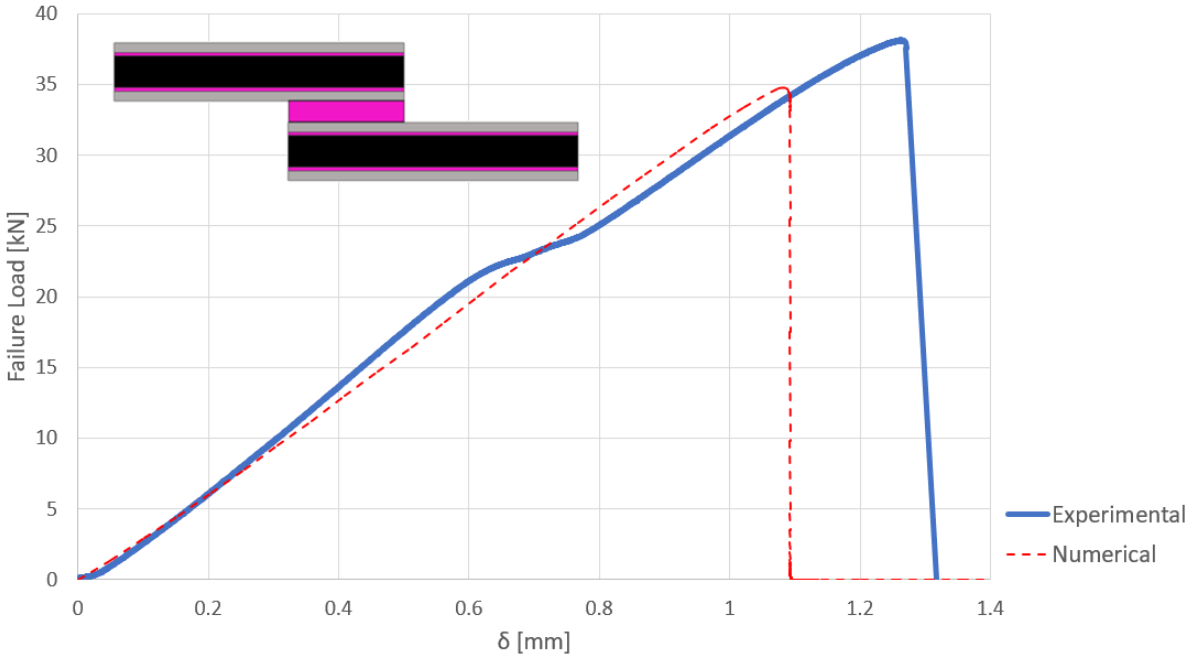

Figure 74: Numerical P-δ curve vs experimental P-δ curve, for a 50 mm overlap SLJ, with the configuration Ti-Adh-CFRP-Adh-Ti.

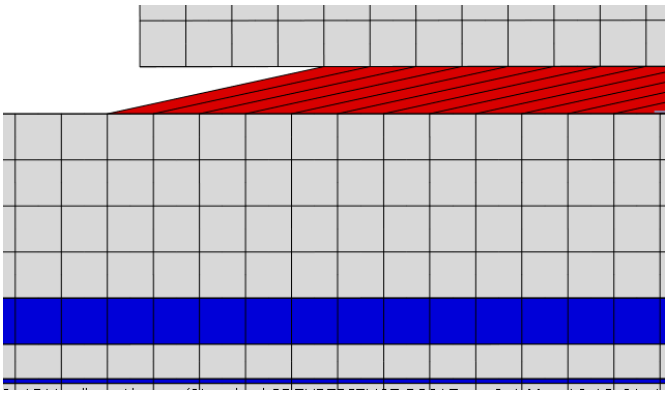

Figure 75: Numerical failure surface, for a 50 mm overlap SLJ, with the configuration Ti-Adh-CFRP-Adh-Ti.

5.6.3 Ti-1/2 Adh-CFRP-1/2 Adh-Ti

Finally, for the configuration defined as Ti-1/2Adh-CFRP-1/2Adh-Ti, the numerical *P-δ* curve is presented in Figure 76. Comparing the numerical curve with the experimental result, it can be observed that the failure load in this configuration is slightly lower than the one that was possible to achieve experimentally.

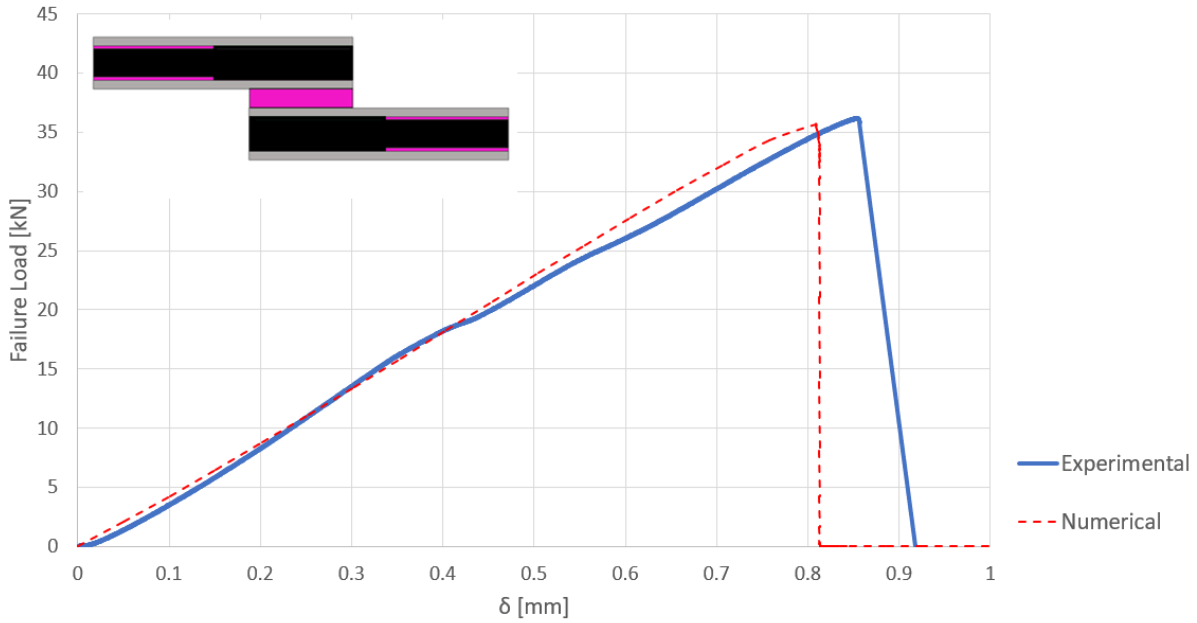

Figure 76: Numerical P-δ curve vs experimental P-δ curve, for a 50 mm overlap SLJ, with the configuration Ti-1/2Adh-CFRP-1/2Adh-Ti.

The failure mode is again coherent with the experimental results and is presented in Figure 77, where a cohesive failure can be observed with the cohesive elements used for the modelling of the adhesive layer being in a state of full degradation.

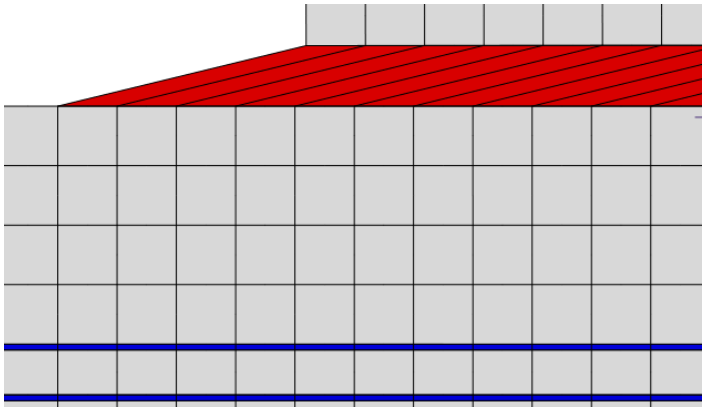

Figure 77: Numerical failure surface, for a 50 mm overlap SLJ, with the configuration Ti-1/2Adh-CFRP-1/2Adh-Ti.

5.7 Numerical analysis under impact conditions

5.7.1 Model description

As analysed in the literature review of this dissertation, the impact loads in the context of aeronautical industry must be to be taken into account to guarantee the safety of the structure and so that structural requirements are met. In this type of structures, impact loads such as collisions with service cars, dropped tools or bird strikes must be considered to avoid failures that can have serious consequences.

To assess the impact behaviour of the lay-up configurations (all with an overlap of 50 mm) suggested during this project, the configurations were at this stage evaluated numerically under impact conditions. For this analysis the *Abaqus*® software was also used and the model applied was similar to the one described regarding the analysis of the tensile tests, with few differences.

For the impact study, the boundary conditions applied to the specimen were altered (left extremity of the joint was fixed in all directions), Figure 78, and, in the right extremity, a mass of a very rigid material was attached to the specimens, to which a velocity field was applied. This velocity creates an acceleration that simulates an impact solicitation to the SLJ.

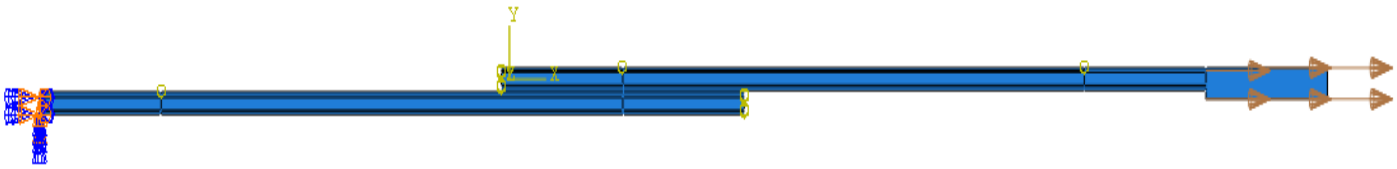

Figure 78: Schematic view of the physical boundary conditions for SLJs under impact conditions in *Abaqus*®.

Another specificity of this model is the element type used for all continuous elements (CFRP and respective metal of each lay-up). Instead of the 8-node biquadratic plane strain quadrilateral elements, 4-node bilinear plane stress quadrilateral elements were used.

The failure load was obtained for all configurations, in the form of a load-time plot, and then compared with the results obtained for the quasi-static conditions analysis.

5.7.2 Results

For the results regarding the configurations where only additional adhesive was used, shown in Figure 79, it can be concluded that with the increase of the introduction of additional adhesive layers used, the numerical failure load under impact conditions tends to decrease. In the more extreme case analysed, the configuration where 3 layers of film adhesive are used on the extremities of the substrate, the failure loads in quasi-static and under impact conditions are already very close.

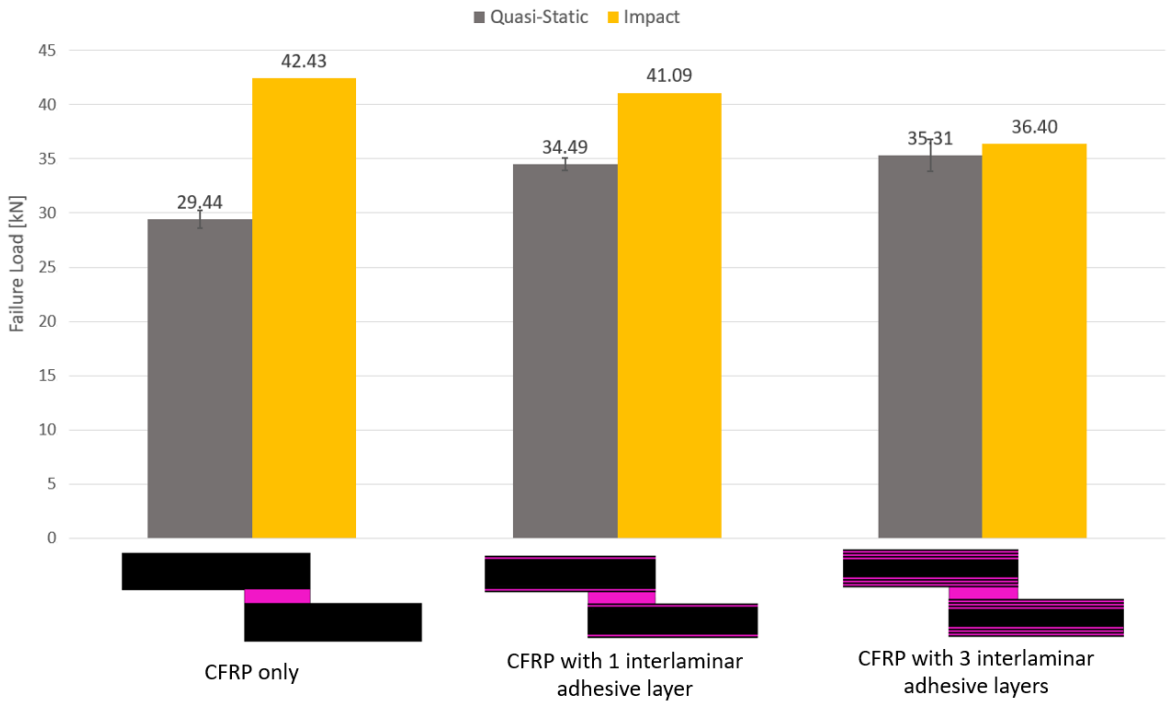

Figure 79: Comparison between numerical and experimental results obtained for the failure loads of SLJ configurations with additional adhesive layers as the reinforcement for the CFRP substrate, under impact and quasi-static conditions, respectively.

For the configurations using metallic plies, with results shown on Figure 80, the same trend of the reduction of the failure load of the SLJ under impact conditions can be observed when additional 0.2 mm adhesive layers are used in the interface between CFRP and metal. Thus, the numerical results obtained show that, with the same adhesive properties used for the quasi-static analysis, to achieve higher failure loads under impact conditions, it is important to moderate the use of additional adhesive to reinforce the substrate.

For the lay-up configuration regarding the utilization of aluminium layers with 0.4 mm of thickness combined with adhesive layers to enhance adhesion in the Al-CFRP interface, the failure load under impact was even lower than the one obtained using the basic

configuration with CFRP only, probably due to the already referred introduction of 0.2 mm thick adhesive layers in both extremities of the adherend, diverging from the original FML concept and consequently from the expected behaviour of an FML.

For the Ti-CFRP-Ti configuration, where no adhesive was used in the substrate - more similar to the original concept of FMLs - the failure load under impact is, as expected, higher than the one obtained for the CFRP only lay-up, being this coherent with the results of similar studies regarding the behaviour of FMLs under impact load already presented in the literature review of this dissertation.

The best result, in terms of simulation under impact conditions, was obtained with the Ti-1/2Adh-CFRP-1/2Adh-Ti lay-up, where an improvement was registered in comparison with the CFRP only basic configuration and with the Ti-CFRP-Ti configuration (more similar to the FML concept), as had also been seen for the experimental tensile tests performed previously. In this configuration, the fact that the application of the interfacial additional adhesive layer is only in half of the length of the adherend seems to reduce the effect of the lowering of the numerical predictions observed when a cohesive layer to model the adhesive is introduced in the total length of the substrate (Ti-Adh-CFRP-Adh-Ti configuration), or when several layers of interlaminar adhesive are introduced in the adherend (SLJ configurations with additional adhesive layers as the reinforcement for the CFRP substrate).

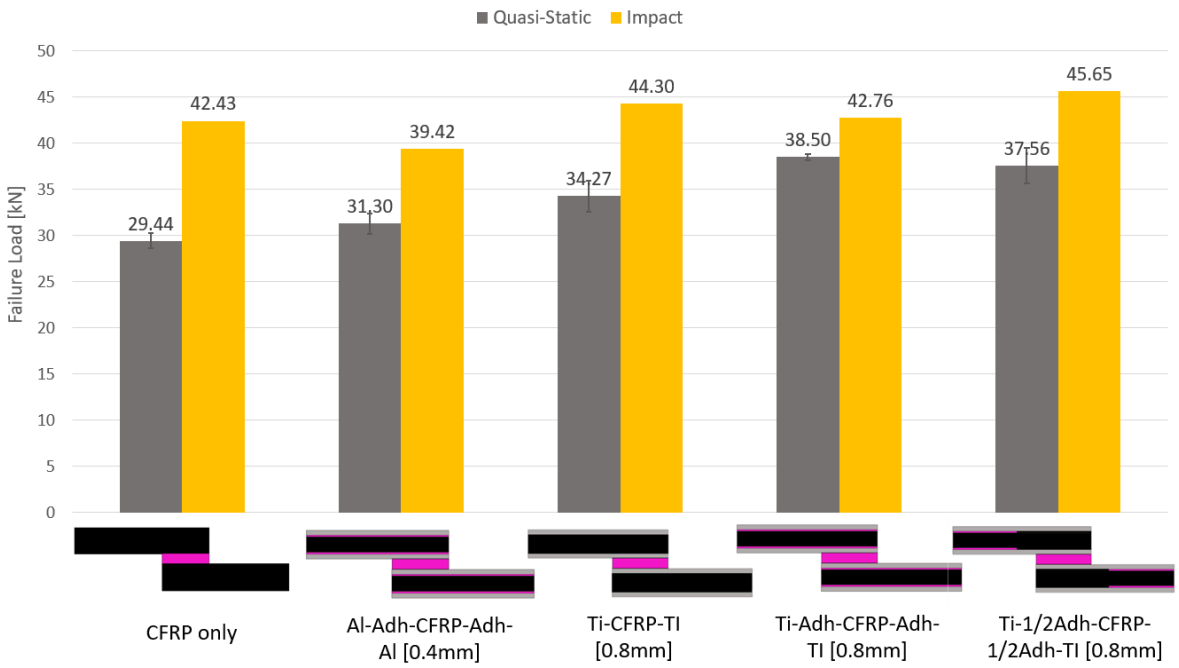

Figure 80: Comparison between numerical and experimental results obtained for the failure loads of SLJ configurations with metal laminates and additional adhesive as the reinforcement for the CFRP substrate, under impact and quasi-static conditions, respectively.

By analysing all the results, it is also possible to observe an increase of the failure load values for all SLJs under impact conditions when compared with the quasi-static situations, being this a general trend for the configurations under study.

For all the suggested lay-up configurations, the predicted failure mode under impact conditions is a cohesive failure in the adhesive, as can be seen, as an example, in the Figure 81.

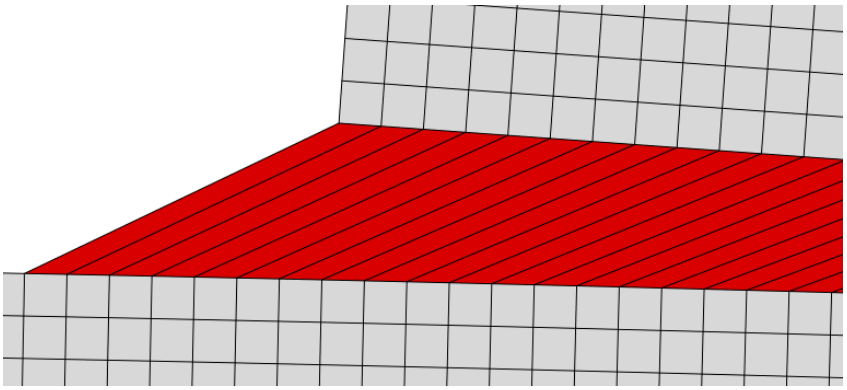

Figure 81: Numerical failure surface of the SLJs under impact conditions, with the exception of the CFRP only configuration.

It is relevant to refer that these results were obtained by performing a numerical analysis, so it will always be needed some experimental work, using the lay-up configurations suggested to validate the models, and to assess if the behaviour verified numerically is confirmed by experimental data. Additionally, as will be suggested in the section regarding suggestions for future works based on this dissertation, it is important to perform a characterization work of the adhesive's properties under different strain rates, so that, the development of models to analyse the impact behaviour of these SLJs, can be supported by the introduction of the correct properties of the adhesive for the specific strain rate that is going to be used for the analysis.

6 Discussions

By comparing the experimental and numerical results, it is possible to assess the suitability of the proposed numerical models to properly predict the failure load and the type of failure occurred during each SLJs tests.

In Figure 82 the evaluation of the results obtained for the basic lay-up configuration and for the SLJs manufactured where additional adhesive layers were used as the reinforcement is presented.

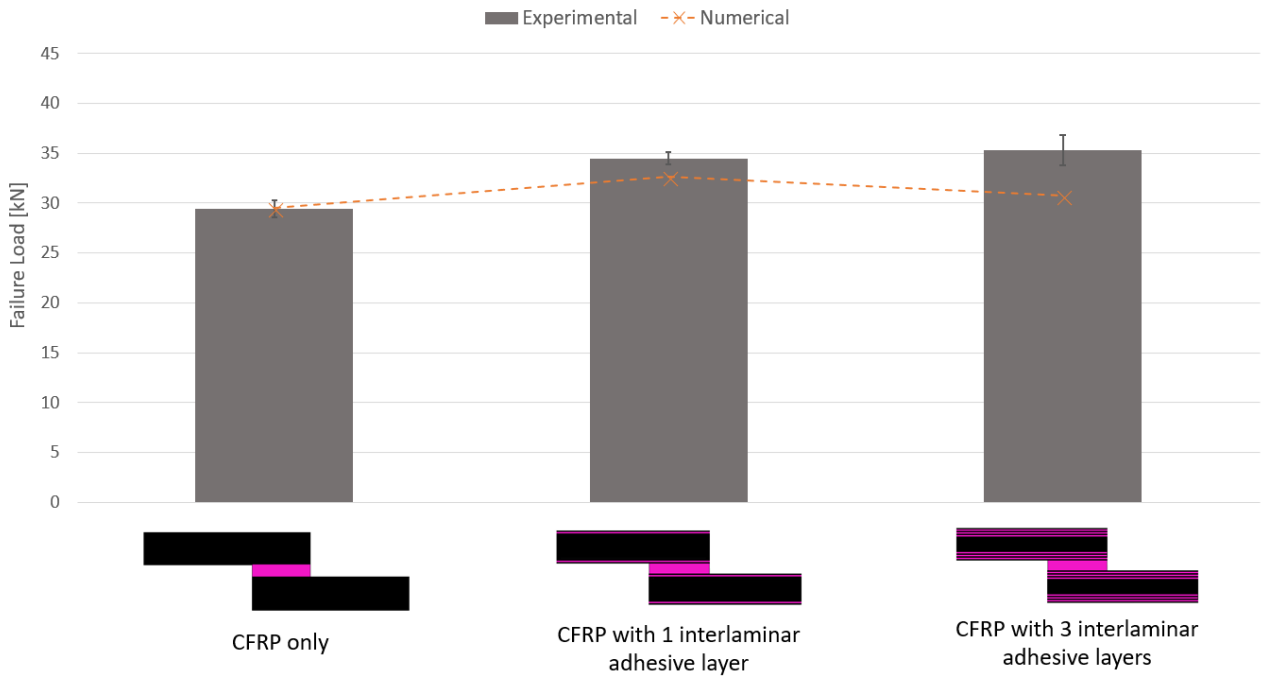

Figure 82: Comparison between numerical and experimental results obtained for the failure loads of SLJ configurations with additional adhesive layers as the reinforcement for the CFRP substrate, under quasi-static conditions.

It can be seen that, for the model regarding the CFRP only lay-up, the numerical failure load value is very similar to the one obtained experimentally. The case in which the experimental and numerical results had more disparity was in the CFRP with 3 interlaminar

adhesive layers configuration, probably because of the effect on the model of stacking many cohesive layers of adhesive material close to one another. In conclusion, the more cohesive layers stacked of adhesive in the adherend, the bigger seems to be the disparity between numerical and experimental data.

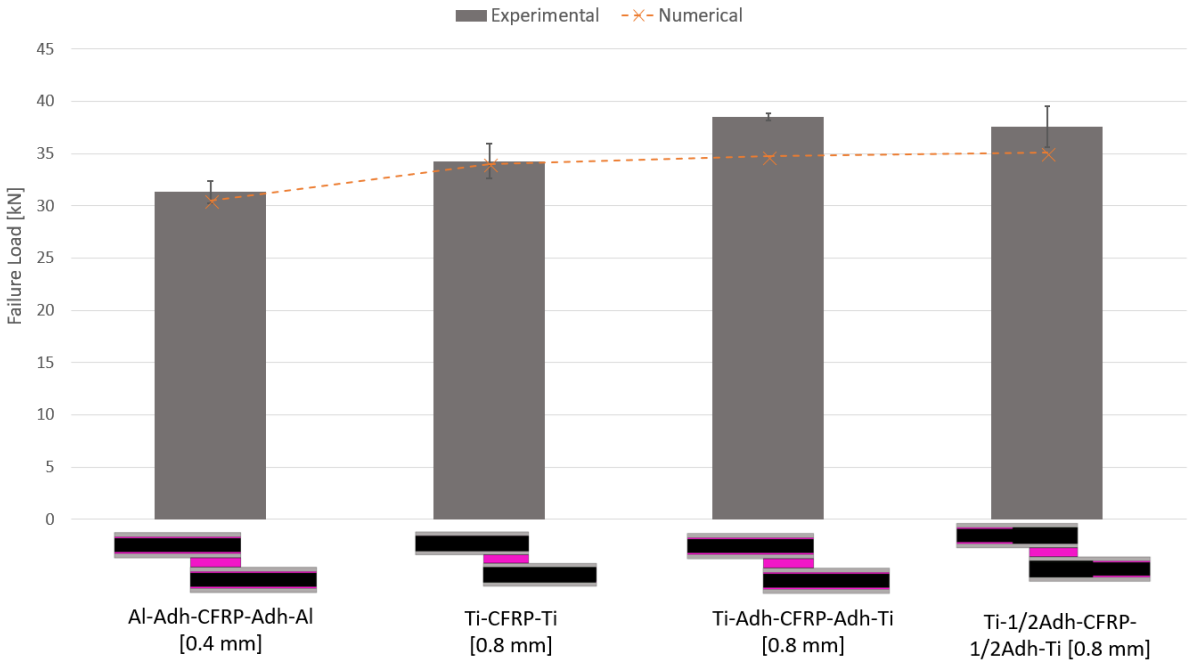

Figure 83: Comparison between numerical and experimental results obtained for the failure loads of SLJ configurations with metal laminates and additional adhesive as the reinforcement for the CFRP substrate, under quasi-static conditions.

For the models involving reinforcements with metallic plies, Figure 83, the model predicts the failure load relatively well although, in some cases, the predicted numerical failure load is lower than that the value obtained experimentally – which can be seen as a positive point when considering a tool to support the design of a real-life structure. The configuration that achieved closer results between numerical and experimental data, was the Ti-CFRP-Ti lay-up, being again this the configuration where the effect of the stacking of cohesive layers in the substrate is minimum. For the Al-Adh-CFRP-Adh-Al, the numerical results were also very close to the experimental ones, being in this case the thickness of the metallic plies 0.4 mm, in opposition to the 0.8 mm used for the titanium configurations, so it is though that the effect of the stacking of the cohesive layers is more prominent with the distance from the adhesive layer of the joint.

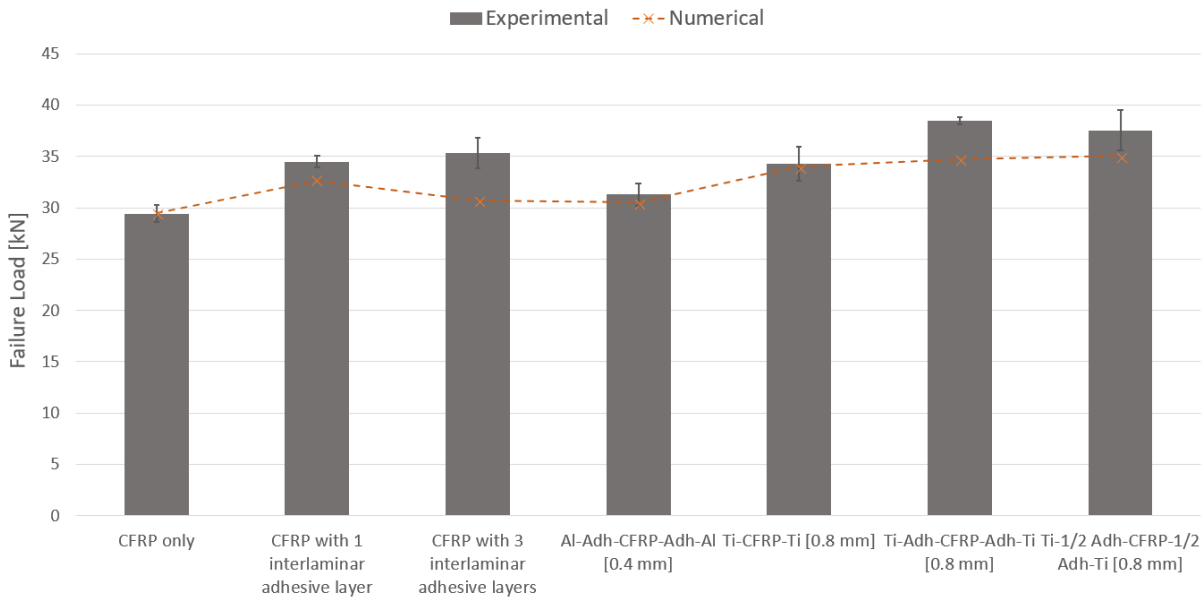

Figure 84: Comparison between numerical and experimental results obtained for the failure loads of all SLJ configurations studied, under quasi-static conditions.

In the Figure 84, the evolution of numerical and experimental results for all the configurations manufactured in this work can be analysed, being possible to check that the best results obtained, in terms of coherency, for the average failure load were registered on the configuration described as Ti-CFRP-Ti, with the utilization of 0.8 mm thick plies of titanium and without film adhesive between the composite and the metallic material, and on the model developed for the CFRP only configuration.

In terms of failure mode obtained, the comparison between numerical and experimental conditions, is summarized and presented in the Table 8, in order to make the analysis of the results easier.

Table 8: Failure mode obtained, experimentally and numerically, for the several lay-up configurations studied (50 mm overlap)

Lay-up Configuration	Schematization	Failure Mode - Experimental	Failure Mode - Numerical
CFRP only		Delamination	Delamination
CFRP with 1 interlaminar adhesive layer		Delamination	Cohesive failure in the adhesive
CFRP with 3 interlaminar adhesive layers		Delamination	Cohesive failure in the adhesive
Al-Adh-CFRP-Adh-Al	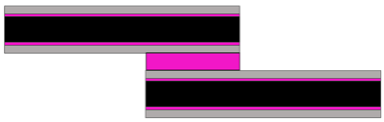	Cohesive failure in the adhesive	Cohesive failure in the adhesive
Ti-CFRP-Ti		Cohesive failure in the adhesive	Cohesive failure in the adhesive
Ti-Adh-CFRP-Adh-Ti		Cohesive failure in the adhesive	Cohesive failure in the adhesive
Ti-1/2Adh-CFRP-1/2Adh-Ti		Cohesive failure in the adhesive	Cohesive failure in the adhesive

For this 50 mm SLJ study, the model just differs on the experimental failure modes obtained in the cases which include CFRP lay-ups where additional interlaminar adhesive layers where used. This can again be explained by the effect of having several layers of cohesive elements too close to each other and the effect that this stacking has on the model.

For all the lay-ups where metallic materials were used, the developed model could replicate correctly all the cohesive failures in the adhesive observed experimentally.

7 Conclusions

The main objective of this project was to explore several lay-up configurations for reinforcing a basic CFRP substrate in order to increase its peel strength, and avoid delamination, as well as increase the adhesively bonded joint strength itself, when hybrid materials are used as adherends.

The work concentrated on two concepts to achieve the defined objective, one using additional interlaminar adhesive layers in between laminas of the CFRP and other, based more on a concept similar to the concept of FML, using metal plies (and in some cases adhesive as well). To apply these concepts several lay-up configurations for SLJs with an overlap of 50 mm and a thickness of 3.2 mm were suggested, manufactured, tested and evaluated in terms of failure load and failure mode.

Additionally, for all the specimens manufactured, a new concept in terms of cure cycle was applied, so that the disadvantage of adhesive bonding and adhesively bonded FRP, regarding the manufacturing time dispended on the cure cycles of both prepregs and adhesive could be tackled. For this purpose, a combined cure cycle was used, based on the information provided by the datasheet of the manufacturer of the adhesive used (AF 163-2K). It was possible to conclude that, using this approach, and for the case of this specific adhesive, the combination of the cure cycle of CFRP and adhesive in a SLJ could have a great impact on the manufacturing time by significantly reducing it, with only a small decrease in the joint performance.

Regarding the configurations where only additional adhesive was used as reinforcement for the CFRP, it was possible to see that, although the delamination presented by the basic CFRP only configuration could not be avoided, the average failure load of the specimens was improved.

For the configurations which use metal and adhesive as reinforcements (based on the concept of FML), in the case where aluminium plies of 0.4 mm thick were used in combination with adhesive, it was possible to avoid the adhesion problems observed in

previous studies made in the adhesive's investigation group of FEUP, being important to refer that, in this study, no phosphoric acid anodizing was used to treat the metallic plies.

For the configurations using 0.8 mm thick titanium plies, the configuration where the best results were reached was the configuration defined as Ti-Adh-CFRP-Adh-Ti, where the average failure load presented by the specimens tested had a good improvement (30.8 %), when compared to the basic CFRP only configuration. For all the configurations tested using metal, the failure modes obtained were also very satisfactory, presenting in every case a cohesive failure in the adhesive layer of the joint.

Regarding the numerical analysis, the results were not as coherent with the experimental results as expected for all the configurations studied, resulting in some cases in numerical failure load values lower than those experimentally obtained. In terms of failure mode obtained numerically, the only configuration in which the numerical failure mode was not a cohesive failure in the adhesive layer, was on the CFRP only lay-up, in which, delamination of the CFRP fibres was predicted numerically, being this a coherent result with the one obtained in the lab.

To summarize, the several experimental and numerical procedures undertaken, strongly indicate that it is possible to reinforce a CFRP joint using either only additional adhesive layers, metallic plies, or a combination of both. The best results are obtained by the introduction of titanium laminates combined with adhesive in the Ti-CFRP interfaces, where a significant increase in the failure load and in the peel strength of a CFRP joint can be observed, with no occurrence of delamination. Under impact conditions, although the introduction of metal laminates seemed to lead to an improvement in terms of failure load, the configurations using one or more additional adhesive layers, seemed to present a decrease in the failure load reachable by the SLJ, so a balanced utilization of adhesive and metal should be studied, in addition to experimental work to validate the data introduced in the model.

8 Future Work

To continue the work developed in this thesis, some suggestions are proposed below with the purpose of improving the knowledge regarding the behaviour of FMLs, of the adhesive tested and of SLJs with hybrid material adherends:

- Study the durability of the bond between adhesive and FML and compare the effects of the different surface treatments;
- Try to improve the trapezoidal traction-separation law developed, in order to better simulate the ductile behaviour of the AF 163-2K adhesive;
- Characterize the AF 163-2K adhesive when loaded with different strain rates, to better simulate the behaviour of SLJs under impact loads;
- Experimentally validate the numerical data obtained from the *Abaqus*® models that were developed to simulate the behaviour of SLJs under impact conditions;
- Do a similar study, regarding the effect of the use of different metals and different lay-up configurations, with a different adhesive, to assess if the improvements observed in this study are reproduceable with other adhesives;
- Try to perform a similar study but with different types of FMLs, for example ARALL or GLARE, or even develop studies with more recent types, such as BARALL, that uses basalt fibres as the reinforcement.

References

1. *The new-technology Boeing 787 dreamliner, which makes extensive use of composite materials, promises to revolutionize commercial air travel.* Aviation Week & Space Technology Market Supplement, 2005. **16201**: p. p. S1-31.
2. Camanho, P.P., et al., *Hybrid titanium–CFRP laminates for high-performance bolted joints.* Composites Part A: Applied Science and Manufacturing, 2009. **40**(12): p. 1826-1837.
3. Sinmazçelik, T., et al., *A review: Fibre metal laminates, background, bonding types and applied test methods.* Materials & Design, 2011. **32**(7): p. 3671-3685.
4. Kinloch, A.J., *Adhesion and adhesives: science and technology*. 1987, London: Chapman and Hall.
5. Adams, R.D., J. Comyn, and W.C. Wake, *Structural adhesive joints in engineering*. 1997: Springer Science & Business Media.
6. Da Silva, L.F., A. Öchsner, and R.D. Adams, *Handbook of adhesion technology*. 2011: Springer Science & Business Media.
7. Täljsten, B., *The importance of bonding—A historic overview and future possibilities.* Advances in Structural Engineering, 2006. **9**(6): p. 721-736.
8. Frauenhofer, D.I.M., *Bonding enables multi-material-mix - Illustrating the possibilities at the new Audi A8*. 2017, Automotive Circle Conference.
9. da Silva, L.F.M., A.G. de Magalhaes, and M.F.S. de Moura, *Juntas adesivas estruturais*. 2007: Publindústria.
10. Da Silva, L.F. and R. Adams, *Techniques to reduce the peel stresses in adhesive joints with composites.* International Journal of Adhesion and Adhesives, 2007. **27**(3): p. 227-235.
11. Banea, M.D. and L.F.M.d. Silva, *Adhesively bonded joints in composite materials: An overview.* Proceedings of the Institution of Mechanical Engineers, Part L: Journal of Materials: Design and Applications, 2009. **223**(1): p. 1-18.
12. Davis, M.J. and D.A. Bond. *The importance of failure mode identification in adhesive bonded aircraft structures and repairs*. in *ICMM 12*. 1999. Paris, France.
13. Ebnesajjad, S. and C. Ebnesajjad, *Surface treatment of materials for adhesive bonding*. 2013: William Andrew.
14. Baldan, A., *Adhesively-bonded joints and repairs in metallic alloys, polymers and composite materials: adhesives, adhesion theories and surface pretreatment.* Journal of materials science, 2004. **39**(1): p. 1-49.
15. Critchlow, G. and D. Brewis, *Review of surface pretreatments for aluminium alloys.* International Journal of Adhesion and Adhesives, 1996. **16**(4): p. 255-275.
16. Vlot, A., L. Vogelesang, and T. De Vries, *Towards application of fibre metal laminates in large aircraft.* Aircraft Engineering and Aerospace Technology, 1999. **71**(6): p. 558-570.
17. Rao, H.J., et al. *Failure Prediction in Fiber Metal Laminates for Next Generation Aero Materials*. in *IOP Conference Series: Materials Science and Engineering*. 2016. IOP Publishing.
18. Kolesnikov, B., L. Herbeck, and A. Fink, *CFRP/titanium hybrid material for improving composite bolted joints.* Composite Structures, 2008. **83**(4): p. 368-380.
19. Council, N.R., *Going to extremes: meeting the emerging demand for durable polymer matrix composites*. 2005: National Academies Press.

20. Agarwal, B.D., L.J. Broutman, and K. Chandrashekhara, *Analysis and performance of fiber composites*. 2017: John Wiley & Sons.
21. Gay, D., *Composite materials: design and applications*. 2014: CRC press.
22. Banea, M. and L.F. da Silva, *Adhesively bonded joints in composite materials: an overview.* Proceedings of the Institution of Mechanical Engineers, Part L: Journal of Materials: Design and Applications, 2009. **223**(1): p. 1-18.
23. Hart-Smith, L., *Analysis and design of advanced composite bounded joints.* 1974.
24. Adams, R., et al., *Stress analysis and failure properties of carbon-fibre-reinforced-plastic/steel double-lap joints.* The Journal of Adhesion, 1986. **20**(1): p. 29-53.
25. Mouritz, A., *Review of z-pinned composite laminates.* Composites Part A: applied science and manufacturing, 2007. **38**(12): p. 2383-2397.
26. Dransfield, K., C. Baillie, and Y.-W. Mai, *Improving the delamination resistance of CFRP by stitching—a review.* Composites Science and Technology, 1994. **50**(3): p. 305-317.
27. Mouritz, A.P., et al., *Review of applications for advanced three-dimensional fibre textile composites.* Composites Part A: applied science and manufacturing, 1999. **30**(12): p. 1445-1461.
28. Asundi, A. and A.Y. Choi, *Fiber metal laminates: an advanced material for future aircraft.* Journal of Materials Processing Technology, 1997. **63**(1-3): p. 384-394.
29. Vogelesang, L.B. and A. Vlot, *Development of fibre metal laminates for advanced aerospace structures.* Journal of Materials Processing Technology, 2000. **103**(1): p. 1-5.
30. Sadighi, M., R. Alderliesten, and R. Benedictus, *Impact resistance of fiber-metal laminates: a review.* International Journal of Impact Engineering, 2012. **49**: p. 77-90.
31. Homan, J., *Fatigue initiation in fibre metal laminates.* International Journal of Fatigue, 2006. **28**(4): p. 366-374.
32. Chang, P.-Y., P.-C. Yeh, and J.-M. Yang, *Fatigue crack initiation in hybrid boron/glass/aluminum fiber metal laminates.* Materials Science and Engineering: A, 2008. **496**(1-2): p. 273-280.
33. Xue, J., et al., *Reduction of thermal residual stress in carbon fiber aluminum laminates using a thermal expansion clamp.* Composites Part A: Applied Science and Manufacturing, 2011. **42**(8): p. 986-992.
34. Miller, J., et al., *Preliminary evaluation of hybrid titanium composite laminates.* The Journal of Adhesion, 1995. **54**(1-4): p. 223-240.
35. Li, X., et al., *Mechanical behaviors of Ti/CFRP/Ti laminates with different surface treatments of titanium sheets.* Composite Structures, 2017. **163**: p. 21-31.
36. Cortes, P. and W. Cantwell, *The prediction of tensile failure in titanium-based thermoplastic fibre–metal laminates.* Composites Science and Technology, 2006. **66**(13): p. 2306-2316.
37. Palmares, M.P., *Strength of Hybrid Laminates Aluminium Carbon-Fibre Joints with Different Lay-up Configurations*. 2016, FEUP: Porto.
38. Martins, J.L.C.H., *CFRP joints with hybrid laminates metal-carbon fibre* in *Department of Mechanical Engineering* 2018, University of POrto: Porto.
39. Vlot, A., E. Kroon, and G. La Rocca. *Impact response of fiber metal laminates*. in *Key Engineering Materials*. 1998. Trans Tech Publ.
40. Vlot, A., *Impact properties of fibre metal laminates.* Composites Engineering, 1993. **3**(10): p. 911-927.
41. Harris, J. and R. Adams, *An assessment of the impact performance of bonded joints for use in high energy absorbing structures.* Proceedings of the Institution of Mechanical Engineers, Part C: Journal of Mechanical Engineering Science, 1985. **199**(2): p. 121-131.
42. Machado, J., E. Marques, and L.F. da Silva, *Adhesives and adhesive joints under impact loadings: An overview.* The Journal of Adhesion, 2017: p. 1-32.
43. Fan, J., W. Cantwell, and Z. Guan, *The low-velocity impact response of fiber-metal laminates.* Journal of Reinforced Plastics and Composites, 2011. **30**(1): p. 26-35.
44. Chai, G.B. and P. Manikandan, *Low velocity impact response of fibre-metal laminates–A review.* Composite Structures, 2014. **107**: p. 363-381.

45. da Silva, L.F., et al., *Analytical models of adhesively bonded joints—Part I: Literature survey.* International Journal of Adhesion and Adhesives, 2009. **29**(3): p. 319-330.
46. Volkersen, O., *Die Nietkraftverteilung in zugbeanspruchten Nietverbindungen mit konstanten Laschenquerschnitten.* Luftfahrtfor schung, 1938. **15**: p. 41-47.
47. Goland, M. and E. Reissner, *The stresses in cemented joints.* J. Applied Mechanics, Trans. ASME, 1944. **66**: p. A-17-A-27.
48. Hart-Smith, L. and A.-B.S.-L. Joints, *NASA contract report.* NASA CR-112236, 1973.
49. Hart-Smith, L. and A.-B.D.-L. Joints, *NASA contract report.* NASA CR-112235, 1973.
50. da Silva, L.F.M. and R.D.S.G. Campilho, *Advances in Numerical Modelling of Adhesive Joints*, in *Advances in Numerical Modeling of Adhesive Joints*. 2012, Springer Berlin Heidelberg: Berlin, Heidelberg. p. 1-93.
51. Zhao, X., R. Adams, and L. Da Silva, *Single lap joints with rounded adherend corners: experimental results and strength prediction.* Journal of Adhesion Science and Technology, 2011. **25**(8): p. 837-856.
52. Adams, R. and J. Harris, *The influence of local geometry on the strength of adhesive joints.* International Journal of Adhesion and Adhesives, 1987. **7**(2): p. 69-80.
53. Adams, R.D., *Adhesive bonding: science, technology and applications*. 2005: Elsevier.
54. Chaves, F.J., et al., *Fracture mechanics tests in adhesively bonded joints: a literature review.* The Journal of Adhesion, 2014. **90**(12): p. 955-992.
55. Ortiz, M. and A. Pandolfi, *Finite-deformation irreversible cohesive elements for three-dimensional crack-propagation analysis.* International Journal for Numerical Methods in Engineering, 1999. **44**(9): p. 1267-1282.
56. Liljedahl, C., et al., *Damage modelling of adhesively bonded joints.* International journal of fracture, 2006. **141**(1-2): p. 147-161.
57. De Moura, M., et al., *Cohesive and continuum mixed-mode damage models applied to the simulation of the mechanical behaviour of bonded joints.* International Journal of adhesion and Adhesives, 2008. **28**(8): p. 419-426.
58. Chandra, N., et al., *Some issues in the application of cohesive zone models for metal–ceramic interfaces.* International Journal of Solids and Structures, 2002. **39**(10): p. 2827-2855.
59. Ribeiro, T., et al., *Damage analysis of composite–aluminium adhesively-bonded single-lap joints.* Composite Structures, 2016. **136**: p. 25-33.
60. Khoramishad, H., et al., *Predicting fatigue damage in adhesively bonded joints using a cohesive zone model.* International Journal of fatigue, 2010. **32**(7): p. 1146-1158.
61. *AF 163-2K Structural Adhesive Film, Technical Datasheet*, M. Scotch-Weld, Editor. 2009.
62. Campilho, R.D.S.G., *Repair of composite and wood structures*. 2009, Universidade do Porto (Portugal).
63. *Titanium Ti-6Al-4V (Grade5), Technical Datasheet* S.M. Centres, Editor. 2017.
64. *Titanium Ti-6Al-4V (Grade5), annealed, Technical Datasheet*, A.A.S.M. Inc., Editor. 1994.
65. Inagaki, I., et al., *Application and features of titanium for the aerospace industry.* Nippon Steel & Sumitomo Metal Technical Report, 2014. **106**: p. 22-27.
66. De Vries, T. and C. Vermeeren, *R-curve testdata: 2024-T3, 7075-T6, GLARE 2 and GLARE 3.* 1994.
67. Molitor, P., V. Barron, and T. Young, *Surface treatment of titanium for adhesive bonding to polymer composites: a review.* International Journal of Adhesion and Adhesives, 2001. **21**(2): p. 129-136.